

Probabilistic Integration: A Role for Statisticians in Numerical Analysis?

François-Xavier Briol¹, Chris. J. Oates^{2,3}, Mark Girolami^{1,4},
Michael A. Osborne⁵ and Dino Sejdinovic⁶

¹Department of Statistics, University of Warwick

²School of Mathematical and Physical Sciences, University of Technology Sydney

³The ARC Centre of Excellence for Mathematical and Statistical Frontiers

⁴The Alan Turing Institute for Data Science

⁵Department of Engineering Science, University of Oxford

⁶Department of Statistics. University of Oxford

September 4, 2022

Abstract

A research frontier has emerged in scientific computation, founded on the principle that numerical error entails epistemic uncertainty that ought to be subjected to statistical analysis. This viewpoint raises several interesting challenges, including the design of statistical methods that enable the coherent propagation of probabilities through a (possibly deterministic) computational pipeline. This paper examines thoroughly the case for probabilistic numerical methods in statistical computation and a specific case study is presented for Markov chain and Quasi Monte Carlo methods. A *probabilistic integrator* is equipped with a full distribution over its output, providing a measure of epistemic uncertainty that is shown to be statistically valid at finite computational levels, as well as in asymptotic regimes. The approach is motivated by expensive integration problems, where, as in krigging, one is willing to expend, at worst, cubic computational effort in order to gain uncertainty quantification. There, probabilistic integrators enjoy the “best of both worlds”, leveraging the sampling efficiency of Monte Carlo methods whilst providing a principled route to assessment of the impact of numerical error on scientific conclusions. Several substantial applications are provided for illustration and critical evaluation, including examples from statistical modelling, computer graphics and uncertainty quantification in oil reservoir modelling.

Keywords: nonparametric statistics, numerical integration, probabilistic numerics, uncertainty quantification.

1 Introduction

This paper presents a statistical perspective on the theoretical and methodological issues pertinent to the emerging area of Probabilistic Numerics. Our aim is to stimulate what we feel is an important discussion about these methods for use in contemporary and emerging statistical applications.

Background Numerical procedures, such as linear solvers, quadrature methods for integration and routines to approximate the solution of differential equations, are the core computational building blocks in modern statistical inference procedures. These are typically considered as computational black-boxes that return a point estimate for a deterministic quantity of interest whose numerical error is considered to be negligible. Numerical methods are thus the only part of the statistical analysis for which uncertainty is not routinely accounted in a fully probabilistic way (although analysis of errors and bounds on these are often available and highly developed). In many situations numerical error will be negligible and no further action is required. However, if numerical errors are propagated through a computational pipeline and allowed to accumulate, then failure to properly account for such errors could potentially have drastic consequences on subsequent statistical inferences (Mosbach and Turner, 2009; Conrad et al., 2015).

Probabilistic Numerics is the study of numerical algorithms from a statistical point of view, where uncertainty is formally due to the presence of an unknown numerical error. The philosophical foundations for Probabilistic Numerics were, to the best of our knowledge, first clearly exposed in the work of Kadane (1985), Diaconis (1988) and O’Hagan (1992). However, elements can be traced back to Poincaré (1912); Erdős and Kac (1940), who discuss a sense in which a deterministic quantity can be uncertain, and Hull and Swenson (1966), who proposed probabilistic models for rounding error in floating point computation. The mathematical tools that underpin these methods, such as linear approximation, do not themselves require any probabilistic semantics; though a probabilistic interpretation has been noted (e.g. Sard, 1963; Larkin, 1972; Wahba, 1990). Further theoretical support comes from the Information Complexity literature (Woźniakowski, 2009), where continuous mathematical operations are approximated by discrete and finite operations to achieve a prescribed accuracy level.

Proponents claim that this approach provides three important benefits. Firstly, it provides a principled approach to quantify and propagate numerical uncertainty through pipelines of computation, allowing for the possibility of errors with complex statistical structure. Secondly, it enables the user to control the uncertainty over the solution of the numerical procedure by identifying key components of numerical uncertainty (using statistical techniques such as analysis of variance), then targeting computational resources at these components. Thirdly, this dual perspective on numerical analysis as an inference task enables new insights, as well as the potential to criticise and refine existing numerical methods. On this final point, recent interest has led to several new and effective numerical algorithms in many areas, including differential equations (Skilling, 1991; Schober et al., 2014; Owhadi, 2016), linear algebra (Hennig, 2015) and optimisation (Hennig and Kiefel, 2013; Mahsereci and Hennig, 2015; Shahriari et al., 2015). Similar ideas have also been used in the context of statistical techniques with Principal Component Analysis (PCA) (Tipping and Bishop, 1999). We point the interested reader to the recent expositions by Hennig et al. (2015) and to the up-to-date bibliography of literature in this emerging area provided at www.probablistic-numerics.org.

Purpose Our aim, with authoring this paper, is to present concrete results that can serve as a basis for discussion on the suitability of probabilistic numerical computation for use in statistical applications. A decision was made to focus on numerical integration (Davis and Rabinowitz, 2007), due to its central role in computational statistics, including frequentist approaches such as bootstrap estimators (Efron and Tibshirani, 1994) and estimators for partial differential equations (Carson et al., 2016), where integration is performed over randomness due to re-sampling, and Bayesian approaches, such as computing conditional distributions, marginal and predictive likelihoods.

For numerical integration, the use of a probabilistic numerics approach was first advocated in Kadane and Wasilkowski (1985); Kadane (1985) who connected the worst-case and average-case numerical errors to Bayesian decision theory. A few years later, Diaconis (1988) and O’Hagan (1991) developed similar ideas independently. In particular, these previous studies all approach integration from the Bayesian perspective. Whilst not strictly necessary (see for example Kong et al. (2003) for a maximum likelihood approach), the Bayesian perspective provides an intuitive route to encode information available about the integration problem at hand, allowing for the design of algorithms which can be tailored to specific prior assumptions, as well as providing a principled approach to the subsequent propagation of uncertainty through a statistical procedure.

The present paper focuses on expensive numerical integrals arising in statistics; specifically, where the cost of evaluating the integrand forms a computational bottleneck. Such problems occur in statistical analysis for scientific applications involving sophisticated computer simulation, including astrophysics (Sozzetti et al., 2013), meteorology (Mizielinski et al., 2014) and, more broadly, in computing sensitivity estimates, such as Sobol indices (Sobol, 1993) and in uncertainty quantification for inverse problems (Dashti and Stuart, 2016). A probabilistic approach to integration could, if the probabilistic arguments hold, confer several advantages in this context. In particular, from a statistical perspective, valid inferences could be drawn at lower computational budgets by explicitly accounting, in a principled way, for the effect of numerical error on the analysis. Given these substantial claims and a surge in recent research activity on probabilistic numerical methods, there is now an imperative for the statistical community to critically examine the foundations of uncertainty in deterministic computation (Hennig et al., 2015).

Novel Contribution Consider a probability measure Π on a state space \mathcal{X} , so that we aim to compute (or, rather, to *estimate*) integrals of the form

$$\Pi[f] := \int_{\mathcal{X}} f \, d\Pi,$$

where $f : \mathcal{X} \rightarrow \mathbb{R}$ or \mathbb{C} is a test function of interest. Our motivation comes from settings where f does not possess a convenient closed-form expression, so that there is epistemic uncertainty over the actual values attained by f at a point \mathbf{x} until the function is actually evaluated at \mathbf{x} , usually at a non-trivial computational cost. The probabilistic integration method that we focus on is known as *Bayesian Quadrature* (BQ), the name being coined

by O’Hagan (1991). The method operates by evaluating the integrand at a set of states $\{\mathbf{x}_i\}_{i=1}^n \subset \mathcal{X}$ and returning a probability distribution \mathbb{P}_n , defined over the real line, that expresses belief about the true value of $\Pi[f]$. As the name suggests, \mathbb{P}_n will be based on a prior that captures certain properties of f , and that is updated, via Bayes’ rule, on the basis of the “data” contained in the function evaluations. The *maximum a posteriori* (MAP) value of \mathbb{P}_n acts as a point estimate of the integral, while the rest of the distribution captures numerical uncertainty due to the fact that we can only evaluate the function at a finite number of locations.

Our first contribution is to explore the claim of the probabilistic approach to integration that, if the prior is well-specified (a non-trivial condition), the probability distribution \mathbb{P}_n will provide a coherent measure of the uncertainty due to the numerical error. This claim is shown to be substantiated by rigorous mathematical analysis of BQ, based on a dual relationship between Bayes decision rules and minimax estimators, as exposed in the Hilbert space setting by Ritter (2000). We further develop that analysis to establish contraction of the posterior \mathbb{P}_n to a point mass centred on the true value $\Pi[f]$, building on recent work in this direction by Briol et al. (2015). These results hold in the important settings of Markov chain Monte Carlo (MCMC) and Quasi-Monte Carlo (QMC) methods, that are the workhorse of much modern statistical computation. Our results demonstrate that posterior contraction occurs under conditions on the sampling approach; in the case of MCMC, uniform ergodicity is sufficient (Meyn and Tweedie, 2012), while for QMC, a particular point set known as a higher-order digital net is proven to provide posterior contraction (Dick and Pillichshammer, 2010). However, these results are all predicated on having a well-specified prior, which is an issue inherited from the Bayesian approach.

Our second contribution is to explore the claim that (appropriate) use of prior information can lead to improved rates of convergence, in the usual (non-probabilistic) sense of the point estimate provided by the MAP estimate. Again, we show how this claim can be substantiated with formal analysis of the BQ estimator, in this case provided in the Kernel Quadrature literature (e.g. Sommariva and Vianello, 2006). Going further, we demonstrate that the same conclusion holds for the full BQ posterior; rates of contraction can be improved via the (appropriate) inclusion of prior information. These results serve to highlight the inefficiency of some basic approaches to integration that are sometimes employed in the statistical literature.

Finally, we investigate the extent to which probabilistic integrators are applicable in contemporary statistical applications¹. In doing so, we have developed strategies for (i) model evidence evaluation via thermodynamic integration, where a large number of candidate models are to be compared, (ii) inverse problems arising in partial differential equation models for oil field fluid flow, (iii) logistic regression models involving high-dimensional latent random effects, and (iv) spherical integration, as used in the rendering of virtual objects in prescribed environments. In each case the relative advantages and disadvantages of the probabilistic approach to integration are presented for critical evaluation.

¹Computer codes and scripts in R to reproduce experiments reported in this paper can be downloaded from www.warwick.ac.uk/fxbriol/probabilistic_integration

Outline The paper is structured as follows. Sec. 2 provides background on BQ and outlines an analytic framework for the method that is rooted in Hilbert spaces. Sec. 3 describes our extension of BQ to MCMC and QMC methods and provides an associated theoretical analysis of their properties. Sec. 4 is devoted to a discussion of practical issues, including the important issue of prior specification. Sec. 5 presents several novel applications of probabilistic integration in modern computational statistics. Sec. 6 concludes with a critical appraisal of the suitability of probabilistic numerical methods for statistical computation.

2 Background

Below we provide the reader with relevant background material. Sec. 2.1 provides a formal description of BQ. Secs. 2.2 and 2.3 explain how the analysis of BQ is dual to minimax analysis in functional regression, and Sec. 2.4 relates these ideas to established MCMC and QMC methods.

Set-Up Let $(\Omega, \mathcal{F}, \mu)$ be a probability space and $(\mathcal{X}, \mathcal{B})$ be a measurable space, whose state space \mathcal{X} will either be a compact subspace of \mathbb{R}^d or more general compact manifolds (e.g. the sphere \mathbb{S}^d), in each case equipped with the Borel σ -algebra $\mathcal{B} = \mathcal{B}(\mathcal{X})$. Also let $\mathbf{X} : \Omega \rightarrow \mathcal{X}$ be a measurable function (random variable). We denote the distribution of \mathbf{X} by Π and consider integration over the measure space $(\mathcal{X}, \mathcal{B}, \Pi)$. Our integrand is assumed to be a measurable function $f : \mathcal{X} \rightarrow \mathbb{R}$ or \mathbb{C} whose expectation, $\Pi[f]$, is the goal of computation.

Notation Write $\|f\|_2^2 := \int_{\mathcal{X}} f^2 d\Pi$ and write $L^2(\Pi)$ for the set of (measurable) functions which are square-integrable with respect to Π (i.e. $\|f\|_2 < \infty$). Note the un-conventional use of $L^2(\Pi)$; here we are *not* referring to equivalence classes of functions. For vector arguments, we also denote $\|\mathbf{u}\|_2 = (u_1^2 + \dots + u_d^2)^{1/2}$. We will make use of the notation $[u]_+ = \max\{0, u\}$. For vector-valued functions $\mathbf{f} : \mathcal{X} \rightarrow \mathbb{R}^m$ or \mathbb{C}^m we write $\Pi[\mathbf{f}]$ for the $m \times 1$ vector whose i th element is $\Pi[f_i]$. The relation $a_l \asymp b_l$ is taken to mean that there exist $0 < C_1, C_2 < \infty$ such that $C_1 a_l \leq b_l \leq C_2 a_l$.

A *quadrature rule* describes any functional $\hat{\Pi} : L^2(\Pi) \rightarrow \mathbb{R}$ that can be written in the linear form

$$\hat{\Pi}[f] = \sum_{i=1}^n w_i f(\mathbf{x}_i), \tag{1}$$

for some states $\{\mathbf{x}_i\}_{i=1}^n \subset \mathcal{X}$ and weights $\{w_i\}_{i=1}^n \subset \mathbb{R}$. The term *cubature rule* is sometimes used when the domain of integration is multi-dimensional (i.e. $d > 1$). The notation $\hat{\Pi}[f]$ is motivated by the fact that this expression can be re-written as the integral of f with respect to an empirical measure $\hat{\Pi} = \sum_{i=1}^n w_i \delta(\cdot - \mathbf{x}_i)$, where $\delta(\cdot)$ is the Dirac delta measure and the weights w_i can be negative and need not sum to one.

2.1 Bayesian Quadrature

Below we formally introduce BQ (O’Hagan, 1991). Probabilistic integration begins by defining a prior probability measure over $L^2(\Pi)$; for BQ this is achieved via a Gaussian process (GP) prior. This choice is motivated in part by analytic tractability but also by the absolute continuity of the posterior with respect to the prior presented in Dashti and Stuart (2016). A GP is a stochastic process f whose finite dimensional distributions are Gaussian, and can thus be characterised by its (measurable) mean function $m : \mathcal{X} \rightarrow \mathbb{R}$, $m(\mathbf{x}) = \mathbb{E}[f(\mathbf{x})]$, and its (product measurable) covariance function $k : \mathcal{X} \times \mathcal{X} \rightarrow \mathbb{R}$, $k(\mathbf{x}, \mathbf{x}') = \mathbb{E}[(f(\mathbf{x}) - \mathbb{E}[f(\mathbf{x})])(f(\mathbf{x}') - \mathbb{E}[f(\mathbf{x}')])]$. The common shorthand $\mathcal{N}(m, k)$ will be employed to denote these priors. Conditioning on (noiseless) “data” $\{\mathbf{x}_i, f_i\}_{i=1}^n$ where $f_i = f(\mathbf{x}_i)$ produces a posterior measure \mathbb{P}_n over $L^2(\Pi)$. Standard conjugacy results imply that \mathbb{P}_n is also a GP, with mean and covariance denoted m_n and k_n (see e.g. Chap. 2 of Rasmussen and Williams, 2006). The final stage is to produce a distribution over $\Pi[f]$ by projecting \mathbb{P}_n down onto \mathbb{R} via the integration operator. Since the distribution \mathbb{P}_n is supported on functions which are consistent with both prior knowledge and data, the projection provides a natural description of quantification over the value of $\Pi[f]$.

A sketch of the procedure is provided in Figure 1 and the relevant formulae are derived below. Denote by $\mathbb{E}_n, \mathbb{V}_n$ the expectation and variance taken with respect to the posterior distribution \mathbb{P}_n . (Later, for measurable A we also write $\mathbb{P}_n[A] = \mathbb{E}_n[1_A]$ where 1_A is the indicator function of the event A .) Write $\mathbf{f} \in \mathbb{R}^n$ for the vector of f_i values, $\mathbf{m} \in \mathbb{R}^n$ for the vector of $m(\mathbf{x}_i)$ values, $X = \{\mathbf{x}_i\}_{i=1}^n$ and $\mathbf{k}(\mathbf{x}, X) = \mathbf{k}(X, \mathbf{x})^T$ for the $1 \times n$ vector whose i th entry is $k(\mathbf{x}, \mathbf{x}_i)$ and \mathbf{K} for the matrix whose i th row and j th column element is $k(\mathbf{x}_i, \mathbf{x}_j)$.

Proposition 1. *The posterior for $\Pi[f]$ is Gaussian with mean and variance*

$$\mathbb{E}_n[\Pi[f]] = \Pi[m] + \Pi[\mathbf{k}(\cdot, X)]\mathbf{K}^{-1}(\mathbf{f} - \mathbf{m}) \quad (2)$$

$$\mathbb{V}_n[\Pi[f]] = \Pi\Pi[k(\cdot, \cdot)] - \Pi[\mathbf{k}(\cdot, X)]\mathbf{K}^{-1}\Pi[\mathbf{k}(X, \cdot)]. \quad (3)$$

Here, $\Pi\Pi[k(\cdot, \cdot)]$ denote the integral of k with respect to each argument. All proofs in this paper are reserved for Supplement A. Inversion of the matrix \mathbf{K} comes with a cost of $O(n^3)$. An important motivation for BQ is the case of expensive functions f , where numerical error is presumed to be non-negligible due to a limited computational budget. In such settings the cost of matrix inversion is often negligible in comparison with the cost of evaluating f , even once.

We now have a probabilistic model for the epistemic uncertainty over the value of the integral that is due to employing a quadrature rule with a finite number n of function evaluations. By re-parametrising $f \mapsto f - m$ we can, without loss of generality, suppose that $m \equiv 0$ for the remainder of the paper. From Eqn. 2, the posterior mean takes the form of a quadrature rule

$$\hat{\Pi}_{\text{BQ}}[f] := \sum_{i=1}^n w_i^{\text{BQ}} f(\mathbf{x}_i) \quad (4)$$

where $\mathbf{w}^{\text{BQ}} := \mathbf{K}^{-1}\Pi[\mathbf{k}(X, \cdot)]$. Furthermore, from Eq. 3 the posterior variance $\mathbb{V}_n[\Pi[f]]$ does not depend on function values $\{f_i\}_{i=1}^n$, but only on the location of the states $\{\mathbf{x}_i\}_{i=1}^n$

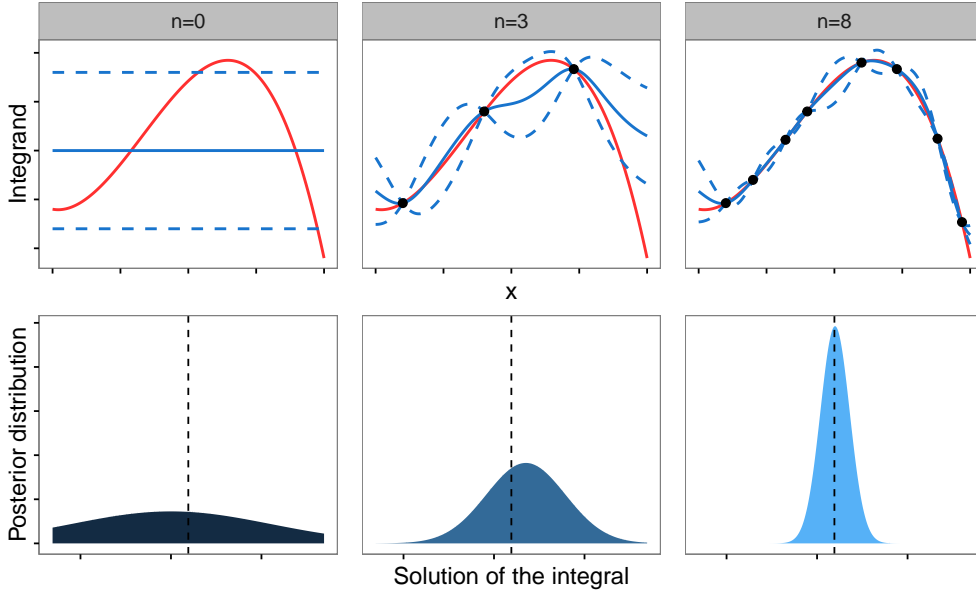


Figure 1: Sketch of Bayesian Quadrature. The top row shows the approximation of the integrand f (in red) by the posterior mean m_n (in blue) as the number n of function evaluations is increased. The dashed lines represent 95% credible intervals. The bottom row shows the Gaussian distribution with mean $\mathbb{E}_n[\Pi[f]]$ and variance $\mathbb{V}_n[\Pi[f]]$ that models uncertainty over $\Pi[f]$ as n increases (the dashed black line gives the true value of the integral). As the number of states n increases, the approximation of f becomes more precise and the posterior distribution over $\Pi[f]$ contracts onto the true value of the integral.

and the choice of covariance function k . This is useful as it allows us to pre-compute state locations and weights that can be used to integrate multiple integrals under the same prior specification. However, it also means that the posterior variance will be driven by our choice of prior, which will have great influence on the performance of the method. A valid quantification of uncertainty relies on a well-specified prior, and we will consider this issue further in Sec. 4.1.

It has long been known that the BQ construction (Eqn. 4) gives rise to several classical quadrature rules for specific choices of covariance function k (Diaconis, 1988). For example, a Brownian covariance function k leads to a posterior mean m_n that is a piecewise linear interpolation of f between the states $\{\mathbf{x}_i\}_{i=1}^n$, i.e. the trapezium rule. As another example, an integrated Brownian covariance function k results in a cubic spline interpolant for m_n , i.e. an instance of Simpson’s rule. Clearly the point estimator $\hat{\Pi}_{\text{BQ}}$ is a natural object; it has also received attention in both the Kernel Quadrature literature (Sommariva and Vianello, 2006) and Empirical Interpolation literature (Kristoffersen, 2013). From the probabilistic perspective, after O’Hagan (1991), subsequent contributions to the BQ literature focus on computational considerations and include Minka (2000); Rasmussen and Ghahramani (2002); Huszar and Duvenaud (2012); Gunter et al. (2014) and Briol et al. (2015). However, BQ has

not yet been extensively studied on a wide range of statistics problems and we provide such an analysis in Sec. 5.

A discussion of computational techniques to accelerate the matrix inversion can largely be deferred to the Kernel Quadrature literature, where an identical calculation is performed (Sommariva and Vianello, 2006). The standard story applies here - smoother kernels lead to worse matrix conditioning (Schaback, 1995). This motivates us to focus on Sobolev spaces in Sec. 3.2, since these afford greater numerical stability relative to smoother spaces associated with e.g. Gaussian kernels. A survey of some more recent ideas is provided in Supplement C.

Finally, we remark that prior measures other than a GP could be taken as the basis for probabilistic integration and may sometimes be more appropriate (e.g. a Student-t process affords heavier tails for values assumed by the integrand).

2.2 Quadrature Rules in Hilbert Spaces

Below we describe how analysis of the approximation properties of the posterior mean $\hat{\Pi}_{\text{BQ}}$ can be carried out in terms of function spaces, and in particular in terms of reproducing kernel Hilbert space (RKHS; Berlinet and Thomas-Agnan, 2004). This can be considered as necessary preparation for analysis of the full posterior \mathbb{P}_n in Sec. 3.

Consider a Hilbert space \mathcal{H} with inner product $\langle \cdot, \cdot \rangle_{\mathcal{H}}$ and associated norm $\| \cdot \|_{\mathcal{H}}$. \mathcal{H} is said to be an RKHS if there exists a symmetric, positive definite function $k : \mathcal{X} \times \mathcal{X} \rightarrow \mathbb{R}$ or \mathbb{C} , called a *kernel*, that satisfies two properties: **(1)** $k(\cdot, \mathbf{x}) \in \mathcal{H}$ for all $\mathbf{x} \in \mathcal{X}$ and; **(2)** $f(\mathbf{x}) = \langle f, k(\cdot, \mathbf{x}) \rangle_{\mathcal{H}}$ for all $\mathbf{x} \in \mathcal{X}$ and $f \in \mathcal{H}$ (the *reproducing* property). It can be shown that every kernel defines an RKHS and every RKHS admits a unique reproducing kernel (Berlinet and Thomas-Agnan, 2004, Sec. 1.3). For simplicity of presentation we generally assume that functions are real-valued below. In this paper all kernels k are assumed to satisfy $R := \int_{\mathcal{X}} k(\mathbf{x}, \mathbf{x}) \Pi(d\mathbf{x}) < \infty$, which guarantees $f \in L^2(\Pi)$ for all $f \in \mathcal{H}$ (see Prop. 4 in Supplement A).

For an RKHS \mathcal{H} with kernel k we define the *kernel mean* map $\mu(\Pi) : \mathcal{X} \rightarrow \mathbb{R}$ as $\mu(\Pi)(\mathbf{x}) := \Pi[k(\cdot, \mathbf{x})]$, which exists in \mathcal{H} as an implication of the assumption $R < \infty$ (Smola et al., 2007). The name is justified by the fact that for all $f \in \mathcal{H}$ we have:

$$\begin{aligned} \Pi[f] &= \int_{\mathcal{X}} f \, d\Pi = \int_{\mathcal{X}} \langle f, k(\cdot, \mathbf{x}) \rangle_{\mathcal{H}} \Pi(d\mathbf{x}) \\ &= \left\langle f, \int_{\mathcal{X}} k(\cdot, \mathbf{x}) \Pi(d\mathbf{x}) \right\rangle_{\mathcal{H}} = \langle f, \mu(\Pi) \rangle_{\mathcal{H}}. \end{aligned}$$

Here the integral and inner product commute due to the existence of $\mu(\Pi)$ as a Bochner integral over an RKHS (Steinwart and Christmann, 2008, p510). The reproducing property permits an elegant theoretical analysis of quadrature rules, with many quantities of interest tractable analytically in \mathcal{H} . In the language of kernel means, quadrature rules of the form in Eqn. 1 can be written in the form $\hat{\Pi}[f] = \langle f, \mu(\hat{\Pi}) \rangle_{\mathcal{H}}$ where $\mu(\hat{\Pi})$ is the approximation to the kernel mean given by $\mu(\hat{\Pi})(\mathbf{x}) = \hat{\Pi}[k(\cdot, \mathbf{x})]$. For fixed $f \in \mathcal{H}$, the integration error

associated with $\hat{\Pi}$ can then be expressed as

$$\hat{\Pi}[f] - \Pi[f] = \langle f, \mu(\hat{\Pi}) \rangle_{\mathcal{H}} - \langle f, \mu(\Pi) \rangle_{\mathcal{H}} = \langle f, \mu(\hat{\Pi}) - \mu(\Pi) \rangle_{\mathcal{H}}.$$

An upper bound for the error is obtained by applying the Cauchy-Schwarz inequality:

$$|\hat{\Pi}[f] - \Pi[f]| \leq \|f\|_{\mathcal{H}} \|\mu(\hat{\Pi}) - \mu(\Pi)\|_{\mathcal{H}}.$$

The expression above decouples the magnitude (in \mathcal{H}) of the integrand f from the approximation accuracy of the kernel mean. The following sections discuss how quadrature rules can be tailored to target the second term.

2.3 Optimality of Bayesian Quadrature

Denote the dual space of \mathcal{H} , consisting of all bounded linear functionals $\mathcal{H} \rightarrow \mathbb{R}$, by \mathcal{H}^* . Its corresponding norm will be denoted by $\|L\|_{\mathcal{H}^*} = \sup_{f \neq 0} L[f] / \|f\|_{\mathcal{H}}$. The performance of quadrature rules can be quantified by the *worst-case error* (WCE) in the RKHS; $e(\hat{\Pi}; \Pi, \mathcal{H}) := \|\hat{\Pi} - \Pi\|_{\mathcal{H}^*}$. The rate at which this WCE vanishes in n is called the *convergence rate* of the quadrature rule $\hat{\Pi}$. We have shown above that the WCE is characterised as the error in estimating the kernel mean:

Proposition 2. $e(\hat{\Pi}; \Pi, \mathcal{H}) = \|\mu(\hat{\Pi}) - \mu(\Pi)\|_{\mathcal{H}}$.

Minimisation of the WCE is natural and corresponds to solving a least-squares problem in the feature space induced by the kernel; such a solution gives minimax properties in the original space (Ritter, 2000, Prop. III.17). This least-squares formulation is analytically tractable: Letting $\mathbf{w} \in \mathbb{R}^n$ denote the vector of weights $\{w_i\}_{i=1}^n$, $\mathbf{z} \in \mathbb{R}^n$ be a vector such that $z_i = \mu(\Pi)(\mathbf{x}_i)$, and $\mathbf{K} \in \mathbb{R}^{n \times n}$ be the matrix with entries $K_{i,j} = k(\mathbf{x}_i, \mathbf{x}_j)$, we obtain the following equality from direct calculation:

Proposition 3. $e(\hat{\Pi}; \Pi, \mathcal{H})^2 = \mathbf{w}^T \mathbf{K} \mathbf{w} - 2\mathbf{w}^T \mathbf{z} + \Pi[\mu(\Pi)]$.

Several optimality properties for integration in RKHS were collated in Sec. 4.2 of Novak and Woźniakowski (2008). Relevant to this work is that an optimal (i.e. minimax) estimate $\hat{\Pi}$ can, without loss of generality, take the form of a quadrature rule (i.e. of the form $\hat{\Pi}$ in Eqn. 1). To be more precise, any non-linear estimator or so-called *adaptive* estimator, which infers f “on-the-fly”, can be matched in terms of WCE by a (linear) quadrature rule as defined above. (Of course, adaptive quadratures may provide superior performance in the context of a *single* fixed function f , and the minimax result is not true outside the RKHS framework.)

To relate these ideas to BQ, consider the challenge of deriving an optimal quadrature rule, conditional on fixed states $\{\mathbf{x}_i\}_{i=1}^n$, that minimises the WCE over weights $\mathbf{w} \in \mathbb{R}^n$. From Prop. 3, the solution to this convex problem is easily seen to be $\mathbf{w} = \mathbf{K}^{-1} \mathbf{z}$. This shows that the posterior mean in BQ, based on a prior covariance function k , is identical to the optimal quadrature rule in the RKHS whose reproducing kernel is k (Kadane and Wasilkowski, 1985;

Ritter, 2000). (Of course, this is a particular instance of the more general result that Bayes estimates are minimax.) Furthermore, the expression for the WCE in Prop. 3 shows that, for any other quadrature rule $\hat{\Pi}$ based on the same states $\{\mathbf{x}_i\}_{i=1}^n$,

$$\mathbb{V}_n[\Pi[f]] = e(\hat{\Pi}_{\text{BQ}}; \Pi, \mathcal{H})^2 \leq e(\hat{\Pi}; \Pi, \mathcal{H})^2$$

with equality if and only if the BQ weights are employed. Regarding optimality, the problem is thus reduced to selection of states $\{\mathbf{x}_i\}_{i=1}^n$.

Our analysis in this paper is reliant on the (strong) assumption that the integrand f belongs to the RKHS \mathcal{H} ; in particular, this is stronger than the assumption that the integrand f is in the support of the prior measure. Further discussion is provided in Sec. 6.

2.4 Selection of States for Quadrature in RKHS

Whilst BQ provides an analytic expression for quadrature weights, it remains open how best to select states for function evaluation. An optimal choice involves an exploration-exploitation trade-off. First, as states concentrate around regions of high probability mass under Π , the values of the kernel mean vector \mathbf{z} will increase and the posterior variance will decrease; this encourages exploitation. However, as states get closer to each other, the eigenvalues of \mathbf{K} will increase and therefore the eigenvalues of \mathbf{K}^{-1} will decrease, leading to an increase of the posterior variance; this encourages exploration. In earlier work, O’Hagan (1991) used the same states that are employed in classical Gauss-Hermite quadrature. Later Rasmussen and Ghahramani (2002) generated states using MC, calling the approach *Bayesian* MC (BMC). Recent work by Gunter et al. (2014); Briol et al. (2015) selected states using experimental design by targeting posterior variance, both directly and indirectly. We briefly review some of these approaches below.

2.4.1 Monte Carlo Methods

We define a *Monte Carlo* (MC) method to be a quadrature rule based on uniform weights $w_i^{\text{MC}} := 1/n$ and states $\{\mathbf{x}_i\}_{i=1}^n$ that are formally considered as random variables. The simplest of those methods consists of sampling states $\{\mathbf{x}_i^{\text{MC}}\}_{i=1}^n$ independently from Π (Fig. 2, left). For un-normalised densities π , MCMC methods proceed similarly but induce a dependence structure among the $\{\mathbf{x}_i^{\text{MCMC}}\}_{i=1}^n$. We denote these (random) estimators by $\hat{\Pi}_{\text{MC}}$ (when $\mathbf{x}_i = \mathbf{x}_i^{\text{MC}}$) and $\hat{\Pi}_{\text{MCMC}}$ (when $\mathbf{x}_i = \mathbf{x}_i^{\text{MCMC}}$) respectively. Uniformly weighted estimators are well-suited to many challenging integration problems since they provide a dimension-independent convergence rate for the WCE of $O_P(n^{-1/2})$ (Thm. 1 below). They are also widely applicable and straight-forward to analyse; for instance the central limit theorem (CLT) gives that $\sqrt{n}(\hat{\Pi}_{\text{MC}}[f] - \Pi[f]) \rightarrow \mathcal{N}(0, \tau_f^{-1})$ where $\tau_f^{-1} = \Pi[f^2] - \Pi[f]^2$ and the convergence is in distribution. However, the CLT is not well-suited as a measure of *epistemic* uncertainty (i.e. as an explicit model for numerical error) since (i) it is only valid asymptotically, and (ii) τ_f is unknown, depending on the integral $\Pi[f]$ that we are computing.

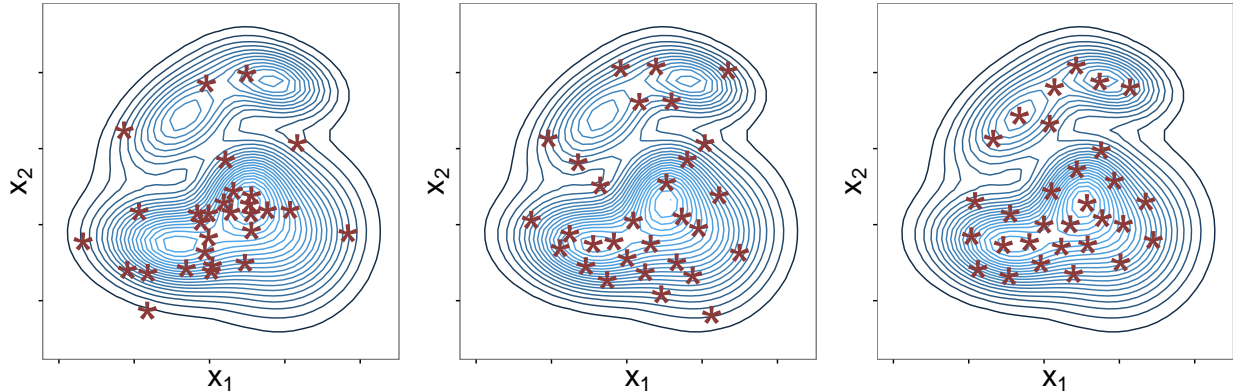


Figure 2: Illustration of states used for quadrature, based on a Gaussian mixture Π . *Left*: Monte Carlo (MC) sampling from Π . *Middle*: A *Sobol sequence*, a specific type of Quasi-MC (QMC) point sequence, mapped to Π . *Right*: States from an experimental design scheme based on the Frank-Wolfe (FW) algorithm. Estimators based on QMC or FW typically outperform estimators based on MC due to their better coverage of Π .

A related class of methods is Quasi Monte Carlo (QMC) (Hickernell, 1998). These methods exploit knowledge of the RKHS \mathcal{H} to spread the states in an efficient, deterministic way over the domain \mathcal{X} (Figure 2, middle). QMC also approximates integrals using a quadrature rule $\hat{\Pi}_{\text{QMC}}[f]$ that has uniform weights $w_i^{\text{QMC}} := 1/n$. These methods benefit from an extensive theoretical literature (Dick and Pillichshammer, 2010). The (in some cases) optimal convergence rates as well as sound statistical properties of QMC have recently led to interest within the statistics community (e.g. Hickernell et al., 2005; Gerber and Chopin, 2015; Oates et al., 2016c).

2.4.2 Experimental Design Schemes

An *Optimal* BQ (OBQ) rule selects states $\{\mathbf{x}_i\}_{i=1}^n$ to globally minimise the posterior variance (equivalent to globally minimising the WCE). Särkka et al. (2016) recently showed that OBQ corresponds to classical quadrature rules (e.g. Gauss-Hermite) for specific choices of covariance function k . Indeed, the average case analysis literature (Ritter, 2000) contains upper and lower bounds for the WCE that map directly onto statements about convergence rates for OBQ as $n \rightarrow \infty$. However OBQ can generally not be implemented; the problem of finding optimal states is in general NP-hard (Schölkopf and Smola, 2002, Sec. 10.2.3).

A more pragmatic approach to select states is using experimental design methods, such as the greedy algorithm sequentially minimising the posterior variance at each iteration. This rule, called *Sequential* BQ (SBQ), is straightforward to implement, e.g. using general-purpose numerical optimisation, and is a probabilistic integration method that is often used in practice (Osborne et al., 2012; Gunter et al., 2014). More sophisticated optimisation algorithms have also been used to select states. For example, in the QMC literature Nuyens and Cools (2006) framed the construction of lattice rules as an optimisation problem, in

the least-squares approximation literature Maday et al. (2009) proposed a greedy algorithm to generate approximate Fekete states. In the Empirical Interpolation literature Eftang and Stamm (2012) proposed adaptive procedures that iteratively divide the domain of integration into sub-domains. In the BQ literature Briol et al. (2015) used conditional gradient algorithms (also called Frank-Wolfe algorithms) that, in effect, produce a linear approximation to the posterior variance based on its derivative (Figure 2, right).

However there are a number of weaknesses with such experimental design schemes that motivate the present work. Firstly, they do not possess the computational efficiency that we have come to expect from advanced MCMC and QMC methods. Secondly, they do not scale well to high-dimensional settings due to the need to repeatedly solve high-dimensional optimisation problems and have no theoretical guarantees of optimality of design.

3 Methods

This section presents novel theoretical results on probabilistic integration schemes, based on the output of MCMC and QMC algorithms, for application in computational statistics. Sec. 3.1 introduces the proposed approach, while Sec. 3.2 establishes theoretical properties.

3.1 Bayesian MCMC and Bayesian QMC

The sampling methods of MCMC (Robert and Casella, 2013) and, to a lesser extent, QMC (Dick and Pillichshammer, 2010) are central to much of contemporary statistical computation. Here we pursue the idea of using these methods to generate states for BQ, with the aim to exploit BQ within statistical applications to account for the possible impact of numerical error on inferences. More precisely, this paper studies the two-step procedure that first uses MCMC or QMC in order to select states and then assigns BQ (minimax) weights to those states. In the MCMC case it is possible that two states $\mathbf{x}_i = \mathbf{x}_j$ are identical, for example in a Metropolis-Hastings chain with a positive probability of rejection. To prevent the kernel matrix \mathbf{K} from becoming singular, one of these states should be discarded (this is justified since the information contained in function evaluations $f_i = f_j$ is the same). Thus we define

$$\begin{aligned}\hat{\Pi}_{\text{BMCMC}}[f] &:= \sum_{i=1}^n w_i^{\text{BQ}} f(\mathbf{x}_i^{\text{MCMC}}) \\ \hat{\Pi}_{\text{BQMC}}[f] &:= \sum_{i=1}^n w_i^{\text{BQ}} f(\mathbf{x}_i^{\text{QMC}})\end{aligned}$$

This two-step procedure requires no modification to existing MCMC or QMC sampling schemes; this can hence be seen as a post-processing scheme. Moreover each estimator is associated with a full posterior probability distribution described in Sec. 2.1.

A moment is taken to emphasise that the apparently simple act of re-weighting MCMC samples can have a dramatic improvement on convergence rates in estimation. This is a well-known fact from the Kernel Quadrature literature and we point the interested reader

toward Sommariva and Vianello (2006). Our aim is not to provide methods for efficient point estimation. Rather, our primary aim is to explore the suitability of BQ as a statistical model for numerical integration error.

To date we are not aware of any previous use of BMCMC, presumably due to analytic intractability of the kernel mean; we provide one possible solution in the following sections. BQMC has been described by Hickernell et al. (2005); Marques et al. (2013); Särkka et al. (2016). To the best of our knowledge there has been no theoretical analysis of the posterior distributions associated with either method. The goal of the next section is to establish theoretical guarantees for consistency of these point estimators and contraction of their associated posterior distributions.

3.2 Theoretical Results

In this section we present the main theoretical properties of BMC, BMCMC and BQMC. Our primary focus here is on integration in Sobolev spaces. This is due to the fact that numerical conditioning is known to be better behaved in these spaces compared to spaces of smoother functions (Schaback, 1995). In addition, there is an elegant characterisation of these spaces in terms of the number of (weak) derivatives of the integrand. Thus from a practical perspective, it is straight-forward, at least in principle, to select a suitable space of functions.

3.2.1 Bayesian Monte Carlo

As a baseline, we begin by noting a general result for MC estimation. This requires a slight strengthening of the assumption on the kernel: $k_{\max} := \sup_{\mathbf{x} \in \mathcal{X}} k(\mathbf{x}, \mathbf{x})^{1/2} < \infty$. This implies that f is bounded on \mathcal{X} . Recall that in MC, states are sampled independently from Π and weighted uniformly. For MC estimators, Lemma 33 of Song (2008) show that, under $k_{\max} < \infty$, the WCE converges in probability at the classical root- n rate:

Lemma 1 (MC Methods). $e(\hat{\Pi}_{MC}; \Pi, \mathcal{H}) = O_P(n^{-1/2})$.

While MC is something of a straw-man, it is nevertheless widely used in statistical applications, in part due to its weak assumption of $f \in L^2(\Pi)$.

Turning now to BMC, we will obtain rates for the WCE that improve on the MC rate in certain cases. Consider the compact manifold $\mathcal{X} = [0, 1]^d$, with Π uniform on \mathcal{X} . Write \mathfrak{F} for the Fourier transform operator and define the *Sobolev* space $\mathcal{H}_\alpha := \{f \in L^2(\Pi) \text{ such that } \|f\|_{\mathcal{H}_\alpha} < \infty\}$, equipped with the norm $\|f\|_{\mathcal{H}_\alpha} := \|\mathfrak{F}^{-1}[(1 + \|\boldsymbol{\xi}\|_2^2)^{\alpha/2} \mathfrak{F}[f]]\|_2$. Here α is the *order* of the space. It can be shown that \mathcal{H}_α is the set of functions f whose weak derivatives $(\partial x_1)^{u_1} \dots (\partial x_d)^{u_d} f$ exist in $L^2(\Pi)$ for $u_1 + \dots + u_d \leq \alpha$ (Triebel, 1992).

To emphasise the level of generality here: a function with derivatives up to order α belongs to \mathcal{H}_α and satisfies our theoretical conclusions below. Derivative counting can hence be a principled approach for practitioners to choose a kernel. In fact, our results are more general than Sobolev spaces, in the sense that any radial kernel $k(\mathbf{x}, \mathbf{x}') = \phi(\mathbf{x} - \mathbf{x}')$ whose Fourier transform decays at a rate $\mathfrak{F}[\phi(\boldsymbol{\xi})] \asymp (1 + \|\boldsymbol{\xi}\|_2^2)^{-\alpha}$, where $\alpha > d/2$, (e.g. Matérn

kernel) induces an RKHS that is norm-equivalent to \mathcal{H}_α (Wendland, 2005, Cor. 10.13). (Two norms $\|\cdot\|$, $\|\cdot\|'$ on a vector space \mathcal{H} are *equivalent* when there exists constants $0 < C_1, C_2 < \infty$ such that for all $h \in \mathcal{H}$ we have $C_1\|h\| \leq \|h\|' \leq C_2\|h\|$.) All results below apply to RKHS \mathcal{H} that are norm-equivalent to \mathcal{H}_α , permitting flexibility in the choice of kernel. Specific examples of kernels are provided in Sec. 4.2.

Our analysis below is based on the scattered data approximation literature (Wendland, 2005). A minor assumption, that enables us to simplify the presentation of results below, is that the set $X = \{\mathbf{x}_i\}_{i=1}^n$ may be augmented with a finite, pre-determined set $Y = \{\mathbf{y}_i\}_{i=1}^m$ where m does not increase with n . Clearly this has no bearing on asymptotics. Define $I_D = [\Pi[f] - D, \Pi[f] + D]$ to be an interval of radius D centred on the true value of the integral. We will be interested in $\mathbb{P}_n[I_D^c]$, the posterior mass on $I_D^c = \mathbb{R} \setminus I_D$, in particular how quickly this mass vanishes as the number n of function evaluations is increased.

Theorem 1 (BMC in \mathcal{H}_α). *Let \mathcal{H} be norm-equivalent to \mathcal{H}_α , where $\alpha \in \mathbb{N}$ and $\alpha > d/2$. Then*

$$e(\hat{\Pi}_{BMC}; \Pi, \mathcal{H}) = O_P(n^{-\alpha/d+\epsilon})$$

and

$$\mathbb{P}_n[I_D^c] = o_P(\exp(-Cn^{2\alpha/d-\epsilon})),$$

where $\epsilon > 0$ can be arbitrarily small.

The proof follows as a special case of Thm. 2 below. This result shows the posterior distribution is well-behaved; probability mass concentrates on the true solution as n increases. Hence, if our prior is well-specified (see Sec. 4.1), the posterior distribution provides valid uncertainty quantification over the solution of the integral as a result of performing a finite number n of function evaluations. It is also shown that accuracy is significantly improved, relative to MC, in settings where it is reasonable to assume a level $\alpha > d/2$ of smoothness on the integrand. An information-theoretic lower bound on the WCE in this setting is $O_P(n^{-\alpha/d-1/2})$ (Novak and Woźniakowski, 2010). Thus BMC is at most one MC rate away from being optimal. Our proof does not show whether or not BMC is optimal; we explore this empirically later.

Bach (2015) obtained a similar result for fixed n and specific importance sampling distribution (often intractable in practice); his analysis does not directly imply our asymptotic results and *vice versa*.

3.2.2 Bayesian Markov Chain Monte Carlo

The analysis of BMCMC generalises that for BMC, with additional technical detail required to account for possible dependence of the states. Below the measure Π will be assumed to admit a density with respect to a reference measure σ on $(\mathcal{X}, \mathcal{B})$, denoted by $\pi : \mathcal{X} \rightarrow [0, \infty)$. Here we present the most compact statement of the result, which can be generalised in several directions as described in the text below:

Theorem 2 (BMCMC in \mathcal{H}_α). *Take $\mathcal{X} = [0, 1]^d$, with σ the Lebesgue measure. Suppose π is bounded away from zero on \mathcal{X} . Let \mathcal{H} be norm-equivalent to \mathcal{H}_α where $\alpha > d/2$, $\alpha \in \mathbb{N}$.*

Suppose states are generated by a reversible, uniformly ergodic Markov chain that targets Π . Then

$$e(\hat{\Pi}_{\text{BMCMC}}; \Pi, \mathcal{H}) = O_P(n^{-\alpha/d+\epsilon})$$

and

$$\mathbb{P}_n[I_D^c] = o_P(\exp(-Cn^{2\alpha/d-\epsilon})),$$

where $\epsilon > 0$ can be arbitrarily small.

The results for BMC and BMCMC point estimation demonstrate the improved accuracy of kernel-based quadrature relative to MC, supporting its use in the case of expensive integration problems. It would not be practical in settings where the number n of MCMC samples is large, due to the $O(n^3)$ cost, however in such settings the contribution from numerical error is likely to be negligible. As a default STAN stores $n = 4000$ samples; this is about the limit for BQ on a modern computer without recourse to more sophisticated linear algebraic methods. Our theoretical results show that the posterior distribution provides effective (if not best-possible) uncertainty quantification at a rate that exceeds the CLT.

Both Theorems 1 and 2 can be easily generalised in several directions. Firstly, we can consider more general domains \mathcal{X} . Specifically, the scattered data approximation bounds that are used in our proof apply to any compact domain $\mathcal{X} \subset \mathbb{R}^d$ that satisfies an *interior cone condition* (Wendland, 2005, p.28). In addition, we can consider other spaces \mathcal{H} , such as the RKHS obtained from popular Gaussians, multi-quadrics, inverse multi-quadrics and thin-plate splines kernels. For example, an extension of Thm. 2 shows that the Gaussian kernel leads to exponential rates for the WCE and super-exponential rates for posterior contraction. We refer the interested reader to the extended results available in Supplement B.

3.2.3 Bayesian Quasi Monte Carlo

The previous section showed that BMC is close to rate-optimal in \mathcal{H}_α . BQMC allows one to obtain optimal rates for \mathcal{H}_α . To avoid repetition, here we consider more interesting spaces of functions whose *mixed* partial derivatives exist, for which even faster convergence rates can be obtained using BQMC methods. To formulate BQMC we must posit an RKHS *a priori* (i.e. specifying all kernel parameters) and consider collections of states $\{\mathbf{x}_i^{\text{QMC}}\}_{i=1}^n$ that constitute a QMC point set tailored to that space.

As before, consider the compact manifold $\mathcal{X} = [0, 1]^d$ with Π be uniform on \mathcal{X} . Define the Sobolev space of *dominating mixed smoothness* $\mathcal{S}_\alpha := \{f \in L^2(\Pi) \text{ such that } \|f\|_{\mathcal{S}, \alpha} < \infty\}$, equipped with the norm $\|f\|_{\mathcal{S}, \alpha} := \|\mathfrak{F}^{-1}[\prod_{i=1}^d (1 + \xi_i^2)^{\alpha/2} \mathfrak{F}[f]]\|_2$. Here α is the *order* of the space. It can be shown that \mathcal{S}_α is the set of functions f whose weak derivatives $(\partial x_1)^{u_1} \dots (\partial x_d)^{u_d} f$ exist in $L^2(\Pi)$ for $u_i \leq \alpha$, $i = 1, \dots, d$. To build intuition, note that \mathcal{S}_α is norm-equivalent to the RKHS generated by a tensor product of Matérn kernels (Sickel and Ullrich, 2009), or indeed a tensor product of any other univariate Sobolev space -generating kernel. Observe that $\mathcal{S}_\alpha \subset \mathcal{H}_\alpha$, but not *vice versa*.

For a specific space such as \mathcal{S}_α , we seek an appropriate QMC point set. The *higher-order digital* $(t, \alpha, 1, \alpha m \times m, d)$ -net construction is an example of a QMC point set for \mathcal{S}_α .

Intuitively, digital nets aim to spread states evenly across the domain \mathcal{X} in order to obtain efficient (un-weighted) quadrature rules; we refer the reader to Dick and Pillichshammer (2010) for details of this construction, which goes beyond the scope of this paper.

Theorem 3 (BQMC in \mathcal{S}_α). *Let \mathcal{H} be norm-equivalent to \mathcal{S}_α , where $\alpha \geq 2$, $\alpha \in \mathbb{N}$. Suppose states are chosen according to a higher-order digital $(t, \alpha, 1, \alpha m \times m, d)$ net over \mathbb{Z}_b for some prime b where $n = b^m$. Then*

$$e(\hat{\Pi}_{BQMC}; \Pi, \mathcal{H}) = O(n^{-\alpha+\epsilon})$$

and

$$\mathbb{P}_n[I_D^c] = o(\exp(-Cn^{2\alpha-\epsilon})),$$

where $\epsilon > 0$ can be arbitrarily small.

This is the optimal rate for any deterministic quadrature rule in \mathcal{S}_α (Dick, 2011). These results should be understood to hold on the sub-sequence $n = b^m$, as QMC methods do not in general give guarantees for all $n \in \mathbb{N}$. It is not clear how far this result can be generalised, in terms of Π and \mathcal{X} , compared to results for B(MC)MC, since this would require the use of a different QMC point set. The case of QMC for the Gaussian kernel was recently studied in Fasshauer et al. (2012); the results therein for Smolyak point sets imply (exponential) convergence and contraction rates for BQMC in via the same arguments that we have made explicit for the space \mathcal{S}_α in this section.

3.2.4 Summary

This concludes the presentation of our main theoretical results. We have focused on establishing optimal and near-optimal rates of convergence and contraction for BMC, BMCMC and BQMC in general Sobolev space settings. These results are essential since they establish the sound properties of the probability measure \mathbb{P}_n , which is shown to contract to the truth as more evaluations are made of the test function. Moreover, kernel quadrature rules are shown to be asymptotically efficient relative to the simple MC estimator that is widely used in statistical applications. An interesting question is whether kernel quadrature rules ought to be more widely adopted, irrespective of the probabilistic semantics that are under investigation in this paper, given that most integrands that occur in computational statistics exhibit some non-trivial degree of smoothness.

Before exploring these estimators on concrete examples, the next section discusses methodological considerations relevant to the implementation of these methods, including specification of the prior distribution.

4 Implementation

So far we have established sound theoretical properties for BMCMC and BQMC under the assumption that the prior is well-specified. Unfortunately, prior specification complicates

the situation in practice since, given a test function f , there are an infinity of RKHS that f belongs to and the specific choice of this space will impact upon estimator performance. In particular, the scale of the prior will have a significant bearing on the suitability of the uncertainty quantification and could lead to over-confident inferences, which mitigates the advantages of the probabilistic formalism. Below we discuss this, along with a number of other practical considerations.

4.1 Prior Specification

The theoretical results above deal with asymptotic behaviour, but a question remains over the choice of prior in relation to the performance afforded for finite n . i.e. whether the scale of the posterior uncertainty provides an accurate reflection of the actual numerical error in practice. For BQ, this corresponds to the well-studied problem of “choosing the kernel” that is itself a research area in machine learning (Duvenaud, 2014).

At this point we highlight a distinction between B(MC)MC and both BQMC and experimental design BQ schemes; for the former the choice of states does not depend on the RKHS. For B(MC)MC this allows for the possibility of off-line specification of the kernel after evaluations of the integrand have been obtained, whereas for alternative methods the kernel must be stated up-front. Our discussion below therefore centres on prior specification in relation to B(MC)MC, where statistical techniques offer several possibilities.

Consider a parametric kernel $k(\mathbf{x}, \mathbf{x}'; \theta_l, \theta_s)$, with a distinction drawn here between *scale parameters* θ_l and *smoothness parameters* θ_s . The former are defined as parametrising the norm on \mathcal{H} , whereas the latter affect the set \mathcal{H} itself. Calibration based on data can only be successful in the absence of acute sensitivity to these parameters. For scale parameters a wide body of empirical evidence demonstrates that this is usually not a concern, but this is not true for smoothness parameters. Indeed, selection of smoothness is an active area of theoretical research (e.g. Szabó et al., 2015). In many cases it is possible to elicit a smoothness parameter from physical or mathematical considerations, such as the number of derivatives that the integrand is known to possess. Our attention below is therefore focused on calibrating kernel scale parameters; in the spirit that hyper-priors cannot be applied in infinite regress, at some point the practitioner must input concrete information. Several possible approaches are discussed below in relation to their suitability for BQ.

Marginalisation A natural approach, from a Bayesian perspective, is to set a prior $p(\theta_l)$ on parameters θ_l and then to marginalise over θ_l to obtain a posterior over $\Pi[f]$. Recent results for the Gaussian kernel establish minimax optimal adaptive rates in $L^2(\Pi)$ for this approach, including in the practically relevant setting where Π is supported on a low-dimensional sub-manifold of the ambient space \mathcal{X} (Yang and Dunson, 2013). However, the act of marginalisation itself involves an intractable integral. While the computational cost of evaluating this integral will often be dwarfed by that of the integral $\Pi[f]$ of interest, marginalisation nevertheless introduces an additional undesirable computational challenge that might require several approximations (e.g. Osborne, 2010).

Cross-Validation One approach to kernel choice would be k -fold cross-validation, where the data $\{\mathbf{x}_i\}_{i=1}^n$ are split into k subsets, $k-1$ subsets being used to elicit the parameters and the last subset used to assess performance. However, cross-validation performs poorly when the number n of data is small, since the data needs to be further reduced into training and test sets. The performance estimates are also known to have large variance in those cases (Chap. 5 of Rasmussen and Williams, 2006). Since the small n scenario is one of our primary settings of interest for BQ, we felt that cross-validation was unsuitable for use in applications below. Here the computational cost of re-fitting many GPs may also be undesirable.

Empirical Bayes An alternative to the above approaches is *empirical Bayes* (EB) selection of scale parameters, choosing θ_l to maximise the log-marginal likelihood of the data $f(\mathbf{x}_i)$, $i = 1, \dots, n$ (Sec. 5.4.1 of Rasmussen and Williams, 2006). EB has the advantage of providing an objective function that is easier to optimise relative to cross-validation. However, we also note that EB can lead to over-confidence when n is very small, since the log-marginal likelihood is usually multimodal, and the full irregularity of the test function has yet to be uncovered (Szabó et al., 2015). To overcome this, one can incorporate prior beliefs on the scale parameters via a prior $p(\theta_l)$ as with marginalisation, that forms an additional term in the objective function and can act to bias θ_l away from small values.

For the remainder, we chose to focus on the EB approach. Empirical results support the use of EB here, though we do not claim that this is in any sense an optimal strategy and we invite further investigation.

4.2 Tractable and Intractable Kernel Means

BQ requires that the kernel mean $\mu(\Pi)(\mathbf{x}) = \Pi[k(\cdot, \mathbf{x})]$ is available in closed-form. This is the case for several kernel-distribution pairs (k, Π) and a subset of these pairs are recorded in Table 1. These pairs are widely applicable; for example the gradient-based kernel in Oates et al. (2016a,b) provides a closed-form expression for the kernel mean whenever the gradient $\partial \log \pi(\mathbf{x})$ is available, and is compatible with un-normalised densities that arise in MCMC sampling.

In the event that the kernel-distribution pair (k, Π) of interest does not lead to a closed-form kernel mean, it is sometimes possible to determine another kernel-density pair (k', Π') for which $\Pi'[k'(\cdot, \mathbf{x})]$ is available and such that (i) Π is absolutely continuous with respect to Π' , so that the Radon-Nikodym derivative $d\Pi/d\Pi'$ exists, and (ii) $f d\Pi/d\Pi' \in \mathcal{H}(k')$. Then one can construct an importance sampling estimator

$$\Pi[f] = \int_{\mathcal{X}} f d\Pi = \int_{\mathcal{X}} f \frac{d\Pi}{d\Pi'} d\Pi' = \Pi' \left[f \frac{d\Pi}{d\Pi'} \right]$$

and proceed as above (O'Hagan, 1991).

One side-contribution of this paper is to provide a novel and generic approach to accommodate intractability of the kernel mean in BQ. We propose *approximate Bayesian Quadrature*, ${}_a\hat{\Pi}_{\text{BQ}}$, where the weights ${}_a\mathbf{w}_{\text{BQ}} = \mathbf{K}^{-1} {}_a\Pi[\mathbf{k}(X, \cdot)]$ are an approximation to

\mathcal{X}	Π	k	Reference
$[0, 1]^d$	Unif(\mathcal{X})	Wendland TP	Oates et al. (2016c)
$[0, 1]^d$	Unif(\mathcal{X})	Matérn Weighted TP	Sec. 5.2.3
$[0, 1]^d$	Unif(\mathcal{X})	Exponentiated Quadratic	Use of error function
\mathbb{R}^d	Mixt. of Gaussians	Exponentiated Quadratic	O’Hagan (1991)
\mathbb{S}^d	Unif(\mathcal{X})	Gegenbauer	Sec. 5.2.4
Arbitrary	Unif(\mathcal{X}) / Mixt. of Gauss.	Trigonometric	Integration by parts
Arbitrary	Unif(\mathcal{X})	Splines	Wahba (1990)
Arbitrary	Known moments	Polynomial TP	Briol et al. (2015)
Arbitrary	Known $\partial \log \pi(\mathbf{x})$	Gradient-based Kernel	Oates et al. (2016a,b)

Table 1: A non-exhaustive list of distribution Π and kernel k pairs that provide a closed-form expression for the kernel mean $\mu(\Pi)(\mathbf{x}) = \Pi[k(\cdot, \mathbf{x})]$ and the initial error $\Pi[\mu(\Pi)]$. Here TP refers to the tensor product of one-dimensional kernels.

the optimal BQ weights based on an approximation ${}_a\Pi[\mathbf{k}(X, \cdot)]$ of the kernel mean. The following lemma demonstrates that we can bound the contribution of this error and inflate our posterior $\mathbb{P}_n \mapsto {}_a\mathbb{P}_n$ to reflect the additional uncertainty due to the approximation, so that an uncertainty quantification is still provided. The statistical foundations of such an approach, where updating of belief occurs via an approximation to the likelihood function, are discussed in the recent work of Bissiri et al. (2016).

Lemma 2 (Approximate kernel mean). *Consider an auxiliary approximation ${}_a\Pi$ to Π of the form ${}_a\Pi = \sum_{j=1}^m {}_aw_j\delta(\cdot - {}_a\mathbf{x}_j)$, a quadrature rule based on weights ${}_aw_j$ and states ${}_a\mathbf{x}_j$. Then BQ can be performed analytically with respect to ${}_a\Pi$; denote this estimator by ${}_a\hat{\Pi}_{BQ}$. It follows that $e({}_a\hat{\Pi}_{BQ}; \Pi, \mathcal{H})^2 \leq e(\hat{\Pi}_{BQ}; \Pi, \mathcal{H})^2 + \sqrt{n}e({}_a\Pi; \Pi, \mathcal{H})^2$.*

Under this method, the posterior variance ${}_a\mathbb{V}_n[\Pi[f]] := e({}_a\hat{\Pi}_{BQ}; \Pi, \mathcal{H})^2$ cannot be computed in closed-form, but computable upper-bounds can be obtained and these can then be used to propagate numerical uncertainty through the remainder of our statistical task. Further discussion is provided in Supplement C.4.

We pause to briefly discuss the utility and significance of such an approach. Obviously, the new approximation problem (that of approximating Π with ${}_a\Pi$) could also be computed with a BQ method, and we may hence end up in an “infinite regress” scenario (O’Hagan, 1991), where the new kernel mean is itself unknown and so on. However, one level of approximation may be enough in many scenarios. Indeed, by using standard Monte Carlo to select $\{{}_ax_j\}_{j=1}^m$ and increasing m sufficiently faster than n , the error term $\sqrt{n}e({}_a\Pi; \Pi, \mathcal{H})^2$ can be made to vanish faster than $e(\hat{\Pi}_{BQ}; \Pi, \mathcal{H})$ and hence the WCE for ${}_a\hat{\Pi}_{BQ}$ will be asymptotically identical to the WCE for the (intractable) exact BQ estimator $\hat{\Pi}_{BQ}$. Therefore, it will be reasonable to expend computational effort on raising m in settings where evaluation of the integrand constitutes the principal computational. This is because approximating the kernel mean only requires sampling m times, but does not require us to evaluate the integrand.

5 Results

Above we have provided theoretical support for the use of BQ in statistical computation, with a focus on obtaining coherent quantification of the uncertainty due to numerical error. The aims of the following section are two-fold; (i) to validate the preceding theoretical analysis and (ii) to explore the applicability and effectiveness of probabilistic integrators in a range of challenging integration problems arising in contemporary statistical applications.

To be clear, we are not aiming to achieve accurate point estimation at low computational cost. This is a well-studied problem that reaches far beyond the methods of this paper. Indeed, much about point estimation is known from the Kernel Quadrature literature. Rather, we are aiming to assess the suitability of the probabilistic description for numerical error that is provided by these probabilistic integrators, motivated by the case where numerical error is most problematic; expensive integrands .

5.1 Assessment of Uncertainty Quantification

The empirical performance of Bayesian Quadrature will be extensively studied in Sec. 5.2. Instead, our focus below is on the quality of uncertainty quantification and, in particular, the performance of the EB prior specification. Our motivation is expensive integrands, but to perform assessment in a controlled environment we considered inexpensive test functions of varying degrees of irregularity, whose integrals can be accurately approximated by brute force, these included an “easy” test function $f_1(\mathbf{x}) = \exp(\sin(5\|\mathbf{x}\|_2)^2 - \|\mathbf{x}\|_2^2)$ and a “hard” test function $f_2(\mathbf{x}) = \exp(\sin(20\|\mathbf{x}\|_2)^2 - \|\mathbf{x}\|_2^2)$. The “hard” test function is highly variable and will hence be more difficult to approximate (see Fig. 3). One realisation of states $\{\mathbf{x}_i\}_{i=1}^n$ generated independently and uniformly over $\mathcal{X} = [-5, 5]^d$ (initially $d = 1$) was used to estimate the $\Pi[f_i]$. We work in an RKHS characterised by tensor products of Matérn kernels

$$k_\alpha(\mathbf{x}, \mathbf{x}') = \lambda^2 \prod_{i=1}^d \frac{2^{1-\alpha}}{\Gamma(\alpha)} \left(\frac{\sqrt{2\alpha}|x_i - x'_i|}{\sigma^2} \right)^\alpha K_\alpha \left(\frac{\sqrt{2\alpha}|x_i - x'_i|}{\sigma^2} \right),$$

where K_α is the modified Bessel function of the second kind. Closed-form kernel means exist in this case for $\alpha = p + 1/2$ whenever $p \in \mathbb{N}$. In this set-up, EB was used to select the length-scale parameter $\sigma \in (0, \infty)$ of the kernel, while magnitude parameter was initially fixed at $\lambda = 1$ and the smoothness parameter was at $\alpha = 7/2$ (note all test functions will be in the space \mathcal{H}_α for any $\alpha > 0$ and there is a degree of arbitrariness in this selection).

Results are shown in Fig. 3. Error-bars are used to denote the 95% posterior credible regions for the value of the integral and we also display the values $\hat{\sigma}_n$ selected for σ by EB at each sample size n . The values for $\hat{\sigma}_n$ appear to converge rapidly as $n \rightarrow \infty$; this is encouraging but we emphasise that we do not provide theoretical guarantees for EB in this work. On the negative side, if the prior is not well-specified, over-confidence is possible at small values of n . Indeed, the BQ posterior will be over-confident under EB, since in the absence of evidence to the contrary, EB selects large values for σ that correspond to more regular functions; this is most evident in the “hard” case. Results for varying dimension

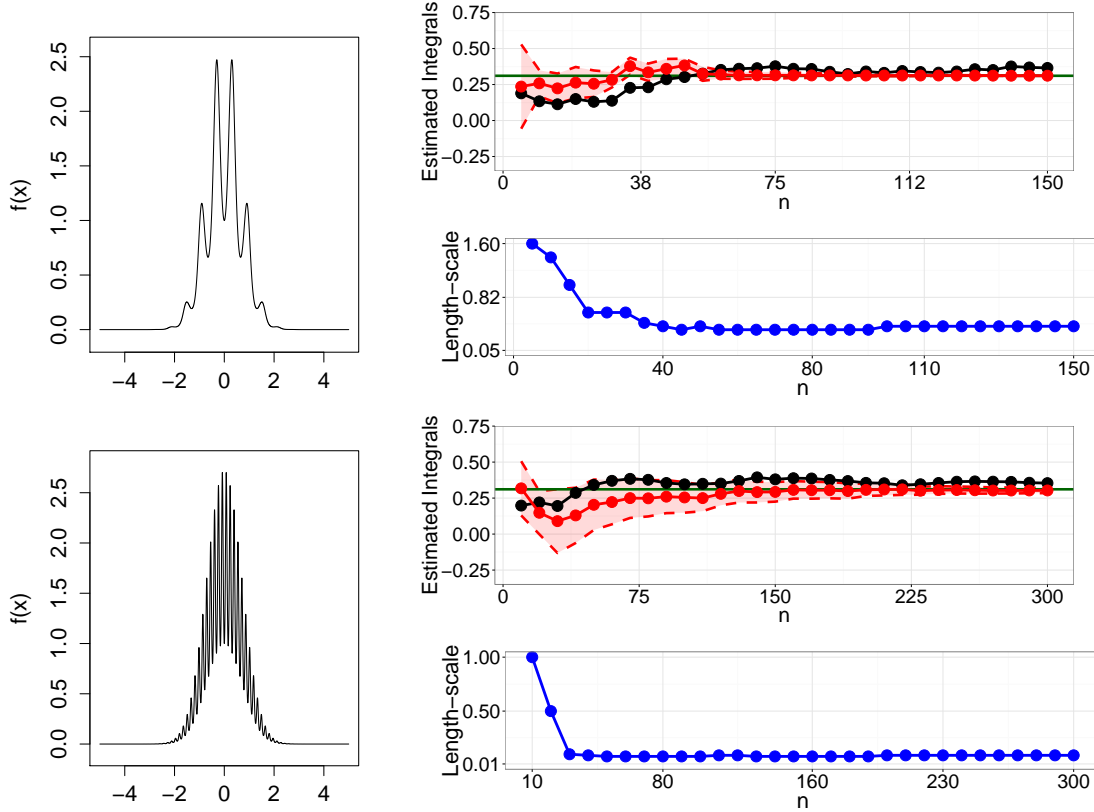


Figure 3: Evaluation of uncertainty quantification provided by empirical Bayes (EB). *Left:* The test functions f_1 (top), f_2 (bottom) in $d = 1$ dimension. *Right:* Solutions provided by Monte Carlo (MC; black) and Bayesian MC (BMC; red), for one typical realisation. BMC was based on a Matérn kernel of order $\alpha = 7/2$. 95% credible regions are shown for BMC and the green horizontal line gives the true value of the integral. The blue curve gives the corresponding lengthscale parameter selected by EB.

d are provided in Supplement D.1. We also point out that optimising over both (σ, λ) is possible, but this is a noticeably harder problem and will usually require a larger number of evaluations to provide good uncertainty quantification. Extended results for this case can be found also be found in Supplement D.1.

For each test function it is seen that the credible sets typically contain the true value $\Pi[f]$. To compute coverage frequencies for $100(1 - \gamma)\%$ credible regions, at sample size n , the process was repeated over many realisations of the states $\{\mathbf{x}_i\}_{i=1}^n$, shown in Fig. 4. It may be seen that the uncertainty quantification provided by EB is slightly loose for the easier function f_1 , whilst being very accurate for the more complicated functions such as f_2 . As expected, we also observed that the coverage improves for larger values of n . Performance was subsequently investigated for varying smoothness α and dimension d , with results shown in Supplement D.1.

Finally, to understand whether theoretical contraction rates are realised in practice, we

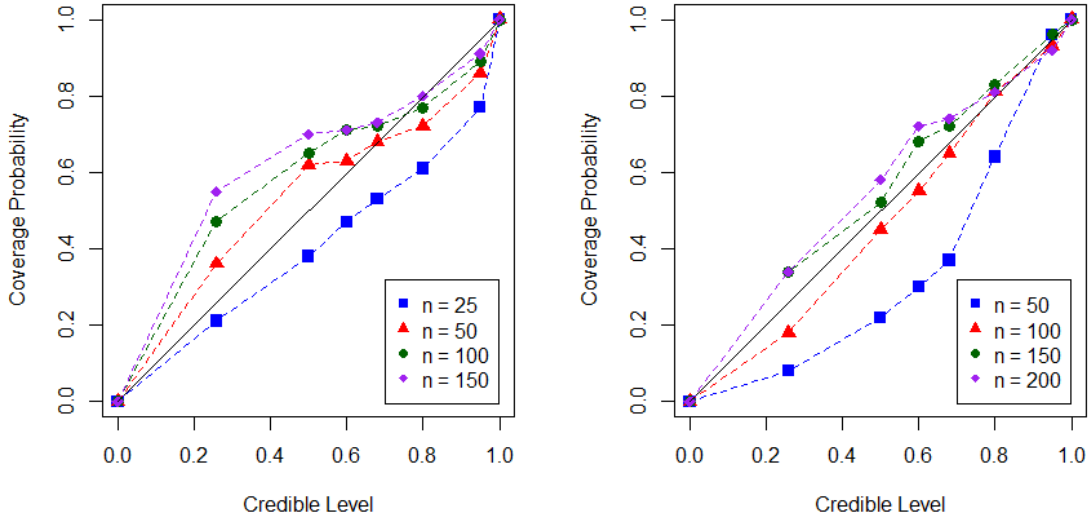


Figure 4: Evaluation of uncertainty quantification provided by empirical Bayes. Coverage frequencies $C_{n,\alpha}$ (computed from 100 realisations) were compared against notional $100(1 - \alpha)\%$ Bayesian credible regions for varying level α and number of observations n . Curves on the upper-left quadrant show conservative credible intervals whilst curve on the lower-right quadrant show over-confident credible intervals. *Left*: “Easy” test function f_1 . *Right*: “Hard” test function f_2 .

note (in the absence of EB) that the posterior variance is independent of the integrand and may be plotted as a function of the number n of data. Results in Supplement D.2 demonstrate that theoretical convergence rates are observed in practice; indeed convergence appears to be slightly faster than the upper bounds we provided. At large values of n numerical instability is observed; this is a well-known computational issue for kernel quadrature and a more complete theoretical and empirical investigation of numerical stability is provided in Supplement C.3.

The results on test functions provided in this section therefore demonstrate that adequate uncertainty quantification is possible using a BQ approach. In particular, we have shown that our calibration approach provided credible bounds with good frequentist coverage after an initial number of samples is obtained. The following section discusses the utility of the probability distribution \mathbb{P}_n in the context of several statistical inference tasks.

5.2 Case Studies

For the remainder we explore possible roles for BMCMC and BQMC in contemporary statistical applications. To this end, we undertook four distinct case studies, carefully chosen to highlight both the strengths and the weaknesses of the probabilistic approach to integration. Brief critiques of each study are presented below, the full details of which can be found in

the accompanying materials (see Supplement E).

5.2.1 Case Study #1: Model Selection via Thermodynamic Integration

Consider the problem of selecting a single best model among a set $\{\mathcal{M}_1, \dots, \mathcal{M}_M\}$, based on data \mathbf{y} assumed to arise from a true model in this set. The Bayesian solution, assuming a uniform prior over models, is to select the *maximum a posteriori* (MAP) model \mathcal{M}_k where $k := \arg \max_{i \in \{1, \dots, M\}} p(\mathcal{M}_i | \mathbf{y})$. We focus on the case with uniform prior on models $p(\mathcal{M}_i) = 1/M$, and this problem hence reduces to finding the largest marginal likelihood $p_i = p(\mathbf{y} | \mathcal{M}_i)$. These terms are usually intractable integrals over the parameters $\boldsymbol{\theta}_i$ associated with model \mathcal{M}_i . One widely-used approach to model selection is to estimate each p_i in turn, say by \hat{p}_i , then to take the maximum of the \hat{p}_i over $i \in \{1, \dots, M\}$. In particular, thermodynamic integration is an effective approach to approximation of marginal likelihoods p_i for individual models (Gelman and Meng, 1998; Friel and Pettitt, 2008).

In many contemporary applications the MAP model is not well-identified, for example in variable selection where there are very many candidate models. Then, the MAP becomes sensitive to numerical error in the \hat{p}_i , since an incorrect model \mathcal{M}_i , $i \neq k$ can be assigned an overly large value of \hat{p}_i due to numerical error, in which case it could be selected in place of the true MAP model. Below we explore the potential to exploit probabilistic integration to surmount this problem.

Thermodynamic Integration To simplify notation below we consider computation of p_i and suppress dependence on the index i corresponding to model \mathcal{M}_i . Denote the parameter space by Θ . For $t \in [0, 1]$ (an *inverse temperature*) define the *power posterior* Π_t , a distribution over Θ with density $\pi_t(\boldsymbol{\theta}) \propto p(\mathbf{y} | \boldsymbol{\theta})^t p(\boldsymbol{\theta})$. The thermodynamic identity is formulated as a double integral:

$$\log p(\mathbf{y}) = \int_0^1 dt \int_{\Theta} \log p(\mathbf{y} | \boldsymbol{\theta}) \Pi_t[d\boldsymbol{\theta}].$$

The thermodynamic integral can be re-expressed as

$$\log p(\mathbf{y}) = \int_0^1 g(t) dt, \quad g(t) = \int_{\Theta} f(\boldsymbol{\theta}) \Pi_t[d\boldsymbol{\theta}],$$

where $f(\boldsymbol{\theta}) = \log p(\mathbf{y} | \boldsymbol{\theta})$ and therefore $g(t) = \Pi_t[\log p(\mathbf{y} | \boldsymbol{\theta})]$. Standard practice is to discretise the outer integral and estimate the inner integral using MCMC: Letting $0 = t_1 < \dots < t_m = 1$ denote a fixed *temperature schedule*, we thus have (e.g. using the trapezium rule)

$$\log p(\mathbf{y}) \approx \sum_{i=2}^m (t_i - t_{i-1}) \frac{\hat{g}_i + \hat{g}_{i-1}}{2}, \quad \hat{g}_i = \frac{1}{n} \sum_{j=1}^n \log p(\mathbf{y} | \boldsymbol{\theta}_{i,j}), \quad (5)$$

where $\{\boldsymbol{\theta}_{i,j}\}_{j=1}^n$ are MCMC samples from Π_{t_i} . Several improvements have been proposed, including the use of higher-order numerical quadrature for the outer integral (Friel et al., 2014; Hug et al., 2015) and the use of control variates for the inner integral (Oates et al., 2016b,c). To date, probabilistic integration has not been explored in this setting.

Probabilistic Thermodynamic Integration This methodology is interesting for probabilistic integration, since nested integrals are prone to propagation and accumulation of numerical error. Several features of the method are highlighted:

Transfer Learning: In the probabilistic approach to thermodynamic integration, the two integrands f and g are each assigned prior probability models. For the inner integral we assign a prior $f \sim \mathcal{N}(0, k_f)$. Our data here are the $nm \times 1$ vector \mathbf{f} where $f_{(i-1)n+j} = f(\boldsymbol{\theta}_{i,j})$. For estimating g_i we have m times as much data as for the estimator \hat{g}_i , in Eqn. 5, which makes use of only n function evaluations. Information transfer across temperatures is made possible by the explicit model for f underpinning the probabilistic integrator (and may suggest a general route to improved estimation for multiple integrals).

In the posterior, $\mathbf{g} = [g(t_1), \dots, g(t_T)]$ is a Gaussian random vector with $\mathbf{g}|\mathbf{f} \sim \mathcal{N}(\boldsymbol{\mu}, \boldsymbol{\Sigma})$ where the mean and covariance are defined by

$$\begin{aligned}\boldsymbol{\mu}_a &= \Pi_{t_a}[\mathbf{k}_f(\cdot, X)]\mathbf{K}_f^{-1}\mathbf{f}, \\ \boldsymbol{\Sigma}_{a,b} &= \Pi_{t_a}\Pi_{t_b}[k_f(\cdot, \cdot)] - \Pi_{t_a}[\mathbf{k}_f(\cdot, X)]\mathbf{K}_f^{-1}\Pi_{t_b}[\mathbf{k}_f(X, \cdot)],\end{aligned}$$

where $X = \{\boldsymbol{\theta}_{i,j}\}_{j=1}^n$ and \mathbf{K}_f is an $nm \times nm$ kernel matrix defined by k_f .

Inclusion of Prior Information: For the outer integral, it is known that discretisation error can be substantial; Friel et al. (2014) proposed a second-order correction to the trapezium rule to mitigate this bias, while Hug et al. (2015) pursued the use of Simpson’s rule. Attacking this problem from the probabilistic perspective, we do not want to place a default prior on $g(t)$, since it is known from extensive empirical work that $g(t)$ will vary more at smaller values of t . Indeed the rule-of-thumb $t_i = (i/m)^5$ is commonly used to inform the choice of quadrature states in accordance with this observation (Calderhead and Girolami, 2009). We would like to encode this information into our prior. To do this, we proceed with an importance sampling step $\log p(\mathbf{y}) = \int_0^1 g(t)dt = \int_0^1 h(t)\pi(t)dt$. The rule-of-thumb implies that taking an importance distribution Π with density $\pi(t) \propto 1/(\epsilon + 5t^{4/5})$ for some small $\epsilon > 0$, which renders the function $h = g/\pi$ approximately stationary (made precise in Supplement E.1). A stationary GP prior $h \sim \mathcal{N}(0, k_h)$ on the transformed integrand h provides an encoding of this prior knowledge.

Propagation of Uncertainty: Under our construction, in the posterior $\log p(\mathbf{y})$ is Gaussian with mean and covariance defined as

$$\begin{aligned}\mathbb{E}_n[\log p(\mathbf{y})] &= \Pi[\mathbf{k}_h(\cdot, T)]\mathbf{K}_h^{-1}\boldsymbol{\mu} \\ \mathbb{V}_n[\log p(\mathbf{y})] &= \underbrace{\Pi\Pi[k_h(\cdot, \cdot)] - \Pi[\mathbf{k}_h(\cdot, T)]\mathbf{K}_h^{-1}\Pi[\mathbf{k}_h(T, \cdot)]}_{(*)} + \underbrace{\Pi[\mathbf{k}_h(\cdot, T)]\mathbf{K}_h^{-1}\boldsymbol{\Sigma}\mathbf{K}_h^{-1}\Pi[\mathbf{k}_h(T, \cdot)]}_{(**)},\end{aligned}$$

where $T = \{t_i\}_{i=1}^m$ and \mathbf{K}_h is an $m \times m$ kernel matrix defined by k_h . The term (*) arises from BQ on the outer integral, while the term (**) arises from propagating numerical uncertainty from the inner integral through to the outer integral.

Simulation Study An experiment was conducted to elicit the MAP model from a collection of 56 candidate logistic regression models in a variable selection setting. This could be

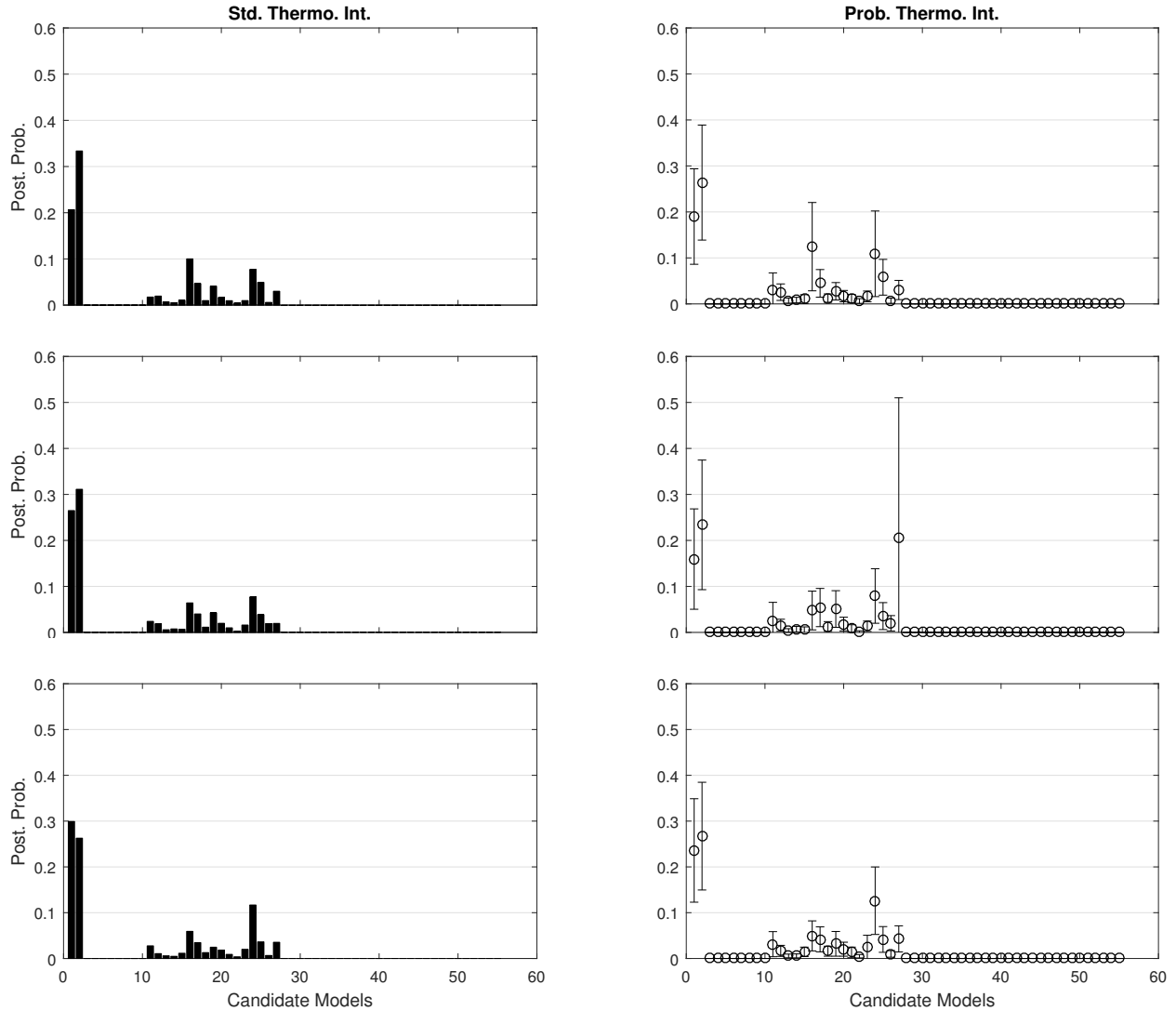


Figure 5: Probabilistic thermodynamic integration; illustration on variable selection for logistic regression (the true model was \mathcal{M}_1). Standard and probabilistic thermodynamic integration were used to approximate marginal likelihoods and, hence, the posterior over models. Each column represents three independent realisations of the MCMC sampler, while the data \mathbf{y} were fixed throughout. *Left*: Standard Monte Carlo, where point estimates for marginal likelihood were assumed to have no associated numerical error. *Right*: Probabilistic integration, where a model for numerical error on each integral was propagated through into the model posterior. This was performed using BMCMC and thermodynamic integration with BQ weights. The probabilistic approach produces a “probability distribution over a probability distribution”, where the numerical uncertainty is modelled on top of the usual uncertainty associated with model selection.

achieved in many ways; our aim was not to compare accuracy of point estimates, but rather

to explore the probability model that, unlike standard methods, is provided by probabilistic integration. Full details are provided in Supplement E.1.

Results are shown in Fig. 5. Here we compared approximations to the model posterior obtained using the standard method versus the probabilistic method, over 3 realisations of the MCMC (the data \mathbf{y} were fixed). We make some observations: (i) The probabilistic approach produces a second-order probability distribution, where the numerical uncertainty is modelled on top of the usual uncertainty associated with model selection. (ii) The computation associated with kernel methods required less time, in total, than the time taken to obtain MCMC samples. (iii) The same model was not always selected as the MAP when numerical error was ignored and depended on the MCMC random seed. In contrast, under the probabilistic approach, either \mathcal{M}_1 or \mathcal{M}_2 could feasibly be the MAP under any of the MCMC realisations. (iv) The middle row of Fig. 5 shows a large posterior uncertainty over the marginal likelihood for \mathcal{M}_{27} . This suggests more computational effort should be expended on this particular integral. (v) The posterior variance was dominated by uncertainty due to discretisation error in the outer integral, rather than the inner integral. This suggests that numerical uncertainty could be reduced by allocating more computational resources to the outer integral rather than the inner integral.

This section is concluded by noting the quite natural connection between algorithm design and numerical uncertainty, as exemplified by points (iv) and (v) above.

5.2.2 Case Study #2: Uncertainty Quantification for Computer Experiments

An important motivation for BQ comes from the statistical analysis of complex computer models. Here we consider an industrial scale computer model for the Teal South oil field (Hajizadeh et al., 2011), situated off the coast of New Orleans (depicted in Fig. 6). Conditional on field data, posterior inference was facilitated using state-of-the-art MCMC methodology (Lan et al., 2016). Oil reservoir models are generally challenging for standard MCMC methods for several reasons. First, simulating from those models can be prohibitively computationally expensive, making the cost of individual MCMC samples from a few minutes to several hours. Second, the posterior distribution will often exhibit strongly non-linear concentration of measure. Below we aim to compute statistics of interest using BMCMC, where the uncertainty quantification afforded by BQ could enable valid inferences in the presence of a relatively small number of posterior samples.

Quantification of the uncertainty associated with the prediction of quantities of interest is a major topic of ongoing research in this field (Mohamed et al., 2010; Hajizadeh et al., 2011; Park et al., 2013) due to the economic consequences associated with inaccurate predictions of quantities such as future oil production rate. A full probability distribution over the solution of integrals associated with prediction could provide a more honest assessment that factors in additional sources of uncertainty.

The particular integrals that we will tackle in this section are posterior means for each parameter, and we compare methods based on estimated mean with a very large number of MCMC runs. BMCMC was employed with a Matérn $\alpha = 3/2$ kernel whose lengthscale-parameter was selected using empirical Bayes. Due to intractability of the posterior distribu-

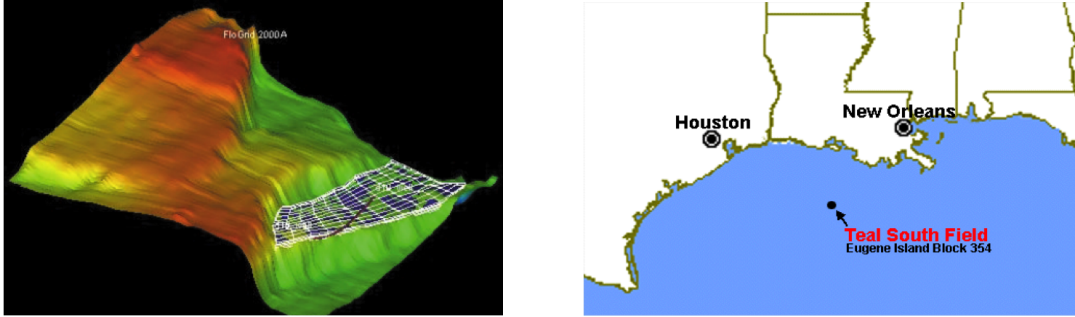


Figure 6: *Left*: Computer model for the Teal South oil field. Simulation of this model requires significant computational resources. This renders any statistical analysis challenging due to the small number of data which can be obtained. *Right*: Location of the oil field.

tion, the kernel mean $\mu(\pi)$ is unavailable in closed form. To overcome this, the methodology in Sec. 4.2 was employed to obtain an empirical estimate of the kernel mean (half of the MCMC samples were used with BQ weights to approximate the integral and the other half with MC weights to approximate the kernel mean). Estimates for posterior means were obtained using both standard MCMC and BMCMC, shown in Fig. 7. For this example the posterior distribution afforded by BMCMC provides sensible uncertainty quantification. We note that the inaccuracies for parameters 2, 4 and 5 are due to the high auto-correlation of the associated Markov chain. We found that the accuracy of the BMCMC estimator matches that of the standard MCMC estimator and does not exceed it. However, the 95% posterior credible intervals overlap with the truth whenever the auto-correlation is not too high, which is not the case for the confidence intervals obtained from the CLT with a plug-in estimate for the asymptotic variance which are overly confident in the non-asymptotic regime. The lack of improved rate of convergence over MCMC appears to be due to inaccurate estimation of the kernel mean and we conjecture that alternative exact approaches, such as Oates et al. (2016b), may provide improved performance in this context.

5.2.3 Case Study #3: High-Dimensional Random Effects

Our aim here is to explore whether the more flexible functional representations afforded by weighted spaces enable probabilistic integration in the challenging high-dimensional setting. The focus is BQMC, but the methodology could be applied to other probabilistic integrators.

Weighted Spaces The formulation of high (and infinite) -dimensional QMC results requires a construction known as a *weighted* Hilbert space. These spaces, defined below, are motivated by the observation that many integrands encountered in applications seem to vary more in lower dimensional projections compared to higher dimensional projections. Our presentation below follows Sec. 2.5.4 and 12.2 of Dick and Pillichshammer (2010), but the idea goes back at least to Wahba (1990, Chap. 10).

As usual with QMC, we work in $\mathcal{X} = [0, 1]^d$, σ is the Lebesgue measure and with Π

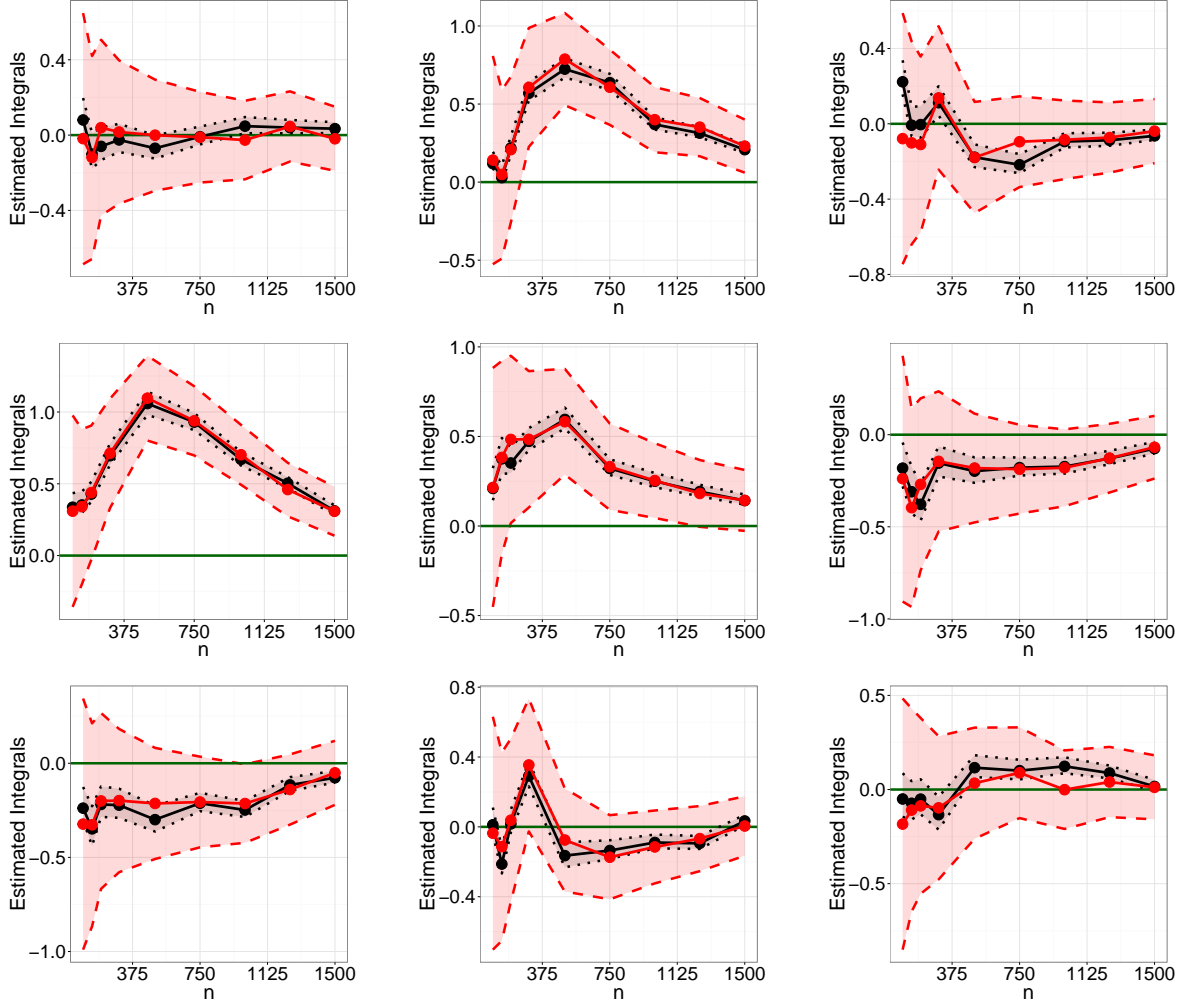


Figure 7: Posterior parameter means for Teal South (centered around the true values). The green line gives the exact solution of the integral. The MCMC (black line) and BMCMC point estimates (red line) give similar performance. The MCMC 95% confidence intervals are based on estimated asymptotic variance (black dotted lines) tend to be over confident whereas with the BMCMC 95% credible intervals (red dotted lines) provide a more accurate coverage when the autocorrelation between MCMC samples is low.

uniform over \mathcal{X} . Let $\mathcal{I} = \{1, 2, \dots, d\}$. For each subset $u \subseteq \mathcal{I}$, define a weight $\gamma_u \in (0, \infty)$ and denote the collection of all weights by $\gamma = \{\gamma_u\}_{u \subseteq \mathcal{I}}$. Consider the space \mathcal{H}_γ of functions of the form $f(\mathbf{x}) = \sum_{u \subseteq \mathcal{I}} f_u(\mathbf{x}_u)$, where f_u belongs to an RKHS \mathcal{H}_u with reproducing kernel k_u and \mathbf{x}_u denotes the components of \mathbf{x} that are indexed by u . We point out that this construction is not restrictive, since any function can be written in this form by considering only $u = \mathcal{I}$. We turn \mathcal{H}_γ into a Hilbert space by defining an inner product $\langle f, g \rangle_\gamma := \sum_{u \subseteq \mathcal{I}} \gamma_u^{-1} \langle f_u, g_u \rangle_u$ where $\gamma = \{\gamma_u : u \subseteq \mathcal{I}\}$. Constructed in this way, \mathcal{H}_γ is an RKHS with

reproducing kernel $k_\gamma(\mathbf{x}, \mathbf{x}') = \sum_{u \subseteq \mathcal{I}} \gamma_u k_u(\mathbf{x}, \mathbf{x}')$. Intuitively, the weights γ_u can be taken to be small whenever the function f does not depend heavily on the $|u|$ -way interaction of the states \mathbf{x}_u . Thus, most of the γ_u will be small for a function f that is effectively low-dimensional. A measure of the dimensionality of the function is given by $\sum_{u \subseteq \mathcal{I}} \gamma_u$; in an extreme case d could even be infinite provided that this sum remains bounded (Dick et al., 2013).

The (canonical) *weighted* Sobolev space of dominating mixed smoothness $\mathcal{S}_{\alpha, \gamma}$ is defined by taking each of the component spaces to be \mathcal{S}_α . In finite dimensions $d < \infty$, we can construct BQMC rules based on a higher-order digital net that attains optimal QMC rates $O(n^{-\alpha+\epsilon})$ for this RKHS; see Supplement E.2 for full details.

Semi-Parametric Random Effects Regression For illustration we observe that the weighted RKHS framework can appropriately model features of integrands that appear in generalised linear models, and focus on a Poisson semi-parametric random effects regression model studied by Kuo et al. (2008, Example 2). The context is inference for the parameters $\boldsymbol{\beta}$ of the following model

$$\begin{aligned} Y_j | \lambda_j &\sim \text{Po}(\lambda_j) \\ \log(\lambda_j) &= \beta_0 + \beta_1 z_{1,j} + \beta_2 z_{2,j} + u_1 \phi_1(z_{2,j}) + \cdots + u_d \phi_d(z_{2,j}) \\ u_j &\sim N(0, \tau^{-1}) \text{ independently.} \end{aligned}$$

Here $z_{1,j} \in \{0, 1\}$, $z_{2,j} \in (0, 1)$ and $\phi_j(z) = [z - \kappa_j]_+$ where $\kappa_j \in (0, 1)$ are pre-determined knots. We took $d = 50$ equally spaced knots in $[\min \mathbf{z}_2, \max \mathbf{z}_2]$. Inference for $\boldsymbol{\beta}$ requires multiple evaluations of the observed data likelihood $p(\mathbf{y} | \boldsymbol{\beta}) = \int_{\mathbb{R}^d} p(\mathbf{y} | \boldsymbol{\beta}, \mathbf{u}) p(\mathbf{u}) d\mathbf{u}$ and therefore is a natural candidate for probabilistic integration methods, in order to propagate the cumulative uncertainty of estimating multiple numerical integrals into the posterior distribution $p(\boldsymbol{\beta} | \mathbf{y})$.

In order to transform this integration problem to the unit cube we perform the change of variables $x_j = \Phi^{-1}(u_j)$ so that we wish to evaluate $p(\mathbf{y} | \boldsymbol{\beta}) = \int_{[0,1]^d} p(\mathbf{y} | \boldsymbol{\beta}, \Phi^{-1}(\mathbf{x})) d\mathbf{x}$. Here $\Phi^{-1}(\mathbf{x})$ denotes the standard Gaussian inverse CDF applied to each component of \mathbf{x} . Probabilistic integration here proceeds under the hypothesis that the integrand $f(\mathbf{x}) = p(\mathbf{y} | \boldsymbol{\beta}, \Phi^{-1}(\mathbf{x}))$ belongs to (or at least can be well approximated by functions in) $\mathcal{S}_{\alpha, \gamma}$ for some smoothness parameter α and some weights $\boldsymbol{\gamma}$. Intuitively, the integrand $f(\mathbf{x})$ is such that an increase in the value of x_j at the knot κ_j can be compensated for by a decrease in the value of x_{j+1} at a neighbouring knot κ_{j+1} , but not by changing values of \mathbf{x} at more remote knots. Therefore we expect $f(\mathbf{x})$ to exhibit strong individual and pairwise dependence on the x_j , but expect higher-order dependency to be much weaker. This motivates the weighted space assumption. Sinescu et al. (2012) provides theoretical analysis for the choice of weights $\boldsymbol{\gamma}$. Here, weights $\boldsymbol{\gamma}$ of *order two* were used; $\gamma_u = 1$ for $|u| \leq d_{\max}$, $d_{\max} = 2$, $\gamma_u = 0$ otherwise, which corresponds to an assumption of low order interaction terms (though f can still depend on all of its arguments).

In terms of point estimation accuracy, results in Fig. 8 demonstrate that this two-way BQMC posterior distribution provides accuracy comparable to the standard QMC estimate,

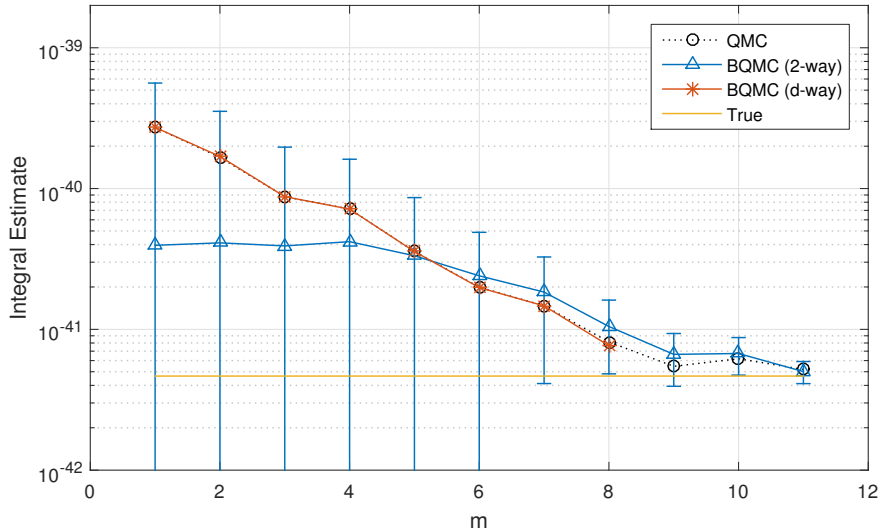


Figure 8: Application to semi-parametric random effects regression in $d = 50$ dimensions, based on $n = 2^m$ samples from a higher-order digital net. [Error bars show 95% credible regions. To improve visibility results are shown on the log-scale; error bars are symmetric on the linear scale. A brute-force QMC estimate was used to approximate the true value of the integral.]

with BQMC more accurate than QMC at smaller sample sizes ($n \leq 2^5$). To understand the effect of the weighted space construction here, we compared against BQMC with d -way interactions ($u \in \{\emptyset, \mathcal{I}\}$). We found that the d -way BQMC closely resembled standard QMC and thus integral estimates based on 2-way interactions were more accurate at smaller sample sizes, although in general the performance of all methods was comparable to standard QMC on this problem. In terms of uncertainty quantification, the 95% posterior credible regions more-or-less cover the truth for this problem, suggesting that the uncertainty estimates are sensible. On the negative side, the BQMC method does not encode non-negativity of the integrand and, consequently, some posterior mass is placed on negative values for the integral, which is not meaningful. This is shown in Fig. 8 where initial credible regions, based on small values of n , cannot be visualised on a log-scale.

5.2.4 Case Study #4: Spherical Integration for Computer Graphics

Probabilistic integration methods can be defined on arbitrary manifolds, with formulations on non-Euclidean spaces suggested as far back as Diaconis (1988) and recently exploited in the context of computer graphics (Brouillat et al., 2009; Marques et al., 2015). This forms the setting for our final case study.

Global Illumination Integrals Below we formulate and analyse BQMC on the d -sphere $\mathbb{S}^d = \{\mathbf{x} = (x_1, \dots, x_{d+1}) \in \mathbb{R}^{d+1} : \|\mathbf{x}\|_2 = 1\}$ in order to estimate integrals of the form $\Pi[f] = \int_{\mathbb{S}^d} f d\Pi$, where Π is the spherical measure (i.e. uniform over \mathbb{S}^d with $\int_{\mathbb{S}^d} d\Pi = 1$).

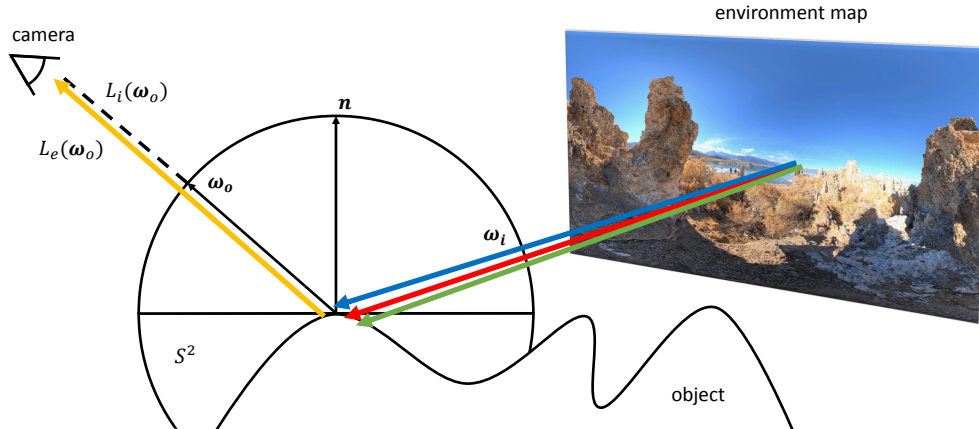


Figure 9: Application to illumination integrals in computer graphics. The cartoon features the California lake environment map that was used in our experiments.

Probabilistic integration is applied to compute global illumination integrals used in the rendering of surfaces (Pharr and Humphreys, 2004), and we therefore focus on the case where $d = 2$ and the measure Π is uniform over \mathbb{S}^2 . The problem of global illumination occurs in the synthesis of photo-realistic images of virtual scenes (e.g. a view of a lake). Uncertainty quantification is motivated by inverse global illumination problems (e.g. Yu et al., 1999), where the task is to make inferences from noisy observation of an object via computer-based image synthesis; a measure of numerical uncertainty could naturally be propagated in such problems. Below, however, we restrict attention to uncertainty quantification in the forward problem to limit scope.

The models involved in global illumination are based on three main factors: a geometric model for the objects present in the scene, a model for the reflectivity of the surface of each object and a description of the light sources (provided by an *environment map* as depicted in Fig. 9). The light emitted from the environment will interact with objects in the scene through reflection. This can be formulated as an illumination integral of the form below²

$$L_o(\omega_o) = L_e(\omega_o) + \int_{\mathbb{S}^2} L_i(\omega_i) \rho(\omega_i, \omega_o) [\omega_i \cdot \mathbf{n}]_+ \Pi(d\omega_i). \quad (6)$$

Here $L_o(\omega_o)$ is the *outgoing radiance*, i.e. the outgoing light in the direction ω_o . $L_e(\omega_o)$ represents the amount of light emitted by the object itself (which we will assume to be known) and $L_i(\omega_i)$ is the light hitting the object from direction ω_i . The term $\rho(\omega_i, \omega_o)$ is the *bidirectional reflectance distribution function* (BRDF), which models the fraction of light arriving at the surface point from direction ω_i and being reflected towards direction ω_o . Here \mathbf{n} is a unit vector normal to the surface of the object. Our investigation is motivated by strong empirical results for BQMC in this context obtained by Marques et al. (2015)³.

²It is noted by Marques et al. (2015) that slightly improved empirical performance can be obtained by replacing the $[\omega_i \cdot \mathbf{n}]_+$ term with the smoother $\omega_i \cdot \mathbf{n}$ term and restricting the domain of integration to the hemisphere $\omega_i \cdot \mathbf{n} \geq 0$. For simplicity we present the problem as an integral over \mathbb{S}^2 .

³The authors call their method BMC, but states arose from a deterministic (spiral point) algorithm.

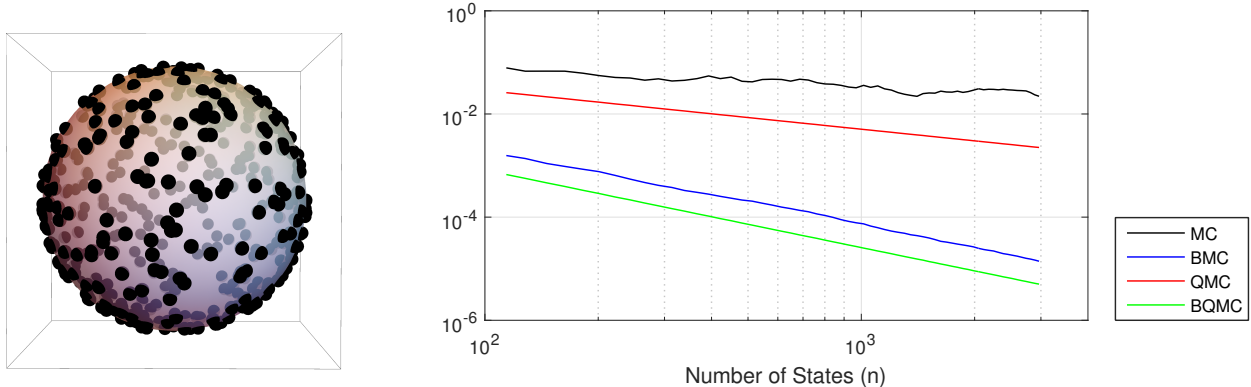


Figure 10: Application to global illumination integrals in computer graphics. *Left*: A spherical t -design over \mathbb{S}^2 . *Right*: The WCE, or worst-case-error, for Monte Carlo (MC), Bayesian MC (BMC), Quasi MC (QMC) and Bayesian QMC (BQMC).

We note that this type of problem can be very expensive in practice since three different integrals (one for each of the RGB channels) of the form in Eqn. 6 need to be computed at every pixel of the image, in order to obtain good rendering.

In order to assess the performance of BQMC we consider a typical illumination integration problem based on the California lake environment map shown in Fig. 9⁴. The goal here is to compute intensities for each of the three RGB colour channels corresponding to observing a virtual object from a fixed direction ω_o . We consider the case of an object directly facing the camera ($\omega_o = \mathbf{n}$). For the BRDF we took $\rho(\omega_i, \omega_o) = (2\pi)^{-1} \exp(\omega_i \cdot \omega_o - 1)$. The integral in Eqn. 6 was viewed here as an integral with respect to a uniform measure Π with integrand $f(\omega_i) = L_i(\omega_i) \rho(\omega_i, \omega_o) [\omega_i \cdot \omega_o]_+$ assumed to be in a Sobolev space of low smoothness. In contrast, Marques et al. (2015) viewed Eqn. 6 as an integral with respect to $\pi(\omega_i) \propto \rho(\omega_i, \omega_o)$ and coupled this with a Gaussian kernel restricted to the hemisphere. The approach that we propose has two advantages; (i) it provides a closed-form expression for the kernel mean, (ii) a rougher kernel may be more appropriate in the context of illumination integrals, as pointed out by Brouillat et al. (2009). The specific function space that we consider is the Sobolev space $\mathcal{H}_\alpha(\mathbb{S}^d)$ for $\alpha = 3/2$, formally defined in Supplement E.1.

Results Both BMC and BQMC were tested on this example. To ensure fair comparison, identical kernels were taken as the basis for both methods. BQMC was employed using a *spherical t -design* (Bondarenko et al., 2013), see Fig. 10 (left). Both BMC and BQMC can be shown to obtain the convergence rate $e(\hat{\Pi}_{\text{BQMC}}; \Pi, \mathcal{H}) = O(n^{-3/4})$ (see Supplement E.1). This is demonstrated empirically on the right hand panel in Fig. 10, where the value of the WCE is plotted for each of the four methods considered (MC, QMC, BMC, BQMC) as the number of states increases. Both BMC and BQMC attain the optimal rate for $\mathcal{H}_{3/2}(\mathbb{S}^2)$, although BQMC provides a constant factor improvement over BMC. Note that $O(n^{-3/4})$ was shown by Brauchart et al. (2014) to be best-possible in the space $\mathcal{H}_{3/2}(\mathbb{S}^2)$.

⁴This environment map is freely available at: <http://www.hdrilabs.com/sibl/archive.html>.

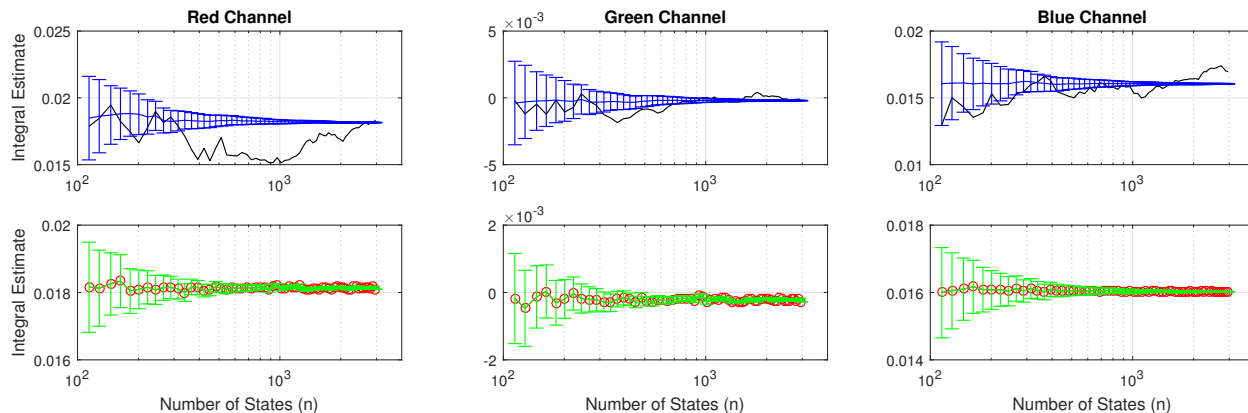


Figure 11: Probabilistic integration over the sphere was employed to estimate the RGB colour intensities for the California lake environment. [Error bars for BMC (blue) and BQMC (green) represent two posterior standard deviations (i.e. 95% credible intervals). MC estimates (black) and QMC estimates (red) are shown for reference.]

Translating this performance into the RGB-space, we see in Fig. 11 that, for this particular test function, the BQMC point estimate was almost identical to the QMC estimate at all values of n . Empirical results reported by Marques et al. (2015), based on Gaussian kernels, showed a RMSE rate of $O(n^{-0.72})$, which is similar to the theoretical $O(n^{-3/4})$ rate that we provide here. Overall, both BMC and BQMC provided sensible quantification of uncertainty for the value of the integral at all values of n that were considered.

6 Conclusion & Discussion

The increasing sophistication of complex computational models, of which numerical integration is one component, demands an improved understanding of how numerical error accumulates and propagates through sequential computation from a statistical perspective. In (now common) settings where integrands are computationally intensive, or very many numerical integrals are required, effective methods are required that make full use of information available about the problem at hand. This is clearly evidenced by the recent success of QMC methods in statistics and engineering disciplines, which account for the smoothness of integrands to gain in quadrature accuracy. Probabilistic Numerics puts the statistician in centre stage and aims to model the numerical error explicitly. This approach was eloquently summarised by Kadane (1985), who proposed the following vision for the future of computation:

“Statistics can be thought of as a set of tools used in making decisions and inferences in the face of uncertainty. Algorithms typically operate in such an environment. Perhaps then, statisticians might join the teams of scholars addressing algorithmic issues.”

This paper explored, from a statistical perspective, the implications of a probabilistic perspective on integration. This investigation attempted to highlight both the advantages and disadvantages of such an approach. On the positive side, the general methodology described provides a unified framework in which existing high-performance quadrature methods based on Monte Carlo point sets are associated with a probability distribution that captures the extent of numerical error associated with the point estimator. Furthermore, the prior information encoded will in some cases lead to faster convergence rates than standard Monte Carlo methods. Theoretical posterior contraction rates were established and form an important, fundamental and novel contribution to the literature. Nevertheless, there remain many substantial open questions and challenges surrounding probabilistic integration, in terms of philosophical foundations, theoretical analysis and practical application.

Philosophy There are several issues concerning the uncertainty which one models with probabilistic numerical methods. In the specific case of integration, there is not yet a complete consensus on how one should interpret uncertainty in the estimation of a constant; is it as simple as “epistemic uncertainty” due to the finite number of evaluations of the integrands? If so, whose epistemic uncertainty is being modelled? The discussion of Kong et al. (2003) is notable by the lack of consensus among statisticians.

An up-to-date discussion of these points is provided in Hennig et al. (2015). There it was argued that the uncertainty being modelled is that of a hypothetical agent “that we get to design”. That is, the statistician selects priors and loss functions for the agent so that it best achieves the statistician’s own goals. These goals typically involve a combination of relatively black-box behaviour, to perform well on a diverse range of problems, and a low computational overhead. Interpretation of the posterior is then more subtle than for subjective inference and many of the points of contention for objective inference also appear in this framework.

Methodology The question of which part of the numerical method should be formally considered to be uncertain is open to debate. In this paper, the integrand f is considered to be uncertain while the distribution Π is considered to be known. However, one could alternatively suppose that f is known and the probability distribution Π is unknown; this approach was pursued in Kong et al. (2003), who incorporated prior information such as invariance to reflection with Lebesgue measure. There the authors concluded that “[...] essentially every Monte Carlo activity may be interpreted as parameter estimation by maximum likelihood in a statistical model”. Another alternative is that both f and Π are known but the continuous mathematical operation of integration is itself uncertain, as in the Information Complexity literature (Woźniakowski, 2009).

Irrespective of where uncertainty is introduced, the scope to design numerical methods that specifically target this source of epistemic uncertainty has close links to statistical decision theory. For example, Briol et al. (2015) consider the choice of quadrature states as a problem in statistical experimental design, providing an iterative approach that is proven to asymptotically minimise posterior variance associated with the numerical uncertainty

measure. This also leads to the question of which statistical tools are most appropriate, and this is likely to be a question with no overall answer, but which will be application dependent and will depend on the philosophical tendencies of the user.

Theory For probabilistic integration, further theoretical work is required. Our results proved several desirable properties of the behaviour of posterior contraction, but did not address coverage at finite sample size, nor the interaction of coverage with the empirical Bayes method for kernel specification. A particularly important question, not addressed here, is the behaviour of BQ when the integrand does not belong to the posited RKHS. Clearly much work in this direction remains before general-purpose probabilistic integrators can be provided as “black-box” (probabilistic) numerical algorithms.

Prior Specification Once a given framework has been adopted, there is still the issue of the elicitation of the prior knowledge available to the person designing the numerical integration scheme. This requires a broad discussion of what prior information should be included, and what information should be ignored. Indeed, practical considerations essentially always demand that some aspects of prior information are ignored. Competing computational, statistical and philosophical considerations are all in play and must be balanced.

For example, the RKHS framework that we studied in this paper has the advantage of providing a flexible way of encoding prior knowledge about the integrand allowing to specify properties such as smoothness, periodicity, non-stationarity and effective low-dimension. On the other hand, several important properties, including positivity, are less easily encoded (see Petersen and Müller, 2016). For BQ, the decomposition of $f\pi$ into a function f and a density π has an element of arbitrariness that appears to preclude the pursuit of a default prior. At a more fundamental level, the constraint that $f \in L^2(\Pi)$ can be critiqued as physically irrelevant (in physical problems where f is meaningful, f^2 can be nonsensical), but this is intrinsic to the Hilbert space approach.

Even within the RKHS framework, there is the issue that integrands f will usually be part of infinitely many RKHS. Selecting an appropriate RKHS is arguably the central open challenge for QMC research at present. From a practical perspective, elicitation of priors over infinite-dimensional spaces is a hard problem. An adequate choice of prior can be very informative for the numerical scheme and can significantly improve the convergence rates of the method. Methods for choosing the kernel automatically would be useful here (e.g. Duvenaud, 2014), but would need to be considered against their suitability for providing correct uncertainty quantification.

The list above is obviously not meant to be exhaustive, but provides many areas of further research which still need to be explored. In summary, it is clear to us that there is an important role for statisticians to play in the development of modern numerical analysis.

Acknowledgements

The authors acknowledge extensive feedback received on an earlier version of this paper from A. Barp, J. Cockayne, J. Dick, D. Duvenaud, A. Gelman, P. Hennig, M. Kanagawa, J. Kronander, X-L. Meng, A. Owen, C. Robert, S. Särkkä, C. Schwab, D. Simpson, J. Skilling, T. Sullivan, Z. Tan, A. Teckentrup and H. Zhu. The authors are very grateful to S. Lan and R. Marques for providing code used in producing these results. FXB was supported by the EPSRC grant [EP/L016710/1]. CJO was supported by the ARC Centre of Excellence for Mathematical and Statistical Frontiers. MG was supported by the EPSRC grant [EP/J016934/1, EP/K034154/1], an EPSRC Established Career Fellowship, the EU grant [EU/259348] and a Royal Society Wolfson Research Merit Award.

References

- F. Bach. On the equivalence between quadrature rules and random features. *arXiv:1502.06800*, 2015. doi: HAL-01118276-v2.
- A. Berlinet and C. Thomas-Agnan. *Reproducing Kernel Hilbert Spaces in Probability and Statistics*. Springer Science+Business Media, New York, 2004.
- P. Bissiri, C. Holmes, and S. Walker. A General Framework for Updating Belief Distributions. *Journal of the Royal Statistical Society Series B: Statistical Methodology*, in press, 2016.
- A. Bondarenko, D. Radchenko, and M. Viazovska. Optimal asymptotic bounds for spherical designs. *Annals of Mathematics*, 178(2):443–452, 2013.
- J. Brauchart, E. Saff, I. H. Sloan, and R. Womersley. QMC designs: Optimal order quasi Monte Carlo integration schemes on the sphere. *Mathematics of Computation*, 83:2821–2851, 2014.
- F.-X. Briol, C. J. Oates, M. Girolami, and M. A. Osborne. Frank-Wolfe Bayesian Quadrature: Probabilistic integration with theoretical guarantees. In *Advances In Neural Information Processing Systems*, 2015.
- J. Brouillat, C. Bouville, B. Loos, C. Hansen, and K. Bouatouch. A Bayesian Monte Carlo approach to global illumination. *Computer Graphics Forum*, 28(8):2315–2329, 2009.
- B. Calderhead and M. Girolami. Estimating Bayes factors via thermodynamic integration and population MCMC. *Computational Statistics and Data Analysis*, 53(12):4028–4045, 2009.
- J. Carson, M. Pollock, and M. Girolami. Unbiased local solutions of partial differential equations via the Feynman-Kac identities. *arXiv:1603.04196*, 2016.
- P. Conrad, M. Girolami, S. Särkkä, A. Stuart, and K. Zygalakis. Probability measures for numerical solutions of differential equations. *arXiv:1506.04592*, 2015.

- M. Dashti and A. Stuart. The Bayesian approach to inverse problems. In *Handbook of Uncertainty Quantification*. 2016.
- P. J. Davis and P. Rabinowitz. *Methods of numerical integration*. Courier Corporation, 2007.
- P. Diaconis. Bayesian numerical analysis. *Statistical Decision Theory and Related Topics IV*, 163–175, 1988.
- J. Dick. Higher order scrambled digital nets achieve the optimal rate of the root mean square error for smooth integrands. *Annals of Statistics*, 39(3):1372–1398, 2011.
- J. Dick and F. Pillichshammer. *Digital Nets and Sequences - Discrepancy Theory and Quasi-Monte Carlo Integration*. Cambridge University Press, 2010.
- J. Dick, F. Y. Kuo, and I. H. Sloan. High-dimensional integration: The quasi-Monte Carlo way. *Acta Numerica*, 22:133–288, 2013.
- D. Duvenaud. *Automatic model construction with Gaussian processes*. PhD thesis, University of Cambridge, 2014.
- B. Efron and R. J. Tibshirani. *An introduction to the bootstrap*. CRC press, 1994.
- J. L. Eftang and B. Stamm. Parameter multi-domain “hp” empirical interpolation. *International Journal for Numerical Methods in Engineering*, 90(4):412–428, 2012.
- P. Erdős and M. Kac. The gaussian law of errors in the theory of additive number theoretic functions. *American Journal of Mathematics*, 62(1):738–742, 1940.
- G. Fasshauer, F. J. Hickernell, and H. Woźniakowski. On dimension-independent rates of convergence for function approximation with Gaussian kernels. *SIAM Journal on Numerical Analysis*, 50(1):247–271, 2012.
- N. Friel and A. N. Pettitt. Marginal Likelihood Estimation via Power Posteriors likelihood estimation via power posteriors. *Journal of the Royal Statistical Society Series B: Statistical Methodology*, 70(3):589–607, 2008.
- N. Friel, M. Hurn, and J. Wyse. Improving power posterior estimation of statistical evidence. *Statistics and Computing*, 24(5):709–723, 2014.
- A. Gelman and X.-L. Meng. Simulating normalizing constants: From importance sampling to bridge sampling to path sampling. *Statistical science*, 13(2):163–185, 1998.
- M. Gerber and N. Chopin. Sequential quasi-Monte Carlo. *Journal of the Royal Statistical Society B: Statistical Methodology*, 77(3):509–579, 2015.
- M. Girolami and B. Calderhead. Riemann manifold Langevin and Hamiltonian Monte Carlo methods. *Journal of the Royal Statistical Society Series B: Statistical Methodology*, 73(2):123–214, 2011.

- T. Gunter, R. Garnett, M. Osborne, P. Hennig, and S. Roberts. Sampling for inference in probabilistic models with fast Bayesian quadrature. In *Advances in Neural Information Processing Systems*, 2789–2797, 2014.
- Y. Hajizadeh, M. Christie, and V. Demyanov. Ant colony optimization for history matching and uncertainty quantification of reservoir models. *Journal of Petroleum Science and Engineering*, 77(1):78–92, 2011.
- P. Hennig. Probabilistic interpretation of linear solvers. *SIAM Journal on Optimization*, 25(1):234–260, 2015.
- P. Hennig and M. Kiefel. Quasi-Newton methods: A new direction. *Journal of Machine Learning Research*, 14:843–865, 2013.
- P. Hennig, M. A. Osborne, and M. Girolami. Probabilistic numerics and uncertainty in computations. *Journal of the Royal Society A*, 471(2179), 2015.
- F. J. Hickernell. A generalized discrepancy and quadrature error bound. *Mathematics of Computation of the American Mathematical Society*, 67(221):299–322, 1998.
- F. J. Hickernell, C. Lemieux, and A. B. Owen. Control variates for quasi-Monte Carlo. *Statistical Science*, 20(1):1–31, 2005.
- S. Hug, M. Schwarzfischer, J. Hasenauer, C. Marr, and F. J. Theis. An adaptive scheduling scheme for calculating Bayes factors with thermodynamic integration using Simpson’s rule. *Statistics and Computing*, 1–15, 2015.
- T. E. Hull and J. R. Swenson. Tests of probabilistic models for propagation of roundoff errors. *Communications of the ACM*, 9(2):108–113, 1966.
- F. Huszar and D. Duvenaud. Optimally-weighted herding is Bayesian quadrature. In *Uncertainty in Artificial Intelligence*, 377–385, 2012.
- J. B. Kadane. Parallel and Sequential Computation : A Statistician’s view. *Journal of Complexity*, 1:256–263, 1985.
- J. B. Kadane and G. W. Wasilkowski. Average case epsilon-complexity in computer science: A Bayesian view. In *Bayesian Statistics 2, Proceedings of the Second Valencia International Meeting*, number July, 361–374, 1985.
- A. Kong, P. McCullagh, X.-L. Meng, D. Nicolae, and Z. Tan. A theory of statistical models for Monte Carlo integration. *Journal of the Royal Statistical Society Series B: Statistical Methodology*, 65(3):585–618, 2003.
- S. Kristoffersen. The empirical interpolation method. Master’s thesis, Department of Mathematical Sciences, Norwegian University of Science and Technology, 2013.

- F. Y. Kuo, W. T. M. Dunsmuir, I. H. Sloan, M. P. Wand, and R. S. Womersley. Quasi-Monte Carlo for highly structured generalised response models. *Methodology and Computing in Applied Probability*, 10(2):239–275, 2008.
- S. Lan, T. Bui-Thanh, M. Christie, and M. Girolami. Emulation of Higher-Order Tensors in Manifold Monte Carlo Methods for Bayesian Inverse Problems. *Journal of Computational Physics*, 308:81–101, 2016.
- F. M. Larkin. Gaussian measure in Hilbert space and applications in numerical analysis. *Journal of Mathematics*, 2(3):379–422, 1972.
- Y. Maday, N. C. Nguyen, A. T. Patera, and G. S. H. Pau. A general, multipurpose interpolation procedure: the magic points. *Commun. Pure Appl. Anal.*, 8:383–404, 2009.
- M. Mahsereci and P. Hennig. Probabilistic line searches for stochastic optimization. In *Advances In Neural Information Processing Systems*, 181-189, 2015.
- R. Marques, C. Bouville, M. Ribardiere, L. P. Santos, and K. Bouatouch. A spherical Gaussian framework for Bayesian Monte Carlo rendering of glossy surfaces. *IEEE Transactions on Visualization and Computer Graphics*, 19(10):1619–1632, 2013.
- R. Marques, C. Bouville, L. Santos, and K. Bouatouch. Efficient quadrature rules for illumination integrals: from Quasi Monte Carlo to Bayesian Monte Carlo. *Synthesis Lectures on Computer Graphics and Animation*, 7(2):1–92, 2015.
- S. P. Meyn and R. L. Tweedie. *Markov chains and stochastic stability*. Springer Science & Business Media, 2012.
- T. Minka. Deriving quadrature rules from Gaussian processes. Technical report, Statistics Department, Carnegie Mellon University, 2000.
- M. S. Mizieliński, M. J. Roberts, P. L. Vidale, R. Schiemann, M.-E. Demory, J. Strachan, T. Edwards, A. Stephens, B. N. Lawrence, M. Pritchard, et al. High-resolution global climate modelling: the upscale project, a large-simulation campaign. *Geoscientific Model Development*, 7(4):1629–1640, 2014.
- L. Mohamed, M. Christie, and V. Demyanov. Comparison of Stochastic Sampling Algorithms for Uncertainty Quantification. *SPE Journal*, 15:31–38, 2010.
- S. Mosbach and A. G. Turner. A quantitative probabilistic investigation into the accumulation of rounding errors in numerical ODE solution. *Computers & Mathematics with Applications*, 57(7):1157–1167, 2009.
- E. Novak and H. Woźniakowski. *Tractability of Multivariate Problems Volume I: Linear Information*. European Mathematical Society Publishing House, EMS Tracts in Mathematics 6, 2008.

- E. Novak and H. Woźniakowski. *Tractability of Multivariate Problems, Volume II : Standard Information for Functionals*. European Mathematical Society Publishing House, EMS Tracts in Mathematics 12, 2010.
- D. Nuyens and R. Cools. Fast component-by-component construction, a reprise for different kernels. In *Monte Carlo and Quasi-Monte Carlo Methods 2004*, 373–387. Springer, 2006.
- C. J. Oates, J. Cockayne, F.-X. Briol, and M. Girolami. Convergence rates for a class of estimators based on Stein’s identity. *arXiv:1603.03220*, 2016a.
- C. J. Oates, M. Girolami, and N. Chopin. Control functionals for Monte Carlo integration. *Journal of the Royal Statistical Society B: Statistical Methodology*, in press, 2016b.
- C. J. Oates, T. Papamarkou, and M. Girolami. The controlled thermodynamic integral for Bayesian model comparison. *Journal of the American Statistical Association*, in press, 2016c.
- A. O’Hagan. Bayes–Hermite quadrature. *Journal of Statistical Planning and Inference*, 29: 245–260, 1991.
- A. O’Hagan. Some Bayesian numerical analysis. *Bayesian Statistics*, 4:345–363, 1992.
- M. A. Osborne. *Bayesian Gaussian processes for sequential prediction, optimisation and quadrature*. PhD thesis, University of Oxford, 2010.
- M. A. Osborne, D. Duvenaud, R. Garnett, C. E. Rasmussen, S. Roberts, and Z. Ghahramani. Active learning of model evidence using Bayesian quadrature. In *Advances In Neural Information Processing Systems*, 46–54, 2012.
- H. Owhadi. Multi-grid with rough coefficients and multiresolution operator decomposition from hierarchical information games. *SIAM Review*, in press, 2016.
- H. Park, C. Scheidt, D. Fenwick, A. Boucher, and J. Caers. History matching and uncertainty quantification of facies models with multiple geological interpretations. *Computational Geosciences*, 17(4):609–621, 2013.
- A. Petersen and H. Müller. Functional data analysis for density functions by transformation to a Hilbert space. *The Annals of Statistics*, 44(1):183–218, 2016.
- M. Pharr and G. Humphreys. *Physically based rendering: From theory to implementation*. Morgan Kaufmann Publishers Inc., 2004.
- H. Poincaré. *Calcul des probabilités*. Gauthier-Villars, 1912.
- C. Rasmussen and C. Williams. *Gaussian Processes for Machine Learning*. MIT Press, 2006.
- C. E. Rasmussen and Z. Ghahramani. Bayesian Monte Carlo. In *Advances in Neural Information Processing Systems*, 489–496, 2002.

- K. Ritter. *Average-Case Analysis of Numerical Problems*. Springer-Verlag Berlin Heidelberg, 2000.
- C. Robert and G. Casella. *Monte Carlo statistical methods*. Springer Science & Business Media, 2013.
- A. Sard. *Linear approximation*, volume 9. American Mathematical Soc., 1963.
- S. Särkka, J. Hartikainen, L. Svensson, and F. Sandblom. On the relation between Gaussian process quadratures and sigma-point methods, *Journal of Advances in Information Fusion*, in press, 2016.
- R. Schaback. Error estimates and condition numbers for radial basis function interpolation. *Advances in Computational Mathematics*, 3:251–264, 1995.
- M. Schober, D. Duvenaud, and P. Hennig. Probabilistic ODE solvers with Runge-Kutta means. In *Advances in Neural Information Processing Systems*, 739–747, 2014.
- B. Schölkopf and A. Smola. *Learning with Kernels: Support Vector Machines, Regularization, Optimization and Beyond*. MIT Press, 2002.
- B. Shahriari, K. Swersky, Z. Wang, R. P. Adams, and N. de Freitas. Taking the Human Out of the Loop: A Review of Bayesian Optimization. *Proceedings of the IEEE*, 104(1):148–175, 2015.
- W. Sickel and T. Ullrich. Tensor products of Sobolev–Besov spaces and applications to approximation from the hyperbolic cross. *Journal of Approximation Theory*, 161(2):748–786, 2009.
- V. Sinescu, F. Y. Kuo, and I. H. Sloan. On the choice of weights in a function space for quasi-Monte Carlo methods for a class of generalised response models in statistics. In *Monte Carlo and Quasi-Monte Carlo Methods*. 2012.
- J. Skilling. Bayesian solution of ordinary differential equations. *Maximum Entropy and Bayesian Methods, Seattle*, 1991.
- A. Smola, A. Gretton, L. Song, and B. Schölkopf. A Hilbert space embedding for distributions. In *Proceedings of the 18th International Conference on Algorithmic Learning Theory*, 13–31, 2007.
- I. Sobol. Sensitivity estimates for non linear mathematical models. *Mathematical Modelling and Computational Experiments*, 1:407–414, 1993.
- A. Sommariva and M. Vianello. Numerical cubature on scattered data by radial basis functions. *Computing*, 76(3-4):295–310, 2006.
- L. Song. *Learning via Hilbert space embedding of distributions*. PhD thesis, School of Information Technologies, University of Sydney, 2008.

- A. Sozzetti, P. Giacobbe, M. G. Lattanzi, G. Micela, R. Morbidelli, and G. Tinetti. Astrometric detection of giant planets around nearby M dwarfs: the gaia potential. *Monthly Notices of the Royal Astronomical Society*, 2013.
- I. Steinwart and A. Christmann. *Support vector machines*. Springer Science & Business Media, 2008.
- B. Szabó, A. van der Vaart, and J. van Zanten. Frequentist coverage of adaptive nonparametric Bayesian credible sets. *The Annals of Statistics*, 43(4):1391–1428, 2015.
- M. E. Tipping and C. M. Bishop. Probabilistic Principal Component Analysis. *Journal of the Royal Statistical Society Series B: Statistical Methodology*, 61(3):611–622, 1999.
- H. Triebel. *Theory of Function Spaces II*. Birkhäuser Basel, 1992.
- A. van Der Vaart and H. van Zanten. Information rates of nonparametric Gaussian process methods. *Journal of Machine Learning Research*, 12:2095–2119, 2011.
- G. Wahba. *Spline models for observational data*, volume 59. SIAM, 1990.
- H. Wendland. *Scattered data approximation*. Cambridge University Press, 2005.
- H. Woźniakowski. What is information-based complexity? *Essays on the Complexity of Continuous Problems*, 2009.
- Y. Yang and D. B. Dunson. Bayesian manifold regression. *arXiv:1305.0617*, 2013.
- Y. Yu, P. Debevec, J. Malik, and T. Hawkins. Inverse Global Illumination: Recovering Reflectance Models of Real Scenes from Photographs. In *Proceedings of the 26th annual conference on Computer graphics and interactive techniques (SIGGRAPH '99)*, 215–224, 1999.

Supplements

These appendices supplement the main text by providing complete proofs for theoretical results, extended numerical results and full details to reproduce the experiments presented in the paper.

A Proof of Theoretical Results

Full technical details are provided to establish the theoretical results from the main text:

Proof of Prop. 1. From standard conjugacy results for GPs we have $\mathbb{P}_n = \mathcal{N}(m_n, k_n)$ where $m_n(\mathbf{x}) = m(\mathbf{x}) + \mathbf{k}(\mathbf{x}, X)\mathbf{K}^{-1}(\mathbf{f} - \mathbf{m})$ and $k_n(\mathbf{x}, \mathbf{x}') = k(\mathbf{x}, \mathbf{x}') - \mathbf{k}(\mathbf{x}, X)\mathbf{K}^{-1}\mathbf{k}(X, \mathbf{x}')$ (Chap. 2 of Rasmussen and Williams, 2006).

Repeated application of Fubini's theorem produces

$$\begin{aligned} \mathbb{E}_n[\Pi[f]] &= \mathbb{E}_n \left[\int_{\mathcal{X}} f \, d\Pi \right] = \int_{\mathcal{X}} \mathbb{E}_n[f] \, d\Pi = \int_{\mathcal{X}} m_n \, d\Pi \\ \mathbb{V}_n[\Pi[f]] &= \int_{\mathcal{F}} \left[\int_{\mathcal{X}} f \, d\Pi - \int_{\mathcal{X}} m_n \, d\Pi \right]^2 \mathbb{P}_n[df] \\ &= \int_{\mathcal{X}} \int_{\mathcal{X}} \int_{\mathcal{F}} [f(\mathbf{x}) - m_n(\mathbf{x})][f(\mathbf{x}') - m_n(\mathbf{x}')] \mathbb{P}_n[df] \Pi(d\mathbf{x})\Pi(d\mathbf{x}') \\ &= \int_{\mathcal{X}} \int_{\mathcal{X}} k_n(\mathbf{x}, \mathbf{x}') \Pi(d\mathbf{x})\Pi(d\mathbf{x}'). \end{aligned}$$

The proof is completed by substituting the expressions for m_n and k_n above. \square

Proposition 4. *Suppose that $R = \int_{\mathcal{X}} k(\mathbf{x}, \mathbf{x}) \Pi(d\mathbf{x}) < \infty$. Then $f \in L^2(\Pi)$ for all $f \in \mathcal{H}$.*

Proof. From the reproducing property and Cauchy-Schwarz:

$$\begin{aligned} \|f\|_2^2 &= \int_{\mathcal{X}} f^2 \, d\Pi = \int_{\mathcal{X}} \langle f, k(\cdot, \mathbf{x}) \rangle_{\mathcal{H}}^2 \Pi(d\mathbf{x}) \\ &\leq \int_{\mathcal{X}} \|f\|_{\mathcal{H}}^2 k(\mathbf{x}, \mathbf{x}) \Pi(d\mathbf{x}) = R \|f\|_{\mathcal{H}}^2, \end{aligned}$$

which establishes the result. \square

Proof of Prop. 3. Combining Prop. 2 with direct calculation gives that

$$\begin{aligned} e(\hat{\Pi}; \Pi, \mathcal{H})^2 &= \|\mu(\hat{\Pi}) - \mu(\Pi)\|_{\mathcal{H}}^2 = \sum_{i,j=1}^n w_i w_j k(\mathbf{x}_i, \mathbf{x}_j) - 2 \sum_{i=1}^n w_i \int_{\mathcal{X}} k(\mathbf{x}, \mathbf{x}_i) \Pi(d\mathbf{x}) \\ &\quad + \int_{\mathcal{X}} \int_{\mathcal{X}} k(\mathbf{x}, \mathbf{x}') \Pi(d\mathbf{x})\Pi(d\mathbf{x}') \\ &= \mathbf{w}^T \mathbf{K} \mathbf{w} - 2\mathbf{w}^T \Pi[\mathbf{k}(X, \cdot)] + \Pi[\Pi[k(\cdot, \cdot)]] \end{aligned}$$

as required. \square

The result, below summarises the conclusion from Sec. 2.3:

Lemma 3 (Bayesian re-weighting). *Let $f \in \mathcal{H}$. Consider the quadrature rule $\hat{\Pi}[f] = \sum_{i=1}^n w_i f(\mathbf{x}_i)$ and the corresponding re-weighted rule $\hat{\Pi}_{BQ}[f] = \sum_{i=1}^n w_i^{BQ} f(\mathbf{x}_i)$; the BQ rule based on \mathcal{H} . Then $e(\hat{\Pi}_{BQ}; \Pi, \mathcal{H}) \leq e(\hat{\Pi}; \Pi, \mathcal{H})$.*

Thus probabilistic integrators provide a point estimate that is *at least as good* as their non-probabilistic versions and consistency of the non-probabilistic integrators is therefore a sufficient condition to prove consistency of the probabilistic counterparts.

The convergence rate of quadrature rules can be shown to be at least as good as the corresponding functional approximation rates in $L^2(\Pi)$. This is summarised as follows:

Lemma 4 (Regression bound). *Let $f \in \mathcal{H}$ and fix states $\{\mathbf{x}_i\}_{i=1}^n \in \mathcal{X}$. Then we have $|\Pi[f] - \hat{\Pi}_{BQ}[f]| \leq \|f - \mathbb{E}_n[f]\|_2$.*

Proof. This is an application of Jensen's inequality:

$$\begin{aligned} |\Pi[f] - \hat{\Pi}_{BQ}[f]|^2 &= \left(\int_{\mathcal{X}} f \, d\Pi - \int_{\mathcal{X}} \mathbb{E}_n[f] \, d\Pi \right)^2 \\ &\leq \int_{\mathcal{X}} (f - \mathbb{E}_n[f])^2 \, d\Pi = \|f - \mathbb{E}_n[f]\|_2^2, \end{aligned}$$

as required. □

Note that this regression bound is not sharp in general (Ritter, 2000, Prop. II.4).

Lemmas 3 and 4 refer to the point estimators provided by BQ rules. However, we also aim to quantify the change in probability mass as the number of samples increases:

Lemma 5 (BQ contraction). *Assume $f \in \mathcal{H}$. Suppose that $e(\hat{\Pi}_{BQ}; \Pi, \mathcal{H}) \leq \delta_n$ where $\delta_n \rightarrow 0$. Define $I_D = [\Pi[f] - D, \Pi[f] + D]$ to be an interval of radius D centred on the true value of the integral. Then $\mathbb{P}_n[I_D^c]$, the posterior mass on $I_D^c = \mathbb{R} \setminus I_D$, vanishes at the rate $\mathbb{P}_n[I_D^c] = O(\delta_n \exp(-(D^2/2)\delta_n^{-2}))$.*

Proof. Assume without loss of generality that $D < \infty$. The posterior distribution over $\Pi[f]$ is Gaussian with mean m_n and variance v_n . Since $v_n = e^2(\hat{\Pi}_{BQ}; \Pi, \mathcal{H})$ we have $v_n \leq \delta_n^2$. Now the posterior probability mass on I_D^c is given by $\mathbb{P}_n[I_D^c] = \int_{I_D^c} \phi(r|m_n, v_n) dr$, where $\phi(r|m_n, v_n)$ is the p.d.f. of the $\mathcal{N}(m_n, v_n)$ distribution. From the definition of D we get the upper bound

$$\begin{aligned} \mathbb{P}_n[I_D^c] &\leq \int_{-\infty}^{\Pi[f]-D} \phi(r|m_n, v_n) dr + \int_{\Pi[f]+D}^{\infty} \phi(r|m_n, v_n) dr \\ &= 1 + \underbrace{\Phi\left(\frac{\Pi[f] - m_n}{\sqrt{v_n}} - \frac{D}{\sqrt{v_n}}\right)}_{(*)} - \underbrace{\Phi\left(\frac{\Pi[f] - m_n}{\sqrt{v_n}} + \frac{D}{\sqrt{v_n}}\right)}_{(*)}. \end{aligned}$$

From the definition of the WCE we have that the terms $(*)$ are bounded by $\|f\|_{\mathcal{H}} < \infty$, so that asymptotically as $v_n \downarrow 0$ we have

$$\begin{aligned} \mathbb{P}_n[I_D^c] &\lesssim 1 + \Phi(-D/\sqrt{v_n}) - \Phi(D/\sqrt{v_n}) \\ &\lesssim 1 + \Phi(-D/\delta_n) - \Phi(D/\delta_n) \\ &\lesssim \operatorname{erfc}(D/\sqrt{2}\delta_n). \end{aligned}$$

The result follows from the fact that $\operatorname{erfc}(x) \lesssim x^{-1} \exp(-x^2/2)$. \square

This result demonstrates that the posterior distribution is well-behaved; probability mass concentrates on the true solution as n increases. Hence, if our prior is well calibrated (see Sec. 4.1), the posterior distribution provides valid uncertainty quantification over the solution of the integral as a result of performing a finite number n of function evaluations.

Define the *fill distance* of the set $X = \{\mathbf{x}_i\}_{i=1}^n$ of states as

$$h_X = \sup_{\mathbf{x} \in \mathcal{X}} \min_{i=1, \dots, n} \|\mathbf{x} - \mathbf{x}_i\|_2.$$

As $n \rightarrow \infty$ the scaling of the fill distance is described by the following:

Lemma 6. *Let $g : [0, \infty) \rightarrow [0, \infty)$ be continuous, monotone increasing, and satisfy $g(0) = 0$ and $\lim_{x \downarrow 0} g(x) \exp(x^{-3d}) = \infty$. Suppose further $\mathcal{X} = [0, 1]^d$, Π has a density π that is bounded away from zero on \mathcal{X} , and $X = \{\mathbf{x}_i\}_{i=1}^n$ are samples from an uniformly ergodic Markov chain targeting Π . Then we have $\mathbb{E}_X[g(h_X)] = O(g(n^{-1/d+\epsilon}))$ where $\epsilon > 0$ can be arbitrarily small.*

Proof. A special case of Lemma 2, Oates et al. (2016a). \square

Proof of Thm. 2. Initially consider fixed states $X = \{\mathbf{x}_i\}_{i=1}^n$ (i.e. fixing the random seed) and $\mathcal{H} = \mathcal{H}_\alpha$. From a now standard result in functional approximation due to Wu and Schaback (1993), see also Wendland (2005, Thm. 11.13) there exists $C > 0$ and $h_0 > 0$ such that, for all $\mathbf{x} \in \mathcal{X}$ and $h_X < h_0$,

$$|f(\mathbf{x}) - \mathbb{E}_n[f(\mathbf{x})]| \leq Ch_X^\alpha \|f\|_{\mathcal{H}}.$$

(For other kernels, alternative bounds are well-known; Wendland, 2005, Table 11.1). We augment X with a finite number of states $Y = \{\mathbf{y}_i\}_{i=1}^m$ to ensure that $h_{X \cup Y} < h_0$ always holds. Then from the regression bound (Lemma 4),

$$\begin{aligned} |\hat{\Pi}_{\text{BMCMC}}[f] - \Pi[f]| &\leq \|f - \mathbb{E}_n[f]\|_2 = \left(\int_{\mathcal{X}} (f(\mathbf{x}) - \mathbb{E}_n[f(\mathbf{x})])^2 \Pi(d\mathbf{x}) \right)^{1/2} \\ &\leq \left(\int_{\mathcal{X}} (Ch_{X \cup Y}^\alpha \|f\|_{\mathcal{H}})^2 \Pi(d\mathbf{x}) \right)^{1/2} = Ch_{X \cup Y}^\alpha \|f\|_{\mathcal{H}}. \end{aligned}$$

It follows that $e(\hat{\Pi}_{\text{BMCMC}}; \Pi, \mathcal{H}_\alpha) \leq Ch_{X \cup Y}^\alpha$. Now, taking an expectation \mathbb{E}_X over the sample path $X = \{\mathbf{x}_i\}_{i=1}^n$ of the Markov chain, we have that

$$\mathbb{E}_X e(\hat{\Pi}_{\text{BMCMC}}; \Pi, \mathcal{H}_\alpha) \leq C \mathbb{E}_X h_{X \cup Y}^\alpha \leq C \mathbb{E}_X h_X^\alpha. \quad (7)$$

From Lemma 6 above, we have a scaling relationship such that, for $h_{XUY} < h_0$, we have $\mathbb{E}_X h_X^\alpha = O(n^{-\alpha/d+\epsilon})$ for $\epsilon > 0$ arbitrarily small. From Markov's inequality, convergence in mean implies convergence in probability and thus, using Eqn. 7, we have $e(\hat{\Pi}_{\text{BMCMC}}; \Pi, \mathcal{H}) = O_P(n^{-\alpha/d+\epsilon})$. This completes the proof for $\mathcal{H} = \mathcal{H}_\alpha$. More generally, if \mathcal{H} is norm-equivalent to \mathcal{H}_α then the result follows from the fact that $e(\hat{\Pi}_{\text{BMCMC}}; \Pi, \mathcal{H}) \leq \lambda e(\hat{\Pi}_{\text{BMCMC}}; \Pi, \mathcal{H}_\alpha)$ for some $\lambda > 0$. \square

Proof of Thm. 3. From Theorem 15.21 of Dick and Pillichshammer (2010), which assumes $\alpha \geq 2$, $\alpha \in \mathbb{N}$, the QMC rule $\hat{\Pi}_{\text{QMC}}$ based on a higher-order digital $(t, \alpha, 1, \alpha m \times m, d)$ net over \mathbb{Z}_b for some prime b satisfies

$$e(\hat{\Pi}_{\text{QMC}}; \Pi, \mathcal{H}) \leq C_{d,\alpha} \frac{(\log n)^{d\alpha}}{n^\alpha} = O(n^{-\alpha+\epsilon})$$

for \mathcal{S}_α the Sobolev space of dominating mixed smoothness order α , where $C_{d,\alpha} > 0$ is a constant that depends only on d and α (but not on n). The result follows immediately from Bayesian re-weighting (Lemma 3) and norm equivalence. The contraction rate is obtained by applying Lemma 5. \square

Proof of Lemma 2. Define $\mathbf{z} = \Pi[\mathbf{k}(X, \cdot)]$ and ${}_a\mathbf{z} = {}_a\Pi[\mathbf{k}(X, \cdot)]$. Let $\boldsymbol{\epsilon} = {}_a\mathbf{z} - \mathbf{z}$, write ${}_a\hat{\Pi}_{\text{BQ}} = \sum_{i=1}^n {}_a w_i^{\text{BQ}} \delta(\cdot - \mathbf{x}_i)$ and consider

$$\begin{aligned} e^2({}_a\hat{\Pi}_{\text{BQ}}; \Pi, \mathcal{H}) &= \|\mu({}_a\hat{\Pi}_{\text{BQ}}) - \mu(\Pi)\|_{\mathcal{H}}^2 \\ &= \left\langle \sum_{i=1}^n {}_a w_i^{\text{BQ}} k(\cdot, \mathbf{x}_i) - \int_{\mathcal{X}} k(\cdot, \mathbf{x}) \Pi(d\mathbf{x}), \sum_{i=1}^n {}_a w_i^{\text{BQ}} k(\cdot, \mathbf{x}_i) - \int_{\mathcal{X}} k(\cdot, \mathbf{x}) \Pi(d\mathbf{x}) \right\rangle_{\mathcal{H}} \\ &= {}_a \mathbf{w}_{\text{BQ}}^T \mathbf{K} {}_a \mathbf{w}_{\text{BQ}} - 2 {}_a \mathbf{w}_{\text{BQ}}^T \mathbf{z} + \Pi[\mu(\Pi)] \\ &= (\mathbf{K}^{-1} {}_a \mathbf{z})^T \mathbf{K} (\mathbf{K}^{-1} {}_a \mathbf{z}) - 2 (\mathbf{K}^{-1} {}_a \mathbf{z})^T \mathbf{z} + \Pi[\mu(\Pi)] \\ &= (\mathbf{z} + \boldsymbol{\epsilon})^T \mathbf{K}^{-1} (\mathbf{z} + \boldsymbol{\epsilon}) - 2 (\mathbf{z} + \boldsymbol{\epsilon})^T \mathbf{K}^{-1} \mathbf{z} + \Pi[\mu(\Pi)] \\ &= e^2(\hat{\Pi}_{\text{BQ}}; \Pi, \mathcal{H}) + \boldsymbol{\epsilon}^T \mathbf{K}^{-1} \boldsymbol{\epsilon}. \end{aligned}$$

We use \otimes to denote the tensor product of RKHS. Now, since

$$\boldsymbol{\epsilon}_i = {}_a z_i - z_i = \mu({}_a\hat{\Pi})(\mathbf{x}_i) - \mu(\Pi)(\mathbf{x}_i) = \langle \mu({}_a\hat{\Pi}) - \mu(\Pi), k(\cdot, \mathbf{x}_i) \rangle_{\mathcal{H}},$$

we have:

$$\begin{aligned} \boldsymbol{\epsilon}^T \mathbf{K}^{-1} \boldsymbol{\epsilon} &= \sum_{i,i'} [\mathbf{K}^{-1}]_{i,i'} \langle \mu({}_a\hat{\Pi}) - \mu(\Pi), k(\cdot, \mathbf{x}_i) \rangle_{\mathcal{H}} \langle \mu({}_a\hat{\Pi}) - \mu(\Pi), k(\cdot, \mathbf{x}_{i'}) \rangle_{\mathcal{H}} \\ &= \left\langle (\mu({}_a\hat{\Pi}) - \mu(\Pi)) \otimes (\mu({}_a\hat{\Pi}) - \mu(\Pi)), \sum_{i,i'} [\mathbf{K}^{-1}]_{i,i'} k(\cdot, \mathbf{x}_i) \otimes k(\cdot, \mathbf{x}_{i'}) \right\rangle_{\mathcal{H} \otimes \mathcal{H}} \\ &\leq \|\mu({}_a\hat{\Pi}) - \mu(\Pi)\|_{\mathcal{H}}^2 \left\| \sum_{i,i'} [\mathbf{K}^{-1}]_{i,i'} k(\cdot, \mathbf{x}_i) \otimes k(\cdot, \mathbf{x}_{i'}) \right\|_{\mathcal{H} \otimes \mathcal{H}}. \end{aligned}$$

From Prop. 2 we have $\|\mu({}_a\hat{\Pi}) - \mu(\Pi)\|_{\mathcal{H}} = e({}_a\hat{\Pi}; \Pi, \mathcal{H})$ so it remains to show that the second term is equal to \sqrt{n} . Indeed,

$$\begin{aligned} \left\| \sum_{i,i'} [\mathbf{K}^{-1}]_{i,i'} k(\cdot, \mathbf{x}_i) \otimes k(\cdot, \mathbf{x}_{i'}) \right\|_{\mathcal{H}}^2 &= \sum_{i,i',l,l'} [\mathbf{K}^{-1}]_{i,i'} [\mathbf{K}^{-1}]_{l,l'} \langle k(\cdot, \mathbf{x}_i) \otimes k(\cdot, \mathbf{x}_{i'}), k(\cdot, \mathbf{x}_l) \otimes k(\cdot, \mathbf{x}_{l'}) \rangle_{\mathcal{H}} \\ &= \sum_{i,i',l,l'} [\mathbf{K}^{-1}]_{i,i'} [\mathbf{K}^{-1}]_{l,l'} [\mathbf{K}]_{il} [\mathbf{K}]_{i'l'} = \text{tr}[\mathbf{K} \mathbf{K}^{-1} \mathbf{K} \mathbf{K}^{-1}] = n. \end{aligned}$$

This completes the proof. \square

B Beyond Sobolev Spaces

In this supplement we extend the theoretical results provided for B(MC)MC in Supplement A to RKHS which are not Sobolev spaces. We show convergence rates for these probabilistic integrators for any RKHS in situations where we have access to an upper bound on the $L^\infty(\mathcal{X})$ error:

$$\sup_{\mathbf{x} \in \mathcal{X}} |f(\mathbf{x}) - \mathbb{E}_n[f(\mathbf{x})]| \leq Cg(h_X) \|f\|_{\mathcal{H}}, \quad (8)$$

where the role of g can be compared with that of the *power function* in the scattered data approximation literature (see Wendland (2005)[Sec. 11.1] for more details on this function). For example, for \mathcal{H}_α we have $g(h_X) = h_X^\alpha$; this was the basis of our analysis of B(MC)MC. The results presented below hold for B(MC)MC, but can also be obtained for various QMC sequences and nets (not presented).

The following is a slight generalisation of Thm. 2:

Theorem 4 (Convergence and contraction rates of B(MC)MC). *Let $\mathcal{X} = [0, 1]^d$ and let Π admit a density π that is bounded away from zero on \mathcal{X} . Consider $X = \{\mathbf{x}_i\}_{i=1}^n$ to be samples from an uniformly ergodic Markov chain targeting Π . Suppose Eqn. 8 is satisfied for all $h_X < h_0$, for some $h_0 < \infty$, where g is a continuous, monotone increasing function $g : [0, \infty) \rightarrow [0, \infty)$ satisfying $g(0) = 0$ and $\lim_{x \downarrow 0} g(x) \exp(x^{-3d}) = \infty$. Then, $e(\hat{\Pi}_{BMC}; \Pi, \mathcal{H}) = O_P(g(m^{-1/d+\epsilon}))$ for all $\epsilon > 0$ arbitrarily small.*

Proof. Following the reasoning of the proof of Thm. 2, we obtain that

$$|\hat{\Pi}_{BMC}[f] - \Pi[f]| \leq Cg(h_{X \cup Y}) \|f\|_{\mathcal{H}},$$

where we have again augmented the data set from X to $X \cup Y$ to ensure $h_{X \cup Y} \leq h_0$. Taking expectations, we then get the following upper bound: $\mathbb{E}_X[e(\hat{\Pi}_{BMC}; \Pi, \mathcal{H})] \leq \mathbb{E}_X[g(h_{X \cup Y})]$. Now, Lemma 6 shows that $\mathbb{E}_X[g(h_{X \cup Y})] = O(g(m^{-1/d+\epsilon}))$, which leads to $\mathbb{E}_X[e(\hat{\Pi}_{BMC}; \Pi, \mathcal{H})] = O(g(m^{-1/d+\epsilon}))$. The result $e(\hat{\Pi}_{BMC}; \Pi, \mathcal{H}) = O_P(g(m^{-1/d+\epsilon}))$ follows by noting that convergence in expectation implies convergence in probability. \square

These generalisations allow us to obtain convergence rates for B(MC)MC and BQMC based on three kernels extensively used in the statistics literature:

- *Gaussian* kernel: $k(\mathbf{x}, \mathbf{y}) = \exp(-\|\mathbf{x} - \mathbf{y}\|_2^2/2\sigma^2)$, $\sigma \in (0, \infty)$.
- *Multi-Quadric* (MQ) kernel: $k(\mathbf{x}, \mathbf{y}) = (-1)^{\lceil \beta \rceil} (c^2 + \|\mathbf{x} - \mathbf{y}\|_2^2)^\beta$, $\beta \in \mathbb{N}_0$ & $c \in \mathbb{R}$.
- *Inverse Multi-Quadric* (Inverse MQ) kernel: $k(\mathbf{x}, \mathbf{y}) = (c^2 + \|\mathbf{x} - \mathbf{y}\|_2^2)^{-\beta}$, $\beta \in \mathbb{N}_0$ & $c \in \mathbb{R}$.

For simplicity we present results for the convergence of WCE, but note that Lemma 5 immediately implies specific rates for posterior contraction:

Corollary 1 (Gaussian, MQ and inverse MQ kernels). *Under the hypotheses of Thm. 4, let k be any of the Gaussian, MQ or inverse MQ kernels. Then there exists $c \in (0, \infty)$ such that $e(\hat{\Pi}_{BMC}; \Pi, \mathcal{H}) = O_P(\exp(-cn^{1/d-\epsilon}))$ for all $\epsilon > 0$ arbitrarily small.*

Proof. Using Table 11.1 in Wendland (2005), we obtain upper bounds on the power function for the Gaussian, MQ and inverse MQ kernels. In the case of the Gaussian, this is given by $g_1(h_X) = \exp(-c_1|\log(h_X)|/h_X) = \exp(-c_1/h_X^{1-\epsilon'})$ for some $c_1 > 0$ and $\epsilon' > 0$ arbitrarily small. For the MQ and inverse MQ kernels this is $g_2(h_X) = \exp(-c_2/h_X)$ for some $c_2 > 0$. We are now interested in the behaviour of the WCE, which we obtain using Theorem 4. For the Gaussian kernel, this is given by

$$e(\hat{\Pi}_{BMC}; \Pi, \mathcal{H}) = O_P(g_1(n^{-1/d+\epsilon})) = O_P(\exp(-c_1n^{1/d-\epsilon''})),$$

where $\epsilon'' > 0$ can be arbitrarily small, whilst for the MQ and inverse MQ we have

$$e(\hat{\Pi}_{BMC}; \Pi, \mathcal{H}) = O_P(g_2(n^{-1/d+\epsilon})) = O_P(\exp(-c_2n^{1/d-\epsilon})).$$

This completes the proof. □

We note that results can also easily be obtained for power kernels, thin-plate splines and Wendland kernels using the bounds provided in (Wendland, 2005, Sec. 11).

Finally, we note that all of the theoretical results in the main text as well as the present section can be generalised to domains satisfying interior cone conditions. Following Wendland (2005)[Sec. 3.3], a domain $\mathcal{X} \in \mathbb{R}^d$ is said to satisfy an *interior cone condition* if there exists an angle $\theta \in (0, \pi/2)$ and a radius $r > 0$ such that $\forall \mathbf{x} \in \mathcal{X}$, a unit vector $\boldsymbol{\xi}(\mathbf{x})$ exists such that the following cone is contained in \mathcal{X} :

$$C(\mathbf{x}, \boldsymbol{\xi}(\mathbf{x}), \theta, r) := \left\{ \mathbf{x} + \lambda \mathbf{y} : \mathbf{y} \in \mathbb{R}^d, \|\mathbf{y}\|_2 = 1, \mathbf{y}^T \boldsymbol{\xi}(\mathbf{x}) \geq \cos \theta, \lambda \in [0, r] \right\}.$$

This condition essentially excludes domains with pinch-points on the boundaries, i.e. regions with a \prec shape. The main step involved in generalisation the domain is to establish Lemma 6 in more general domains. This contribution was made in Oates et al. (2016a).

C Scalability, Stability and Tractability

C.1 Scalability in the Number of States

In situations where f is cheap to evaluate, the naive $O(n^3)$ computational cost associated with kernel matrix inversion renders BQ more computationally intensive relative to the $O(n)$ cost of (MC)MC and QMC methods. However, when f is expensive to evaluate, n will be sufficiently small that BQ methods prove considerably more effective than their standard counterparts. We discuss below several approaches to improving the scalability of BQ, based on the extensive literature on scaling Gaussian processes and other spline-related models.

Exact inversion can be achieved at low cost through exploiting structure in the kernel matrix. Examples include: the use of kernels with compact support (e.g. Wendland, 2005, Sec. 9) to induce sparsity in the kernel matrix; tensor product kernels (e.g. O’Hagan, 1991) in the context of inverting kernel matrices defined by tensor products of point sets in multivariate problems; using Toeplitz solvers for a stationary kernel evaluated on an evenly-spaced point set; and making use of low-rank kernels (e.g. polynomial kernels).

In addition there are many approximate techniques: (i) Reduced rank approximations reduce the computational cost to $O(nm^2)$ where $m \ll n$ is a parameter controlling the accuracy of the approximation, essentially an effective degree of freedom (Quinonero-Candela and Rasmussen, 2005; Bach, 2013; El Alaoui and Mahoney, 2015). (ii) Explicit feature maps designed for additive kernels (Vedaldi and Zisserman, 2012). (iii) Local approximations (Gramacy and Apley, 2015), training only on nearest neighbour data. (iv) Multi-scale approximations, whereby the high-level structure is modelled using a full GP and approximation schemes are applied to lower-level structure (Katzfuss, 2015). (v) Fast multipole methods (Wendland, 2005)[Sec.15.1]. (vi) Random approximations of the kernel itself, rather than the kernel matrix, such as random Fourier features (RFF; Rahimi and Recht, 2007), spectral methods (Lazaro-Gredilla et al., 2010; Bach, 2015) and hash kernels (Shi et al., 2009). (RFF have previously been successfully applied in BQ by Briol et al. (2015).) (vii) Parallel programming provides an alternative perspective on complexity reduction, as discussed in (e.g.) Dai et al. (2014).

This does not represent an exhaustive list of the (growing) literature on GP computation. We note that efficient use of data structures (Wendland, 2005)[Sec. 14] may also provide significant computational improvements. Note that the latter do not come with probability models for the additional source of numerical error introduced by the approximation. This could therefore be considered to be sacrificing the philosophical advantages of the probabilistic numerical framework.

C.2 Scalability in Dimension

High-dimensional integrals that arise in applications are, in many cases, effectively low-dimensional problems. This can occur either (i) when the distribution Π is effectively concentrated in a low-dimensional manifold in \mathcal{X} (this is responsible for the excellent performance of (MC)MC in certain high-dimensional settings), or (ii) when the integrand f depends on

only a subset of its inputs, possibly after a transformation (this is responsible for the excellent performance of QMC methods in certain high-dimensional settings; Dick et al., 2013). The B(MC)MC and BQMC methods that we study provably deliver performance that is at least equivalent to (MC)MC and QMC in settings (i) and (ii) respectively (see Sec. 5.2.3 for an empirical example with $d = 50$). Conversely, when neither Π nor f are effectively low-dimensional, all approaches to integration necessarily suffer from a curse of dimension. For example, for Π uniform on $\mathcal{X} = [0, 1]^d$ and f belonging to a general Sobolev space of order α , no deterministic integration algorithm can exceed the $O(n^{-\alpha/d})$ rate. Clearly this rate becomes arbitrarily slow as d tends to infinity. Nevertheless, we note that BQ estimators remain coherent, reverting to the prior in this degenerate limit. Having weights that tend to zero is natural from a Bayesian point of view since our approximation of the integrand f will become very poor as d grows with n fixed.

We briefly note that a number of alternative approaches exist for problems in which the effective dimensionality is low. In particular, low-dimensional random embeddings project the ambient space into a lower dimensional space using a randomized map, perform computation in that space and then map back the results to the original space (see e.g. Wang et al., 2013, in the context of Bayesian optimisation).

C.3 Regularisation and Noisy Observations

This supplement studies the impact of numerical regularisation of the kernel matrix on estimator performance. Indeed, it is well known that instability in the numerical inversion of the kernel matrix \mathbf{K} can sometimes lead to a loss of performance (Schaback, 1995) (see for example Fig. 13, left-hand side). Several techniques have been developed to counteract this issue. Examples include pre-conditioning of the kernel matrix and change of basis tricks (i.e. finding a different kernel spanning the same space of functions but for which the conditioning of the kernel matrix is improved). We refer the interested reader to Wendland (2005)[Chap. 12] for an overview of available methods.

In this section we focus on a simple trick which consists of replacing \mathbf{K} by $\mathbf{K} + \lambda\mathbf{I}$ for some small $\lambda > 0$. Such regularisation can be interpreted in several ways. If added solely to improve numerical stability, $\lambda\mathbf{I}$ is sometimes referred to as *jitter* or a *nugget* term. However, an alternative interpretation of particular interest here is that the observed function values f_i are corrupted by noise. In this case the posterior variance is naturally inflated (see e.g. Fig. 12). Below we provide a theoretical study of the convergence and contraction of BMC under the assumption of noisy data, which is equivalent to studying the BQ estimator when numerical regularisation is employed.

Consider an homoscedastic Gaussian noise model in which $\mathbf{y} = \mathbf{f} + \mathbf{e}$ is observed, where $\mathbf{e} \sim \mathcal{N}(\mathbf{0}, \tau^{-1}\mathbf{I})$. In this case, using the conjugacy of Gaussian variables, it is possible to get a closed-form expression for the induced quadrature rule $\hat{\Pi}_{\text{BQ}}^{\mathbf{e}}$ and other quantities of interest by replacing \mathbf{f} by \mathbf{y} and adding a constant term to the diagonal of the kernel matrix of size $\lambda = \tau^{-1}$ (Rasmussen and Williams, 2006). This leads to a probabilistic integrator with

$$e^2(\hat{\Pi}_{\text{BQ}}^{\mathbf{e}}; \Pi, \mathcal{H}) = e^2(\hat{\Pi}_{\text{BQ}}; \Pi, \mathcal{H}) + \tau^{-1} \|\mathbf{w}^{\text{BQ}}\|_2^2,$$

see (Bach, 2015, Sec. 3.1). Since the term $\|\mathbf{w}^{\text{BQ}}\|_2$ can in general decay more slowly (as $n \rightarrow \infty$) compared to the WCE term $e(\hat{\Pi}_{\text{BQ}}; \Pi, \mathcal{H})$, it comes as no surprise that convergence rates are slower in the noisy data regime, compared to the noiseless regime. This is made precise in the following:

Lemma 7 (BMC with noisy data). *Let $\mathcal{X} = [0, 1]^d$ and consider data \mathbf{y} generated under the homosecdastic Gaussian noise model. Then:*

1. *If \mathcal{H} is an RKHS in the intersection of the Sobolev space \mathcal{H}_α and the Hölder space \mathcal{C}_α for $\alpha > d/2$, we have $e(\hat{\Pi}_{\text{BMC}}^e; \Pi, \mathcal{H}) = O_P(n^{-\alpha/(2\alpha+d)})$ and $\mathbb{P}_n[I_D^e] = o_P(\exp(-Cn^{2\alpha/(2\alpha+d)}))$.*
2. *If \mathcal{H} is an RKHS with Gaussian kernel we have $e(\hat{\Pi}_{\text{BMC}}^e; \Pi, \mathcal{H}) = O_P(n^{-1/2+\epsilon})$ and $\mathbb{P}_n[I_D^e] = o_P(\exp(-Cn^{1-\epsilon}))$ where $\epsilon > 0$ can be arbitrarily small.*

Proof of Lemma 7. Initially consider fixed states $\{\mathbf{x}_i\}_{i=1}^n$ (i.e. fixing the random seed). Fix a particular integration problem whose true integrand is $f_0 \in \mathcal{H}$. Since the WCE (squared) coincides with the posterior variance, we have from Jensen's inequality

$$e^2(\hat{\Pi}_{\text{BMC}}^e; \Pi, \mathcal{H}) = \mathbb{E}_n[\Pi[f] - \mathbb{E}_n[\Pi[f]]]^2 = \mathbb{E}_n[\Pi[f - \mathbb{E}_n[f]]]^2 \leq \mathbb{E}_n\|f - \mathbb{E}_n[f]\|_2^2.$$

Here $\mathbb{E}_n = \mathbb{E}[\cdot | \{\mathbf{x}_i^{\text{MC}}, y_i\}_{i=1}^n]$ denotes an expectation with respect to the posterior GP that includes a model for the observation noise. Noting that $\mathbb{E}_n[f]$ is the variational minimiser of the posterior least squares loss, we have $\mathbb{E}_n\|f - \mathbb{E}_n[f]\|_2^2 \leq \mathbb{E}_n\|f - f_0\|_2^2$. Now, taking an expectation \mathbb{E}_X over the states $\{\mathbf{x}_i\}_{i=1}^n$, viewed as independent draws from Π , we have

$$\mathbb{E}_X e^2(\hat{\Pi}_{\text{BMC}}^e; \Pi, \mathcal{H}) \leq \mathbb{E}_X \mathbb{E}_n\|f - f_0\|_2^2. \quad (9)$$

Since the left hand side of Eqn. 7 is independent of f_0 , it suffices to exhibit a particular regression problem f_0 for which the right hand side converges at a known rate. Suppose in addition that $f_0 \in \mathcal{C}_\alpha \cap \mathcal{H}_\alpha$ for $\alpha > d/2$ (this includes for example the function $f_0 \equiv 0$). Then from Theorem 5 of van Der Vaart and van Zanten (2011) we have a scaling relationship $\mathbb{E}_X \mathbb{E}_n\|f - f_0\|_2^2 = O(n^{-2\alpha/(2\alpha+d)})$. From Markov's inequality, convergence in mean implies convergence in probability and thus, combining Eqn. 9 with the scaling relationship, we have $e(\hat{\Pi}_{\text{BMC}}^e; \Pi, \mathcal{H}) = O_P(n^{-\alpha/(2\alpha+d)})$.

On the other hand, if we have a Gaussian kernel then we suppose in addition that f_0 is a restriction to $[0, 1]^d$ of an element of $\mathcal{A}^{\gamma,r}(\mathbb{R}^d)$, for $r \geq 1$ and $\gamma > 0$, defined to be the set of functions whose Fourier transform $\mathfrak{F}f_0$ satisfies $\int \exp(\gamma\|\boldsymbol{\xi}\|^r) |\mathfrak{F}f_0|^2(\boldsymbol{\xi}) d\boldsymbol{\xi} < \infty$. Again, the function $f_0 \equiv 0$ belongs to $\mathcal{A}^{\gamma,r}(\mathbb{R}^d)$. This time, from Theorem 10 of van Der Vaart and van Zanten (2011) we have a scaling relationship $\mathbb{E}_X \mathbb{E}_n\|f - f_0\|_2^2 = O((\log n)^{2/r}/n)$. Since the function $f_0 \equiv 0$ belongs to $\mathcal{A}^{\gamma,r}(\mathbb{R}^d)$ for all $r \geq 1$ we conclude, via Markov's inequality as before, that $e(\hat{\Pi}_{\text{BMC}}^e; \Pi, \mathcal{H}) = O_P(n^{-1/2+\epsilon})$ where $\epsilon > 0$ can be arbitrarily small. This completes the proof. \square

Tsybakov (2008) proves that the first result above is in fact minimax for noisy regression problems. Clearly the effect of measurement noise is to destroy the asymptotic efficiency

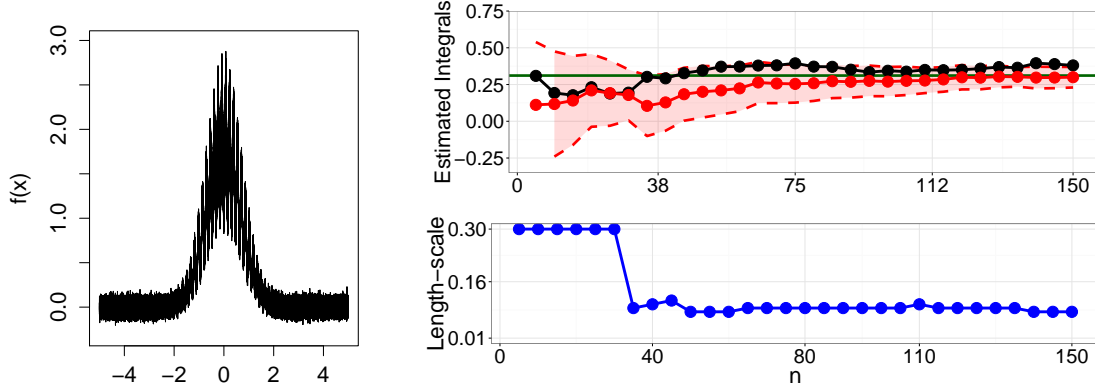


Figure 12: Performance of BMC on test function f_3 with noisy observations. *Left*: Plot of the noisy version of f_3 . *Right*: Estimate of the integral provided by MC (black) and BMC (red) with 95% credible intervals (dotted red lines). BMC performs worse than MC and the calibration provided by EB is over-confident.

of BMC over a simple MC estimator; in fact the BMC estimator can become *worse* than the MC estimator in these instances. This should serve as a warning when dealing with kernel matrices that have poor condition number and necessitate careful monitoring of this condition number in computer code.

We now investigate the issue of noisy data on our test functions from Sec. 5.1, incorporating the fact that we have noisy observations into the BQ estimator. In particular, we consider estimating f_2 with $\mathcal{N}(0, 0.05^2)$ measurement error (see Fig. 12, left). As shown on the left-hand side of Fig. 12, the EB procedure manages to pick up the fact that we are getting noisy observations and adapts uncertainty adequately (here we fix $\lambda = 1$ and optimize σ). In fact, Fig. 13 demonstrates that we get very accurate coverage of the credible intervals obtained using EB for this “hard” test function.

C.4 Intractable Kernel Means

This supplement elaborates on the approach to intractable kernel means proposed in Sec. 4.2. Specifically, we address the point that while ${}_a\hat{\Pi}_{\text{BQ}}$ is available analytically, it is not directly possible to compute the associated posterior variance, which involves the (intractable) kernel mean. The purpose of this section is to establish a computable upper bound for the posterior variance. The idea is to make use of the triangle inequality:

$$e({}_a\hat{\Pi}_{\text{BQ}}; \Pi, \mathcal{H}) \leq e({}_a\hat{\Pi}_{\text{BQ}}; {}_a\Pi, \mathcal{H}) + e({}_a\Pi; \Pi, \mathcal{H}). \quad (10)$$

The first term on the RHS is now available analytically; from Prop. 1 its square is ${}_a\Pi {}_a\Pi [k(\cdot, \cdot)] - {}_a\Pi [k(\cdot, X)] \mathbf{K}^{-1} {}_a\Pi [k(X, \cdot)]$. For the second term, explicit upper bounds exist in the case where states ${}_a\mathbf{x}_i$ are independent random samples from Π . For instance, from (Song, 2008,

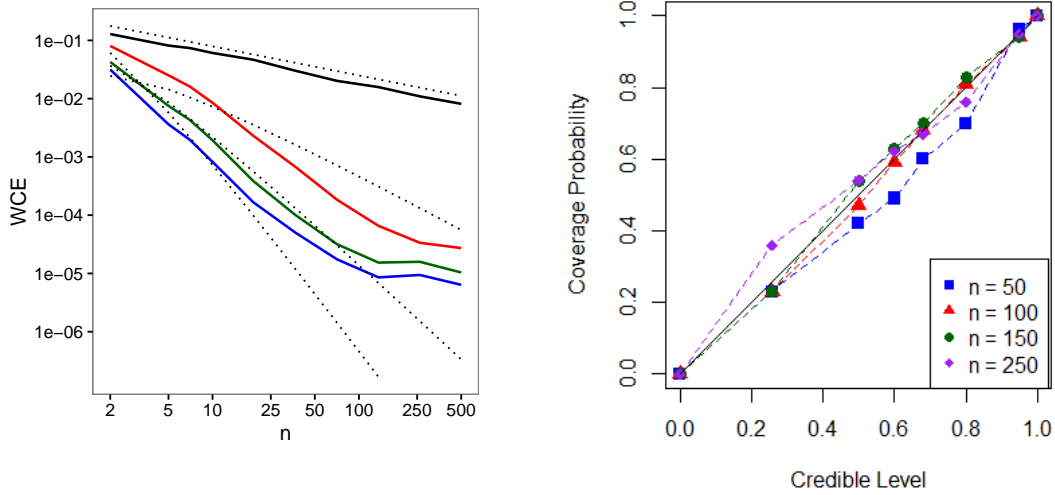


Figure 13: Performance in the noisy data case. *Left*: Plot of the convergence of BMC on $\mathcal{X} = [0.1]$ with length-scale parameter taking value 2. Here, \mathbf{K} is unstable and the nugget term is increased whenever numerical inversion is not possible. Every time this is the case, the rates can be seen to slow down. *Right*: Frequentist coverage of credible intervals for test function f_3 . The empirical Bayes procedure accounts for the observation noise and inflates the credible intervals appropriately.

Thm. 27) we have, for a radial kernel k , uniform ${}_a w_j = m^{-1}$ and independent ${}_a \mathbf{x}_i \sim \Pi$,

$$e({}_a \Pi; \Pi, \mathcal{H}) \leq \frac{2}{\sqrt{m}} \sup_{\mathbf{x}} \sqrt{k(\mathbf{x}, \mathbf{x})} + \sqrt{\frac{\log(2/\delta)}{2m}} \quad (11)$$

with probability at least $1 - \delta$. (For dependent ${}_a \mathbf{x}_j$, the m in Eqn. 11 can be replaced with an estimate for the effective sample size.) Write $C_{n,\alpha,\delta}$ for a $100(1 - \alpha)\%$ credible interval for $\Pi[f]$ defined by the conservative upper bound described in Eqns. 10 and 11. Then we conclude that $C_{n,\alpha,\delta}$ is $100(1 - \alpha)\%$ credible interval with probability at least $1 - \delta$.

Note that, even though the credible region has been inflated, it still contracts to the truth, since the first term on the RHS in Lemma 2 can be bounded by the sum of $e({}_a \hat{\Pi}_{\text{BQ}}; \Pi, \mathcal{H})$ and $e({}_a \Pi; \Pi, \mathcal{H})$, both of which vanish as $n, m \rightarrow \infty$. The resulting (conservative) posterior ${}_a \mathbb{P}_n$ can be viewed as an updating of beliefs based on an approximation to the likelihood function; the statistical foundations of such an approach are made clear in the recent work of Bissiri et al. (2016).

D Additional Numerical Results

This section presents additional numerical results concerning both the calibration of uncertainty and an empirical assessment of the convergence rates proved in this paper.

D.1 Assessment of Uncertainty Quantification

In this subsection, we extend the results of Sec.5.1 to include calibration for multiple parameters and in higher dimensions.

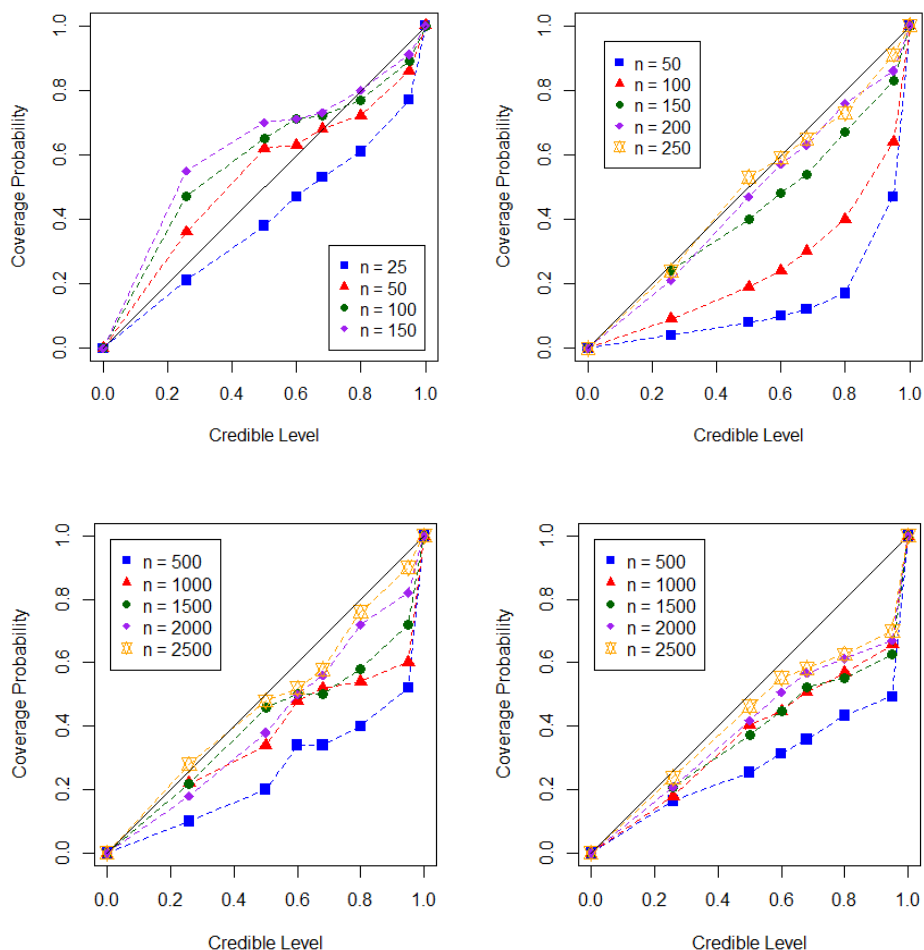


Figure 14: Evaluation of uncertainty quantification provided by EB for the length-scale σ and magnitude λ in $d = 1$ (top plots) or for σ only in $d = 5$ (bottom plots). Coverage frequencies $C_{n,\alpha}$ (computed from 100 (top) or 50 (bottom) realisations) were compared against notional $100(1 - \alpha)\%$ Bayesian credible regions for varying level α . *Left*: function f_1 . *Right*: test function f_2 .

Calibration in 1D In figure 14, we study the quantification of uncertainty provided by empirical Bayes in the same setup as in the main text, but optimizing over both length-scale parameter σ and magnitude parameter λ . For both test functions, we notice that the performance is slightly worse in the “low n ” regime, but becomes accurate for larger n .

Calibration in 5D The experiments of Sec. 5.1, based on BMC, were repeated with the same test functions f_1 and f_2 , with various values of kernel parameter $p = \alpha + 1/2 \in \{3/2, 5/2, 7/2\}$ in dimension $d = 5$. Results are shown in Figs. 14. Clearly, we now require more states to attain a good frequentist coverage of the credible intervals, which is to be expected since covering the space with i.i.d. points will suffer from a curse of dimensionality. However, the coverage becomes accurate for large enough n .

D.2 Posterior Contraction in Sobolev Spaces

Below we empirically validate the theoretical results presented in Sec. 3 for the convergence rates of BMC and BQMC. In particular, we demonstrate that the method satisfies those rates and sometimes even outperforms them.

BMC We study the rates obtained for BMC in the context of Sec. 3.2.1, where the method is proven to have WCE convergence of $O_P(n^{-\alpha/d+\epsilon})$ for any $\alpha > d/2$ and $O_P(n^{-1/2})$ otherwise. Figure 15 (top row) gives the results obtained for $d = 1$ (left) and $d = 5$ (right). In the one dimensional case, the $O_P(n^{-\alpha/d+\epsilon})$ theoretical convergence rates are all attained by the method. At larger values of n , numerical regularisation sees the initially rapid convergence slow down, as predicted by the analysis in Supplement C.3. In the higher dimensional case, the only rate proven in this paper is $O_P(n^{-1/2})$ since $\alpha < d/2$ in all cases $p = \alpha + 1/2 \in \{3/2, 5/2, 7/2\}$ considered. Results show that BMC outperforms the MC rate for all three level of smoothness; further theoretical work is needed to understand this behaviour.

BQMC We study the rates obtained for BQMC based on higher-order digital nets. The theoretical rates provided in Sec. 3.2.3 for this method are $O(n^{-\alpha+\epsilon})$ for any $\alpha > 1/2$. Figure 15 (bottom row) gives the results obtained for $d = 1$ (left) and $d = 5$ (right). In the one dimensional case, the $O(n^{-\alpha+\epsilon})$ theoretical convergence rate is attained by the method in all cases $p = \alpha + 1/2 \in \{3/2, 5/2, 7/2\}$ considered. However, in the $d = 5$ case, the rates are not observed for the number n of evaluations considered. This helps us demonstrate the important point that the rates we provide are asymptotic, and may require large values of n before being observed in practice.

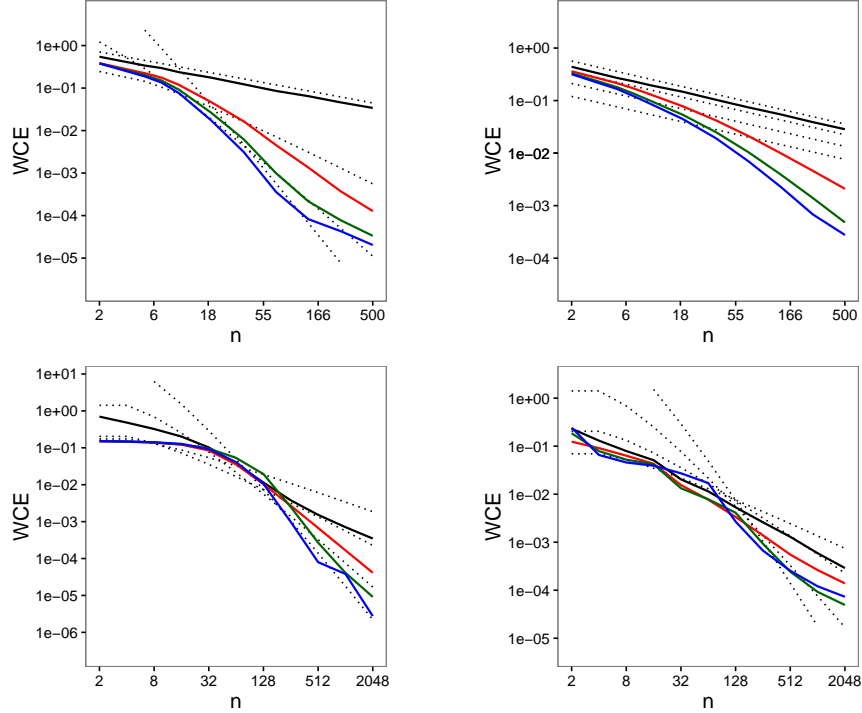


Figure 15: Validation of the BMC & BQMC convergence rates on $[0, 1]^d$ for $d = 1$ (left) and $d = 5$ (right). Here we consider BMC with Sobolev spaces \mathcal{H}_α (top row), and BQMC with Sobolev spaces of mixed dominating smoothness \mathcal{S}_α of dominating mixed smoothness (bottom row). The results are obtained using tensor product Matérn kernels of smoothness $\alpha = 3/2$ (red), $\alpha = 5/2$ (green) and $\alpha = 7/2$ (blue). Dotted lines represent the theoretical convergence rates established for each kernel. The black line represents the corresponding standard Monte Carlo or Quasi-Monte Carlo rate. Kernel parameters were fixed to $(\sigma, \lambda) = (0.02, 1)$ (top left), $(\sigma, \lambda) = (1.2, 1)$ (top right), $(\sigma, \lambda) = (0.005, 1)$ (bottom left) and $(\sigma, \lambda) = (1, 0.5)$ (bottom right).

E Supplementary Information for Case Studies

E.1 Case Study #1

Below we present full details for the simulation study associated with probabilistic thermodynamic integration.

MCMC Established MCMC techniques are available for obtaining samples from power posteriors. In this paper we used the manifold Metropolis-adjusted Langevin algorithm (Girolami and Calderhead, 2011) in combination with population MCMC, a combination also explored by Oates et al. (2016c). Population MCMC shares information across temperatures during sampling, yet previous work has not leveraged evaluation of the log-likelihood f from one sub-chain t_i to inform estimates derived from other sub-chains $t_{i'}, i' \neq i$. In contrast,

this occurs naturally in the probabilistic integration framework, as described in the main text.

Here MCMC was used to generate a small number, $n = 200$, of samples on a per-model basis, in order to simulate a scenario where numerical error in computation of marginal likelihood will be non-negligible. A temperature ladder with $m = 10$ rungs was employed, for the same reason, according to the rule-of-thumb of Calderhead and Girolami (2009). No convergence issues were experienced; the same MCMC set-up has previously been successfully used in Oates et al. (2016c).

Importance Sampling Calderhead and Girolami (2009) advocated the use of a power-law schedule $t_i = (\frac{i-1}{m-1})^5$, $i = 1, \dots, m$, based on an extensive empirical comparison of possible schedules. Observed that a “good” temperature schedule approximately satisfies the criterion

$$|g(t_i)(t_{i+1} - t_i)| \approx m^{-1},$$

on the basis that this allocates equal area to the portions of the curve g that lie between t_i and t_{i+1} , controlling bias for the trapezium rule. Substituting $t_i = (\frac{i-1}{m-1})^5$ into this optimality criterion produces

$$|g(t_i)|((i+1)^5 - i^5) \approx m^4.$$

Now, letting $i = \theta m$

$$|g(\theta^5)|((5\theta^4 m^4 + o(m^4))) \approx m^4.$$

Formally treating θ as continuous and taking the $m \rightarrow \infty$ limit produces

$$|g(\theta^5)| \approx \frac{1}{5\theta^4} \implies |g(t)| \approx \frac{1}{5t^{4/5}}.$$

From this we conclude that the transformed function $h(t) = 5t^{4/5}g(t)$ is approximately stationary and can reasonably be assigned a stationary GP prior. However, in an importance sampling transformation we require that $\pi(t)$ has support over $[0, 1]$. For this reason we took

$$\pi(t) = \frac{1.306}{0.01 + 5t^{4/5}}$$

in our experiments.

Variance Computation The covariance matrix Σ cannot be obtained in closed-form due to intractability of the kernel mean $\Pi_{t_i}[k_f(\cdot, \boldsymbol{\theta})]$. We therefore explored an approximation ${}_a\Sigma$ such that plugging in ${}_a\Sigma$ in place of Σ provides an approximation to the posterior variance $\mathbb{V}_n[\log p(\mathbf{y})]$ for the log-marginal likelihood:

$${}_a\Sigma_{i,j} := {}_a\Pi_{t_i}{}_a\Pi_{t_j}[k_f(\cdot, \cdot)] - {}_a\Pi_{t_i}[\mathbf{k}_f(\cdot, X)]\mathbf{K}_f^{-1}{}_a\Pi_{t_j}[\mathbf{k}_f(X, \cdot)].$$

An empirical distribution ${}_a\Pi = \frac{1}{100} \sum_{i=1}^{100} \delta(\mathbf{x}_i)$ was employed based on the first $m = 100$ samples, while the remaining samples $X = \{\mathbf{x}_i\}_{i=101}^{200}$ were reserved for the kernel computation. This heuristic approach becomes exact as $m \rightarrow \infty$, in the sense that ${}_a\Sigma_{i,j} \rightarrow \Sigma_{i,j}$, but

under-estimated covariance at finite values of m . Results in the main text suggest that the heuristic performs reasonably in practice, in the sense of providing reasonable uncertainty quantification.

We note that the alternative gradient-based kernel construction of Oates et al. (2016a) would permit *exact* computation here, with no need to employ heuristics as above. Our motivation for proceeding with a generic kernel k_f here was not to complicate the presentation by introducing a non-trivial kernel construction.

Kernel Choice In experiments below, both k_f and k_h were taken to be Gaussian (also called squared-exponential) covariance functions; for example: $k_f(\mathbf{x}, \mathbf{x}') = \lambda_f \exp(-\|\mathbf{x} - \mathbf{x}'\|_2^2 / 2\sigma_f^2)$ parametrised by λ_f and σ_f . This choice was made to capture infinite differentiability of both integrands f and h involved in the example below. For this application we found that, while the σ . were possible to learn from data using EB, the λ . required a large number of data to pin down. Therefore for these experiments we fixed $\lambda_f = 0.1 \times \text{mean}(f_{i,j})$ and $\lambda_h = 0.01 \times \text{mean}(h_i)$. In both cases the remaining kernel parameters σ . were selected using EB. Results in Fig. 16 present the posterior estimates for the marginal likelihoods $p_i = p(\mathbf{y}|\mathcal{M}_i)$ that take into account numerical error, contrasted with the single point estimates obtained by ignoring numerical error (the standard approach).

Data Generation As a test-bed that captures the salient properties of model selection discussed in the main text, we considered variable selection for logistic regression:

$$p(\mathbf{y}|\boldsymbol{\beta}) = \prod_{i=1}^N p_i(\boldsymbol{\beta})^{y_i} [1 - p_i(\boldsymbol{\beta})]^{1-y_i}$$

$$\text{logit}(p_i(\boldsymbol{\beta})) = \gamma_1 \beta_1 x_{i,1} + \dots + \gamma_d \beta_d x_{i,d}, \quad \gamma_1, \dots, \gamma_d \in \{0, 1\}$$

where the model \mathcal{M}_k specifies the active variables via the binary vector $\boldsymbol{\gamma} = (\gamma_1, \dots, \gamma_d)$. A model prior $p(\boldsymbol{\gamma}) \propto d^{-\|\boldsymbol{\gamma}\|_1}$ was employed. Given a model \mathcal{M}_k , the active parameters β_j were endowed with independent priors $\beta_j \sim \mathcal{N}(0, \tau^{-1})$, where here $\tau = 0.01$.

A single dataset of size $N = 200$ were generated from model \mathcal{M}_1 with parameter $\boldsymbol{\beta} = (1, 0, \dots, 0)$; as such the problem is under-determined (there are in principle $2^{10} = 1024$ different models) and the true model is not well-identified. The selected model is thus sensitive to numerical error in the computation of marginal likelihood. Here we actually limit the model space to consider only models with $\sum \gamma_i \leq 2$; this speeds up the computation and, in this particular case, only rules out models that have much lower posterior probability than the actual MAP model. There are thus 56 models under comparison.

E.2 Case Study #2

Background on the model The Teal South model is a PDE computer model used for prediction of the performance of oil reservoirs. The model studied is on an 11×11 grid with 5 layers. It has 9 parameters representing physical quantities of interest, for which

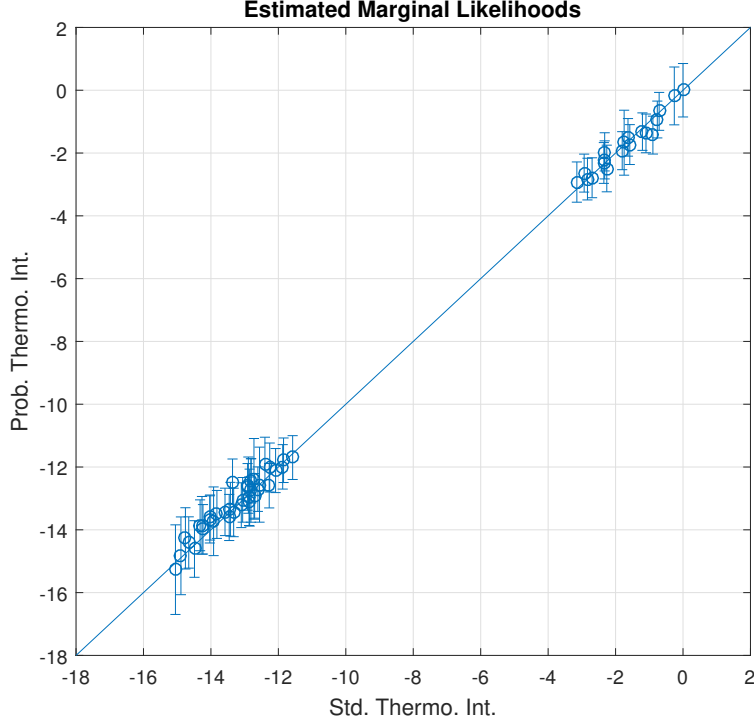


Figure 16: Probabilistic thermodynamic integration; estimates of marginal likelihoods $p_i = p(\mathbf{y}|\mathcal{M}_i)$. On the x-axis we show point estimates obtained by ignoring numerical error (the standard approach). On the y-axis we present the posterior mean estimates and \pm one standard deviation for the marginal likelihoods that take into account numerical error.

we would like to do inference using MCMC Lan et al. (2016). These include horizontal permeabilities for each of the 5 layers, the vertical to horizontal permeability ratio, aquifer strength, rock compressibility and porosity. For our experiments, we used a Gaussian process approximation of the likelihood model in order to speed up the cost of obtaining MCMC samples; however this will usually be undesirable in general due to the additional uncertainty associated with the approximation in the results obtained.

Kernel Choice The numerical results in Sec. 5.2.2 were obtained using a Matérn $\alpha = 3/2$ kernel given by $k(r) = \lambda^2(1 + \sqrt{3}r/\sigma) \exp(-\sqrt{3}r/\sigma)$ where $r = \|\mathbf{x} - \mathbf{y}\|_2$, which generates a Sobolev space $\mathcal{H}_{3/2}$. We note that $f \in \mathcal{H}_{3/2}$ since we know that it has infinitely many weak derivatives. We used empirical Bayes over the length-scale parameter σ , but fixed the magnitude parameter to $\lambda = 1$ (we once again found that this required a lot of data to learn accurately).

Variance Computation We used the approach to deal with intractable kernel means that was presented in Sec. 4.2. Furthermore, we used the framework described in Supplement C.4, and in particular of Eqn. 10 to upper bound the intractable BQ posterior variance. For the

upper bound to hold, states ${}_a\mathbf{x}_j$ must be independent samples from Π , whereas here they were obtained using MCMC and were therefore not independent. In order to ensure that MCMC samples were “as independent as possible” we employed sophisticated MCMC methodology developed by Lan et al. (2016) that provides low autocorrelation. Nevertheless, we emphasise that there is a gap between theory and practice here that we hope to fill in future research. For the results in this paper we always take $\delta = 0.05$, so that $C_{n,\alpha} = C_{n,\alpha,0.05}$ is essentially a $95(1 - \alpha)\%$ credible interval. A formal investigation into the theoretical properties of the uncertainty quantification provided by these methods is not provided in this paper.

E.3 Case Study #3

Below we present fill details for the simulation study associated with high-dimensional probabilistic integration.

Kernel Choice The (canonical) *weighted* Sobolev space $\mathcal{S}_{\alpha,\gamma}$ is defined by taking each of the component spaces \mathcal{H}_u to be Sobolev spaces of dominating mixed smoothness \mathcal{S}_α . i.e. the space \mathcal{H}_u is norm-equivalent to a tensor product of $|u|$ one-dimensional Sobolev spaces, each with smoothness parameter α . Constructed in this way, $\mathcal{S}_{\alpha,\gamma}$ is an RKHS with kernel

$$k_{\alpha,\gamma}(\mathbf{x}, \mathbf{x}') = \sum_{u \subseteq \mathcal{I}} \gamma_u \prod_{i \in u} \left(\sum_{k=1}^{\alpha} \frac{B_k(x_i) B_k(x'_i)}{(k!)^2} - (-1)^\alpha \frac{B_{2\alpha}(|x_i - x'_i|)}{(2\alpha)!} \right),$$

where the B_k are Bernoulli polynomials. For example, taking $\alpha = 1$ we have the kernel

$$k_{1,\gamma}(\mathbf{x}, \mathbf{x}') = \sum_{u \subseteq \mathcal{I}} \gamma_u \prod_{i \in u} \left(\frac{x_i^2}{2} + \frac{(x'_i)^2}{2} - \frac{x_i}{2} - \frac{x'_i}{2} - \frac{|x_i - x'_i|}{2} + \frac{1}{3} \right),$$

and tractable kernel mean $\mu(\Pi)(\mathbf{x}) = \int_{\mathcal{X}} k_{1,\gamma}(\mathbf{x}, \mathbf{x}') d\mathbf{x}' = \gamma_\emptyset$.

Theoretical Results In finite dimensions $d < \infty$, we can construct a higher-order digital net that attains optimal QMC rates for weighted Sobolev spaces:

Theorem 5. *Let \mathcal{H} be an RKHS that is norm-equivalent to $\mathcal{S}_{\alpha,\gamma}$. Then BQMC based on a digital $(t, \alpha, 1, \alpha m \times m, d)$ -net over \mathbb{Z}_b attains the optimal rate $e(\hat{\Pi}_{BQMC}; \Pi, \mathcal{H}) = O(n^{-\alpha+\epsilon})$ for any $\epsilon > 0$, where $n = b^m$. Hence $\mathbb{P}_n[I_D^c] = o(\exp(-Cn^{2\alpha-\epsilon}))$.*

Proof. This follows by combining Thm. 15.21 of Dick and Pillichshammer (2010) with Lemma 3. □

The QMC rules in Theorem 5 do not explicitly take into account the values of the weights γ . An algorithm that tailors QMC states to specific weights γ is known as the *component by component* (CBC) algorithm; further details can be found in (Kuo, 2003). In principle the CBC algorithm can lead to improved rate constants in high dimensions, because effort

is not wasted in directions where f varies little, but the computational overheads are also greater. We did not consider CBC algorithms for BQMC in this paper.

Note that the weighted Hilbert space framework allows us to bound the MMD *independently of dimension* providing that $\sum_{u \in \mathcal{I}} \gamma_u < \infty$ (Sloan and Woźniakowski, 1998). This justifies the use of “high-dimensional” in this context; the posterior variance can be bounded independently of dimension for these RKHSs. Analogous results for functional approximation were provided by Fasshauer et al. (2012) for the Gaussian kernel. Further details are provided in Sec. 4.1 of (Dick et al., 2013).

E.4 Case Study #4

In this section we provide full details for spherical BMC and BQMC.

Kernel Choice The function spaces that we consider are Sobolev-like spaces $\mathcal{H}_\alpha(\mathbb{S}^d)$ for $\alpha > d/2$, obtained using the reproducing kernel $k(\mathbf{x}, \mathbf{x}') = \sum_{l=0}^{\infty} \lambda_l P_l^{(d)}(\mathbf{x} \cdot \mathbf{x}')$, $\mathbf{x}, \mathbf{x}' \in \mathbb{S}^d$, where $\lambda_l \asymp (1+l)^{-2\alpha}$ and $P_l^{(d)}$ are normalised Gegenbauer polynomials (for $d = 2$ these are also known as Legendre polynomials) (Brauchart et al., 2014). A particularly simple expression for the kernel in $d = 2$ and Sobolev-like space $\alpha = 3/2$ can be obtained by taking $\lambda_0 = 4/3$ along with $\lambda_l = -\lambda_0 \times (-1/2)_l / (3/2)_l$ where $(a)_l = a(a+1) \dots (a+l-1) = \Gamma(a+l)/\Gamma(a)$ is the Pochhammer symbol. Specifically, these choices produce

$$k(\mathbf{x}, \mathbf{x}') = \frac{8}{3} - \|\mathbf{x} - \mathbf{x}'\|_2, \quad \mathbf{x}, \mathbf{x}' \in \mathbb{S}^2.$$

This kernel is associated with a tractable kernel mean $\mu(\Pi)(\mathbf{x}) = \int_{\mathbb{S}^2} k(\mathbf{x}, \mathbf{x}') \Pi(d\mathbf{x}') = 4/3$ and hence the initial error is also available $\Pi[\mu(\Pi)] = \int_{\mathbb{S}^2} \mu(\Pi)(\mathbf{x}) \Pi(d\mathbf{x}') = 4/3$.

Theoretical Results The states $\{\mathbf{x}_i\}_{i=1}^n$ could be generated as MC samples. In that case, analogous results to those obtained in Sec. 3.2.2 can be obtained. Specifically, from Thm. 7 of Brauchart et al. (2014) and Bayesian re-weighting (Lemma 3), classical MC leads to slow convergence $e(\hat{\Pi}_{\text{MC}}; \Pi, \mathcal{H}) = O_P(n^{-1/2})$. The regression bound argument (Lemma 4) together with a functional approximation result in Le Gia et al. (2012, Thm. 3.2), gives a faster rate for BMC of $e(\hat{\Pi}_{\text{BMC}}; \Pi, \mathcal{H}) = O_P(n^{-3/4})$ in dimension $d = 2$. (For brevity the details are omitted.)

Rather than focus on MC methods, we present results based on spherical QMC point sets. We briefly introduce the concept of a *spherical t -design* (Bondarenko et al., 2013) which is defined as a set $\{\mathbf{x}_i\}_{i=1}^n \subset \mathbb{S}^d$ satisfying $\int_{\mathbb{S}^d} f d\Pi = \frac{1}{n} \sum_{i=1}^n f(\mathbf{x}_i)$ for all polynomials $f: \mathbb{S}^d \rightarrow \mathbb{R}$ of degree at most t . (i.e. f is the restriction to \mathbb{S}^d of a polynomial in the usual Euclidean sense $\mathbb{R}^{d+1} \rightarrow \mathbb{R}$).

Theorem 6. *For all $d \geq 2$ there exists C_d such that for all $n \geq C_d t^d$ there exists a spherical t -design on \mathbb{S}^d with n states. Moreover, for $\alpha = 3/2$ and $d = 2$, the use of a spherical t -designs leads to a rate $e(\hat{\Pi}_{\text{BQMC}}; \Pi, \mathcal{H}) = O(n^{-3/4})$ and $\mathbb{P}_n[I_D^c] = o(\exp(-Cn^{3/2}))$.*

Proof. This property of spherical t -designs follows from combining Hesse and Sloan (2005); Bondarenko et al. (2013) and Lemma 3. \square

The rate in Thm. 6 is best-possible in the space $\mathcal{H}_{3/2}(\mathbb{S}^2)$ (Brauchart et al., 2014) and, unlike the result for BMC, is fully deterministic. (Empirical evidence in Marques et al. (2015) suggests that BQMC attains faster rates than BMC in RKHS that are smoother than $\mathcal{H}_{3/2}(\mathbb{S}^2)$.) Although explicit spherical t -designs are not currently known in closed-form, approximately optimal point sets have been computed numerically to high accuracy. Our experiments were based on such point sets provided by R. Womersley on his website <http://web.maths.unsw.edu.au/~rsw/Sphere/EffSphDes/sf.html> [Accessed 24 Nov. 2015].

References

- F. Bach. Sharp analysis of low-rank kernel matrix approximations. In *International Conference on Learning Theory*, 185–209, 2013.
- B. Dai, B. Xie, N. He, Y. Liang, A. Raj, M. Balcan, and L. Song. Scalable kernel methods via doubly stochastic gradients. In *Advances in Neural Information Processing Systems*, 3041–3049, 2014.
- A. El Alaoui and M. W. Mahoney. Fast randomized kernel methods with statistical guarantees. In *Advances in Neural Information Processing Systems*, 775–783, 2015.
- R. B. Gramacy and D. W. Apley. Local Gaussian process approximation for large computer experiments. *Journal of Computational and Graphical Statistics*, 24(2):561–578, 2015.
- K. Hesse and I. A. Sloan. Worst-case errors in a Sobolev space setting for cubature over the sphere \mathbb{S}^2 . *Bulletin of the Australian Mathematical Society*, 71(1):81–105, 2005.
- M. Katzfuss. A multi-resolution approximation for massive spatial datasets. *arXiv:1507.04789*, 2015.
- F. Y. Kuo. Component-by-component constructions achieve the optimal rate of convergence for multivariate integration in weighted Korobov and Sobolev spaces. *Journal of Complexity*, 19(3):301–320, 2003.
- M. Lazaro-Gredilla, J. Quinero-Candela, C. E. Rasmussen, and A. R. Figueiras-Vidal. Sparse spectrum Gaussian process regression. *Journal of Machine Learning Research*, 11:1865–1881, 2010.
- Q. T. Le Gia, I. H. Sloan, and H. Wendland. Multiscale approximation for functions in arbitrary Sobolev spaces by scaled radial basis functions on the unit sphere. *Applied and Computational Harmonic Analysis*, 32:401–412, 2012.
- J. Quinero-Candela and C. E. Rasmussen. A unifying view of sparse approximate Gaussian process regression. *Journal of Machine Learning Research*, 6:1939–1959, 2005.

- A. Rahimi and B. Recht. Random features for large-scale kernel machines. In *Advances In Neural Information Processing Systems*, 1177–1184, 2007.
- Q. Shi, J. Petterson, G. Dror, J. Langford, A. Smola, and S. V. N. Vishwanathan. Hash kernels for structured data. *Journal of Machine Learning Research*, 10:2615–2637, 2009.
- I. H. Sloan and H. Woźniakowski. When are Quasi-Monte Carlo algorithms efficient for high dimensional integrals? *Journal of Complexity*, 14(1):1–33, 1998.
- A. B. Tsybakov. *Introduction to nonparametric estimation*. Springer Science & Business Media, 2008.
- A. Vedaldi and A. Zisserman. Efficient additive kernels via explicit feature maps. *IEEE Transactions on Pattern Analysis and Machine Intelligence*, 34(3):480–492, 2012.
- Z. Wang, M. Zoghi, F. Hutter, D. Matheson, and N. De Freitas. Bayesian optimization in high dimensions via random embeddings. In *Proceedings of the Twenty-Third International Joint Conference on Artificial Intelligence.*, 1778–1784, 2013.
- Z. Wu and R. Schaback. Local error estimates for radial basis function interpolation of scattered data. *IMA journal of Numerical Analysis*, 13(1):13–27, 1993.